Cortical Somatosensory Neuroprosthesis for Active Tactile Exploration without Visual Feedback

by

Je Hi An

Department of Biomedical Engineering
Duke University

Date:_____

Approved:

_____
Miguel Nicolelis, Supervisor

_____
Patrick Wolf

_____
Marc Sommer

_____
Michael Platt

_____
Mikhail Lebedev

Dissertation submitted in partial fulfillment of the requirements for the degree of
Doctor of Philosophy in the Department of Biomedical Engineering
in the Graduate School of Duke University

2013

ABSTRACT

Cortical Somatosensory Neuroprosthesis for Active Tactile Exploration

without Visual Feedback

by

Je Hi An

Department of Biomedical Engineering
Duke University

Date:_____

Approved:

_____
Miguel Nicolelis, Supervisor

_____
Patrick Wolf

_____
Marc Sommer

_____
Michael Platt

_____
Mikhail Lebedev

An abstract of a dissertation submitted in partial fulfillment of the requirements for the degree of Doctor of Philosophy in the Department of Biomedical Engineering in the Graduate School of Duke University

2013

Abstract

Brain Machine Interfaces (BMI) strive to restore motor and sensory functions lost due to paralysis, amputation, and neurological diseases by interfacing brain circuitry to external actuators in form of a cursor on a computer screen or a robotic limb. There is a strong clinical need for sensory restoration as lack of somatosensory feedback leads to loss of fine motor control and one of the most common preferences for improvements according to individuals with upper-limb loss is the ability to require less visual attention to perform certain functions and to have a better control of wrist movement. One way to restore sensory functions is using electrical microstimulation of brain sensory areas as an artificial sensory channel; however, the ways of creating such artificial sensory inputs are poorly understood.

This dissertation presents the use of intracortical microstimulation (ICMS) to the primary somatosensory cortex (S1) to guide exploratory arm movements without visual feedback. Two rhesus monkeys were chronically implanted with multielectrode arrays in S1 and primary motor cortex (M1). The monkeys used a hand-held joystick to reach targets with a cursor on a computer screen. ICMS patterns were delivered to S1 when the cursor was placed over the target, mimicking the sense of touch. After the target or the cursor was made invisible, monkeys relied on ICMS feedback instead of vision to perform the task. For an invisible cursor, a random offset was added to the position of

the invisible cursor to rule out the possibility that monkeys relied on joystick position felt through proprioception. Learning to perform these tasks was accompanied by changes in both the parameters of arm movements and representation of those parameters by M1 and S1 neurons at a population and individual neuronal levels.

Offline decoding of single neurons and population of neurons showed that overlapping, but not identical subpopulations of neurons represented movements when ICMS provided feedback instead of vision.

These results suggest that ICMS could be used as an essential source of sensation from prosthetic limbs.

Contents

List of Tables

List of Figures

Acknowledgements

First, I want to thank my advisor Miguel Nicolelis who showed me real passion for science (and soccer).

I am extremely grateful to Mikhail Lebedev, a Senior Research Scientist in the lab, for all his guidance and wisdom.

I also want to thank the rest of my committee members, Dr. Michael Platt, Dr. Marc Sommer, and Dr. Patrick Wolf for their valuable input and encouragement.

I was lucky to be surrounded by wonderful primate lab members who enriched my graduate school experience: Joseph O'Doherty, Andrew Tate, Zheng Li, Timothy Hanson, Katie Zhuang, Peter Ifft, David Schwarz, Vivek Subramanian, Billy Yoon Woo Byun, and our lab manager Tamara Phillips. From the rodent lab side, I would like to thank Gary Lehew, Jim Meloy, Susan Halkiotis, Laura Olivera, and Terry Jones.

I had a great support system outside of the lab in form of friends who were always willing to listen to ups and downs of grad school: Inés Nam, Anna Uger, Aarti Wolenski, Eikar Lai, Rohan Shah, Jaafar Tindi, Cindy Cheng, Amanda Travis, and Dexter.

A special and copious amount of gratitude goes to my fiancé Andrew Tate for his support and *humour*.

Lastly, I know that I would be very far away from here if it wasn't for the sacrifice that my parents made moving across continents and starting over, not once but twice, and doing their very best to enable my dreams.

1 Introduction

1.1 Clinical need for BMIs

Trauma such as vehicle accidents and central nervous system disorders such as cerebral palsy and amyotrophic lateral sclerosis can cause spinal cord injuries (SCI) and the estimated size of the American population with traumatic SCI is 183,000 to 230,000 (McDonald and Sadowsky 2002). Diabetes mellitus, dysvascular disease, trauma, and malignancy of the bone and joint cause an estimated 185,000 Americans to undergo limb amputations each year (Ziegler-Graham, MacKenzie et al. 2008). These injuries can affect the ability of these individual to move and to feel. Treating these conditions is an active area of interdisciplinary research in neuroscience and engineering.

In patients with SCI, the brain gets disconnected from the spinal cord disconnected and it most often means confinement to a wheelchair (McDonald and Sadowsky 2002). A traditional solution to amputations is the use of prosthetics. Although major developments have occurred in prosthetic technology in the areas of biomechanics, materials and robotic devices, it still needs vast enhancements in the area of control and feedback. A subcategory of prosthetics that has recently formed is the field of Brain Machine Interfaces (BMIs) which allow ensembles of cortical neurons to directly control an external actuator such as a robotic manipulator or a cursor on the computer screen (Lebedev and Nicolelis 2006)

1.2 History of BMIs

The inception of BMIs is attributed to Fetz (Lebedev and Nicolelis 2006) with his 1969 study in which he showed that rhesus macaques could be conditioned to modulate the firing rates of single M1 neurons to receive a food reward (Fetz 1969). The cells' firing rates increased 50 to 500 % of their baseline level once the macaque was conditioned to food pellet and auditory cues but once that association was extinguished the firing rate returned to the preconditioned level.

The idea of using activity of motor cells to control an external device for immobile patients was reported first by Edward Schmidt in 1980 (Schmidt 1980) . In his article, he reported that intracortical electrodes could be chronically implanted in monkeys to establish a long-term connection to the brain. Furthermore he showed that monkeys could modulate the firing rate of a single motor neuron according to the displayed target. It is worth noting that Humphrey and Schmidt (Humphrey, Schmidt et al. 1970) had also previously shown that using multiple electrodes simultaneously to record from different brain areas and to predict the force generated by the monkey's movement of a handle was possible.

The next huge step to the conception of BMIs was the discovery that the *combination* or a population of a widely tuned individual motor cells coded a precise

movement direction was published in 1986 by Georgopoulos and colleagues (Georgopoulos, Schwartz et al. 1986).

It was in 1995 that Nicolelis and colleagues were able to show that chronic multielectrode recording was possible across multiple brain structures in the rat trigeminal sensory system (Nicolelis, Baccala et al. 1995). Finally, Chapin and his group (Chapin, Moxon et al. 1999) showed for the first time that rats with chronically implanted multiwire arrays could modulate their motor cortical and ventrolateral thalamic neural populations to control a robotic arm in real time.

From this period, several landmark BMI studies were published in a relatively short period: Wessberg (Wessberg, Stambaugh et al. 2000) and colleagues demonstrated monkeys could control a robotic arm in both one and three dimensional movements just using their motor cortical activity (Wessberg, Stambaugh et al. 2000). Taylor et al. 2002 (Taylor, Tillery et al. 2002) showed that three dimensional brain control of a cursor was possible in a closed loop system in which the visual feedback and constant update of decoder parameters were incorporated to the system. Carmena (Carmena, Lebedev et al. 2003) showed that reaching and grasping with a robotic arm was possible using real-time decoding of neuronal activity in different regions of the cortex and that neuronal tuning changes during learning of BMI control. Even a cognitive neural prosthesis was reported in 2004 (Musallam, Corneil et al. 2004) which mainly activity from the medial

intraparietal area (MIP), which is part of the parietal reach region thought to represent reaching movements and the goals of the reach in visual space, was used to decode the monkeys' intention to move a cursor in the screen.

Further experiments have shown that monkeys can use their motor cortical activity to control a robotic arm with five degrees of freedom for self-feeding (Velliste, Perel et al. 2008). Moritz and colleagues demonstrated that it is possible to control paralyzed muscles directly with the activity of motor cortical neurons (Moritz, Perlmutter et al. 2008) using functional electrical stimulation (FES) delivered to the paralyzed muscle based on motor cell firing. In 2012, restoration of grasp of paralyzed muscles was also shown to be possible by predicting the desired muscle activity using a large population of neurons and delivering FES to the temporarily paralyzed flexor muscles in the forearm and hand (Ethier, Oby et al. 2012). As described here, there have been multiple studies and advances in decoding of movement from cortical motor activity.

However, an area that remains poorly explored is spatial sensory restoration in which a patient can regain the sensation of limb position and the location of objects. One of the most common preferences for improvements according to individuals with upper-limb loss is the ability to require less visual attention to perform certain functions and to have a better control of wrist movement (Atkins, Heard et al. 1996). In addition,

restoration of sensory feedback that can aid reaching movements for those suffering of diminished or lack of somatosensory feedback and alleviate phantom limb pain caused by somatosensory cortical reorganization (Flor, Elbert et al. 1998). This is not surprising given that a projected movement is often modified according to sensory information.

Incorporation of multiple sensory modalities improves BMI control as shown by Suminski and colleagues (Suminski, Tkach et al. 2010). They found that providing both visual and proprioceptive feedback improved performance of brain-controlled movement by decreasing both time to target and path length. Lesion to the sensory cortex has been found to negatively affect the ability of monkeys to discriminate the speed of moving tactile stimuli (Zainos, Merchant et al. 1997). Vision can provide feedback for proprioception and kinesthesia and even dominate over other senses in certain cases (Gallace and Spence 2008). However, visual feedback might not be sufficient in some cases such as those requiring precise movement (Blank, Okamura et al. 2008). Studies in patients suffering from large fiber sensory neuropathy who have lost their sense of position, touch, and vibration but with intact muscle strength show errors in reaching for visual targets and a large increase in variability of limb position compared to intact sensory subjects (Ghez, Gordon et al. 1995). Deafferented monkeys have a degraded timing and fine control of their movements than the intact animals and this impairment worsens as the speed of task increases or when vision is eliminated

unless if it involves an activity that the monkey was overtrained (Taub, Goldberg et al. 1975). These studies are some selective of the many that substantiate the importance of the role of sensory feedback during movement.

1.3 Sensory substitution

Somatosensory processing is intricate due to the involvement of tactile, proprioceptive, and temperature sensation when touching an object. It is not surprising then to find that there are different and mixed neural response types dispersed in the primary somatosensory cortex (Rincon-Gonzalez, Warren et al. 2011). Given the complexity of the sensory system, one approach to sensory restoration has been sensory substitution which instead of replicating the body's natural sensory feedback seeks to replace an affected sensory channel with an artificial channel.

1.3.1 *Periphery: robotics and prosthetics*

One goal of prosthetics is for the artificial limb to move and feel like one's own. Carroza and colleagues have developed an artificial hand with proprioceptive sensors with this goal in mind capable of processing EMG signals from two antagonist muscles in the forearm to control the robotic actuator (Carrozza, Vecchi et al. 2003). This is a promising device but it will require much more development to be user-friendly and to have any clinical efficiency.

Kuiken and his colleagues tackled the same problem by rerouting residual nerves of amputees to healthy muscles thus enabling a finer and a more natural control of prosthetics calling it targeted reinnervation. In an article published in 2004, they reported using this technique in a 54 year old patient who had lost both arms in an accident. They innervated what was left of the brachial plexus and median nerves to the healthy pectoralis major muscles. Then the surviving nerves connected to muscles were able to control a two degree of freedom prosthesis (Kuiken, Dumanian et al. 2004). Furthermore, in a later study they reported two patients who regained sensation of the hand by the same targeted reinnervation of the sensory nerves that used to innervate the amputated limb to the overlying chest skin so when that patch of skin was touched, the patients felt as if the missing limbs were touched (Kuiken, Marasco et al. 2007).

1.3.2 Periphery: mechanical and electrical stimulation

One approach to restore proprioception has been to obtain proprioceptive information from artificial sensors (position, speed, and joint angles) and relay that information to the other sensory modalities. Vibration and cutaneous electrical stimulation have been used extensively to mimic proprioceptive information. Mann and Reimers observed that amplitude modulated vibratory feedback near the stump of the joint angle in above-elbow amputees reduced errors by 50% when they performed reaching tasks with an EMG controlled prosthesis (Mann and Reimers 1970). Similarly,

Alles has also investigated the use of vibration with the ultimate goal of delivering elbow joint angle information (Alles 1970).

Another approach to peripheral stimulation is using electrical stimulation of the skin. Nohama and his colleagues have developed a system using the tactile phi phenomenon. In this phenomenon, through two or more pairs of electrodes produce a feeling of a moving image as if they are placed next to each other and if the amplitude of stimulation changes temporally and complementarily (Nohama, Lopes et al. 1995). This approach has the advantage of decreasing the number of stimulating points while improving quantity of information transmitted.

The drawback of transferring feedback from artificial sensors to other parts of the body is that the patient has to learn the new feedback which interferes with physiologically relevant signals and that this particular feedback cannot be used in paralyzed patients and amputees without residual sensation in their body.

1.3.3 Microstimulation in the brain for somatosensory sensation

It has been shown that electrical stimulation in small areas of the sensory cortex, known as microstimulation, can be used to evoke artificial sensation in awake, behaving monkeys (Dobelle, Mladejovsky et al. 1976, Romo, Hernandez et al. 1998, Fitzsimmons, Drake et al. 2007, London, Jordan et al. 2008, O'Doherty, Lebedev et al. 2009). Thus,

cortical microstimulation has been shown to evoke sensation that can reproduce some characteristics of normal tactile sensations.

The discovery that electrical stimulation of the mammalian cortex could produce movements contralateral to applied stimulation was made in 1870 by Fritch and Hitzig (Fritsch and Hitzig 1870), and since then cortical electrical stimulation has been used to study brain function. In particular, Penfield and colleagues studied the effect of electrical stimulation of the human cortex (Penfield and Boldrey 1937, Penfield and Perot 1963). Stimulation applied to different points in the brain produced particular movements and sensations in a localized part of the body ranging from movement and sensation of the tongue to the leg and foot (Penfield and Boldrey 1937), as well as visual and auditory hallucinations. They observed that electrical stimulation near the central sulcus (both anterior and posterior) produced sensations of numbness, tingling, movement (or desire of movement), and sometimes pain.

Operant conditioning to electrical stimulation in cats was demonstrated by Doty and colleagues in 1956 (Doty, Rutledge et al. 1956). In these experiments, cats responded by lifting the forelimb when electrical stimulation was applied to various points in cortex.

A seminal study in the field of electrical stimulation to the brain was the one by Romo and colleagues (Romo, Hernández et al. 1998) in which monkeys were able to

discriminate different flutter frequencies delivered by vibration to the skin and via microstimulation.

Graziano and colleagues (Graziano, Taylor et al. 2002) showed that microstimulation can elicit complex movements involving the eyes, shoulder, and the hand when applied to the ventral intraparietal area of the macaque brain, an area that responds to both visual and tactile stimuli.

Another use of microstimulation has been to guide a rat through a maze (Talwar, Xu et al. 2002). By applying microstimulation in S1 as the cue for either left or right direction and applying microstimulation to the medial forebrain bundle as the "reward center", rats were successfully able to navigate through a maze.

Similar sensations are reported in stimulation of the somatosensory thamalus performed on patients undergoing deep brain stimulation (DBS) during surgery. Continuous and cycling high frequency stimulation (185 Hz, 0.21 ms pulse duration) in the thalamus elicited different kinds of sensations in different patients but most people have reported tingling, movement, mechanical, pain, and temperature sensations. After the DBS electrodes were implanted for a mean of 29.1 months, more people have expressed "unnatural" sensations than when tested immediately after implantation (Heming, Choo et al. 2011).

Further recent studies support the premise that electrical stimulation to the somatosensory cortex can be a reliable and potential solution for providing sensory feedback with BMI devices. Johnson and colleagues 2013 (Johnson, Wander et al. 2013) applied electrical stimulation to the somatosensory cortex in humans undergoing surgical treatment for intractable epilepsy using electrocorticography electrodes. They applied stimulation to the cortical sites corresponding to somatic sensation of the right hand in one patient and the lower lip and the middle finger in the other patient. Using amplitudes of 7-9.8 mA in one patient and 3-3.6 mA on the other, much greater than the one used for ICMS, and frequencies of 50-100 Hz, they found that both patients were able to discriminate different frequencies and amplitudes. These results suggest that changing the parameters of stimulation applied to the surface of the brain can produce different and reliable sensations. However, long term adaptation, effects of sub and suprathreshold stimulation and more complex and repetitive stimulation patterns using microwires still have to be investigated.

Fitzsimmons and colleagues in the Nicolelis lab have demonstrated that delivering different spatial and temporal microstimulation patterns in the primary somatosensory cortex can be interpreted by monkeys as directional instructions for reaching movements (Fitzsimmons, Drake et al. 2007). This is a direct demonstration that microstimulation can be used as an artificial sensory channel. Furthermore, the

monkeys learned new microstimulation patterns more rapidly as compared to initial training. This could indicate that microstimulation can be used as reliable and stable artificial sensory channel. Soon after, O'Doherty and colleagues in the Nicolelis lab have shown that simultaneous recording of non-sensory cortical areas and active sensing of artificial tactile feedback based on ICMS of the sensory cortex can be achieved (O'Doherty, Lebedev et al. 2009).

Microstimulation has also been applied to areas that handle proprioceptive information. London and colleagues have used electrical stimulation in area 3a corresponding to the proprioceptive cortex and have successfully trained a monkey to use microstimulation as a cue to reach left or right using a manipulandum (London, Jordan et al. 2008).

Recent uses of microstimulation push beyond the boundaries of not just replacing bodily sensations but to crossing modalities such as perceiving invisible infrared (IR) light through microstimulation to S1 (Thomson, Carra et al. 2013) and to establishing a brain-to-brain interface (Pais-Vieira, Lebedev et al. 2013). Adult rats wearing an IR detector actively searched for a IR-emitting port out of three that would provide a reward with the correct cue was given by ICMS (Thomson, Carra et al. 2013). In the brain-to-brain machine interface, two rats exchanged behaviorally relevant information such as press of the correct lever that provided reward from the encoder rat

(the one that sent the information) to the decoder rat (the one that received the information) through microstimulation, and the performance of the decoded rat back to the encoder rat which affected the behavioral performance of the encoder rat (Pais-Vieira, Lebedev et al. 2013).

Electrical stimulation of neural circuitry potentially offers better resolution and information capacity compared to stimulation of the peripheral receptors. Another advantage of electrical stimulation in S1 is that the anatomy and the physiology of the receptors in the area have been studied extensively and computational models can even predict the spiking responses of different sensory receptors (Weber, Friesen et al. 2012). The drawbacks of microstimulation in the somatosensory cortex are the need for an invasive brain surgery and potential activation of misleading sensation such as phantom limb syndrome (Micera, Navarro et al. 2008).

1.3.4 Microstimulation outside of somatosensation

1.3.4.1 Vision

A classic use of visual cortex stimulation is to enable 'Braille' reading to blind patients by eliciting cortical phosphenes (Dobelle, Mladejovsky et al. 1976). Brindley and Lewin reported that stimulation in the occipital cortex caused a blind patient to see phospenes (Brindley and Lewin 1968) and stimulating through several electrodes simultaneously allowed the patient to see more complex patterns. Dobelle and

colleagues took this idea and they studied the effects of stimulation parameters and electrode configuration more systematically in more subjects to create a visual prosthesis for blind patients (Dobelle and Mladejovsky 1974).

Furthermore, microstimulation in cortical areas processing vision has been demonstrated to influence behavior in animals. Stimulation in the middle temporal visual area (MT) biased monkeys' perception of direction of motion (Salzman, Britten et al. 1990).

Marzullo and colleagues (Marzullo, Lehmkuhle et al. 2010) stimulated the visual cortex of the rat and combined it with motor cortex activity modulation in order to develop a closed loop brain machine interface. Given the extensive ability of the visual cortex to react to microstimulation, Murphey and Mounsell explored the microstimulation threshold needed to evoke a behavioral percept in monkeys and found that there was no significant difference in threshold among the five visual areas tested V1,V2,V3A,MT, and the inferotemporal cortex (Murphey and Maunsell 2007).

1.3.4.2 Auditory

Microstimulation to the auditory cortex has been used to restore hearing as in the case of cochlear implants (Wilson and Dorman 2008) and as behavioral cues (Otto, Rousche et al. 2005). In a controlled experimental setting, microstimulation can elicit more accurate discrimination than natural auditory feedback (Otto, Rousche et al. 2005).

1.3.4.3 Face perception

Microstimulation was also used to bias face categorization by monkeys. Stimulation of the inferior temporal cortex influences monkeys to choose faces rather than non-faces and this effect is increased as the duration of stimulation increases (Afraz, Kiani et al. 2006).

1.4 Movement planning and the role of visual and proprioceptive feedback

Planning and executing a movement is a complex process that involves constant feedback and involvement of several areas of the brain. In normal contexts, when a reach toward an object needs to be performed, the location of the object is detected through multiple sensory integration such as visual and proprioceptive feedback and this information is then transformed into different coordinate frames (Batista, Buneo et al. 1999, Sober and Sabes 2003).

Sober and Sabes (Sober and Sabes 2005) found that the brain uses different combinations of feedback modalities depending on the type of target and composition of the feedback. They found that a target indicated by the position of the left hand relied less on visual feedback than the purely visual target. The exact mechanisms of the combination of visual and proprioceptive feedback are still not clear. What is known is that both feedback modalities contribute to movement direction. The target position is

usually given by visual feedback and the arm movement is initiated by visual feedback but its relative position during movement is given both by visual and proprioceptive feedback. It is thought that proprioception plays a role in control of movement distance.

Given all the evidence of the importance of both visual and somatosensory feedback during movement it is important to develop a means to deliver somatosensory feedback to the brain for BMI users to ensure that their experience is as efficacious and useful as possible.

1.5 Current state of BMIs in human

Brain-Computer-Interfaces (BCIs) using electroencephalography (EEG) signals recorded at the scalp have been developed as a non-invasive method of providing control of motor intention to people suffering from motor diseases and paralysis. However it has the disadvantage of having very low spatial resolution and training. An intermediate level of invasiveness between BCIs with EEG and BMIs with single neuron recording is BCI with electrocorticographic (ECoG) activity. This technology in humans has been shown to be successful in controlling a cursor (Leuthardt, Schalk et al. 2004) although of less accuracy of a cortical microwire array.

Invasive BMIs have been implemented in humans with some success. A patient with advanced stage of Amytrophic Lateral Sclerosis (ALS) with locked-in syndrome

was implanted with a neurotrophic electrode which contained neurotrophic factors in the right motor cortex and appeared to have stable signals (Kennedy and Bakay 1998). Hochberg and colleagues showed that a tetraplegic man was able to control a cursor on a computer screen using his motor cortical neurons and successfully used a computer interface that simulated some daily activities such as opening an email, controlling the volume and channel of a TV and displayed initial success in controlling robotic arms (Hochberg, Serruya et al. 2006). In 2012, they showed that two people with tetraplegia were able to use their neuronal activity to perform reach and grasp movements with a robotic arm such as drinking coffee from a bottle (Hochberg, Bacher et al. 2012).

2. Experimental methodology

2.1. Background

2.1.1. Multielectrode arrays

There are mainly two types of multielectrode arrays being used nowadays in the BMI field: silicon based electrodes and microwire electrodes made of a metal with a coating of insulating material. The two main subtypes of silicon-based arrays are the Utah Electrode Array, which is created from one single block with needle-like recording electrode tips, and the Michigan probes which are planar arrays of electrode shanks with recording sites along the shank (Polikov, Tresco et al. 2005). The Nicolelis lab has pioneered the microwire multielectrode array technique (Nicolelis, Dimitrov et al. 2003, Nicolelis 2007). An array containing up to 96 microwires made of stainless steel usually coated with Teflon is attached to a printed circuit board (PCB) which is then connected to the tips of the microwires. A high-density, miniature connector is attached to the opposite side of the PCB (Nicolelis, Dimitrov et al. 2003). Since these early designs, microwire multielectrode array technology has been improved to include customized movable microwires that deliver robust recording signal quality for as long as four years post-implantation as described in the later section of this chapter.

It is important to notice that although silicon micromachined electrodes have the capability of complex design, current silicon based arrays do not offer any major

advantage compared to microarray design and many of these kind have been found to be unreliable for chronic recording applications in the CNS (Polikov, Tresco et al. 2005) .

2.1.2. Biocompatibility of chronically implanted electrodes

In the brain there are mainly three types of tissues: neurons, glial cells and vascular-related tissue. The proximity of the electrode's site to the neurons will affect the signal quality of the recording. Among the glial cells, the oligodendrocytes make up the myelin wrapping the axons of the neurons while astrocytes and microglia react to the presence of electrodes (Polikov, Tresco et al. 2005) .

2.1.2.1. Acute response

When the electrode is lowered into the cortex, capillaries, extracellular matrix, glial and neuronal cell processes can be damaged. The insertion of the electrode causes edema and necrosis and the brain initiates the release of red blood cells, platelets, clotting factors and macrophage recruitment to heal the wound. Activated microglia and re-absorption decreases edema and cellular debris 6-8 days after electrode insertion (Polikov, Tresco et al. 2005).

2.1.2.2. Chronic response

The presence of electrodes produces a chronic foreign body response in the brain. Astrocytes form a glial scar forming an encapsulated layer around the electrodes and activate microglia that will attempt to phagocytose the electrodes (Polikov, Tresco et

al. 2005, Grill, Norman et al. 2009). The glial scar layer can lead to electrode signal degradation although its effect seems to be different even in the same electrode implanted at different locations in the same animal.

2.2. Experimental setup

2.2.1. Subjects, cortical implants, and electrophysiological recordings

All animal procedures were performed in accordance with the National Research Council's Guide for the Care and Use of Laboratory Animals and were approved by the Duke University Institutional Animal Care and Use Committee.

Two rhesus monkeys (Macacca Mulatta), one female (monkey N, 6.4 $\pm$ 0.6 kg) and one male (monkey M, 8.2 $\pm$ 0.7 kg) were chronically implanted with microelectrode arrays in both hemispheres. A total of 113-120 and 111-118 units were recorded per experimental session in monkeys N and M, respectively. After the monkeys were placed in the experimental setup, head stage amplifiers were attached to the connectors embedded in the implant. Flexible cables connected the headstages to a 128 channel Multichannel Acquisition Processor (MAP, Plexon, Inc., TX, USA). Neuronal units were sorted in real time using the templates defined in MAP software.

2.3 Surgery

The surgery was performed by a neurosurgeon who has significant experience in multielectrode array implantation in a sterile environment. The head of the monkey was shaved, disinfected, the skin opened, and then small parts of the skull and dura were removed to allow implantation of arrays. While the animal was under anesthesia its blood pressure, ECG, and oxygen level were closely monitored. The head was placed in a stereotax apparatus to allow exact placement of the arrays. The electrode arrays were placed and fixed with surgical acrylic. Screws were placed to hold the cap together and a layer of acrylic was used to hold all the elements together (Nicolelis 2007, Lebedev, Tate et al. 2011). Both monkeys had four arrays implanted in 2009: two arrays in each hemisphere. Each array contained 96 channels that could be used for recording and stimulation and covers areas M1 or S1 of each hemisphere (Figure 2.1).

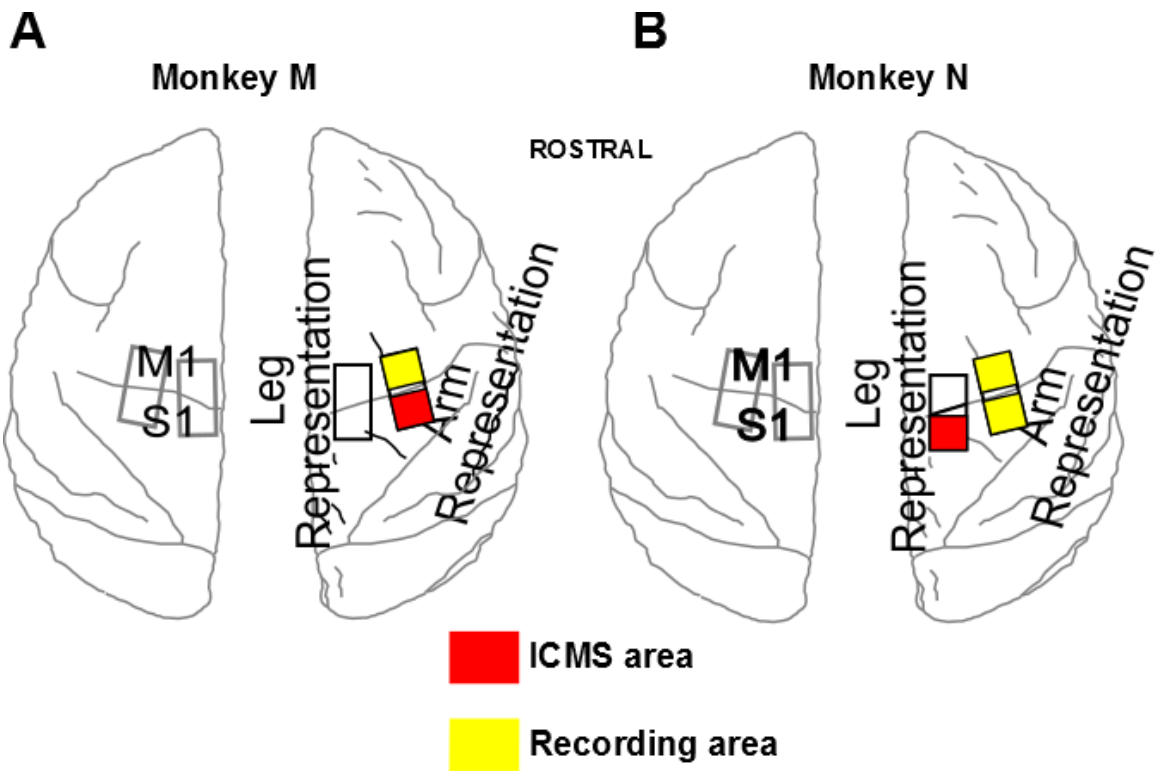

Figure 2.1. Multielectrode array implantation sites for both monkeys. A. In monkey M, M1 and part of the S1 area of the arm representation was recorded and part of the S1 area of the arm representation was used to for ICMS. B. In monkey N, the M1 and S1 areas of the arm representation were recorded and the leg representation of the S1 area was used to for ICMS.

2.3. Multielectrode recording

Multielectrode implants has proven to be a reliable way to simultaneously record of large numbers of neurons in long term. Recording a large number of neurons allows better predictive power and allows for obtaining information about multiple areas of the brain (Lebedev and Nicolelis 2006). Furthermore they allow electrical stimulation of a

specific area of the brain and also different combinations of simulation sites which is important for delivery of sensory feedback.

Each array contained 32 screws, 3 connectors for recording headstages, and 96 microwires grouped into triplets (Figure 2.2). Each screw moved three electrodes independently of others according to recording needs.

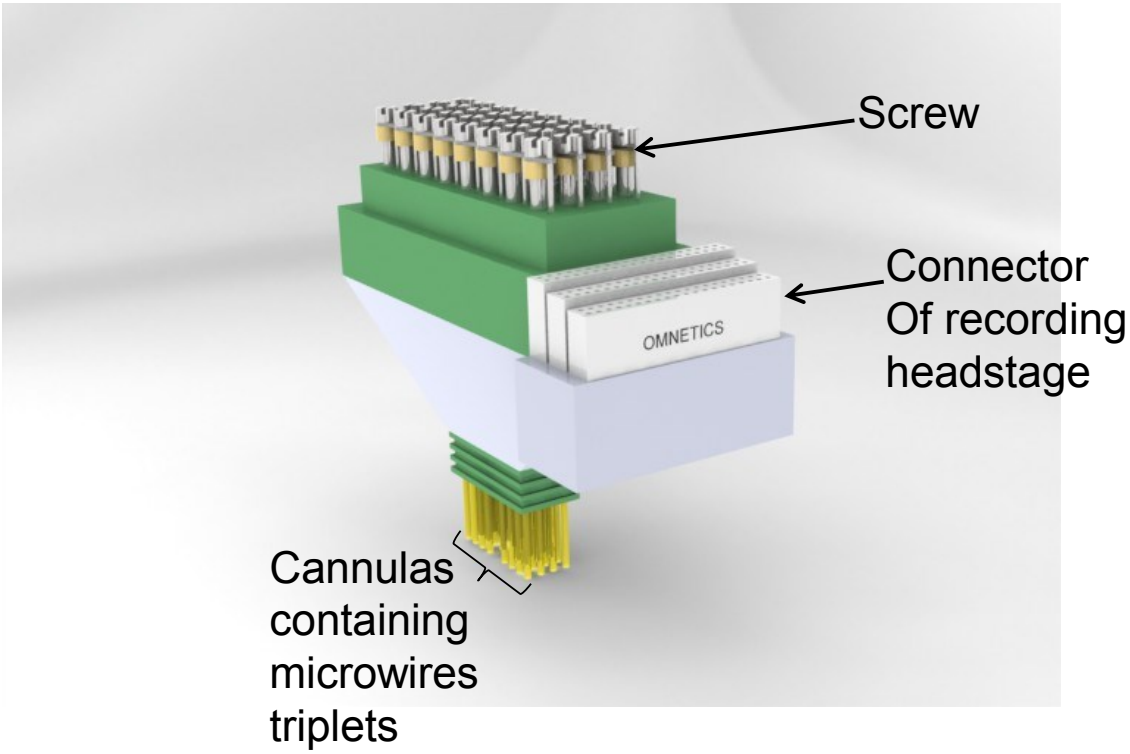

Figure 2.2. Rendering of a complete multielectrode array.

These arrays were contained in a headcap with a removable top (Figure 2.3.).

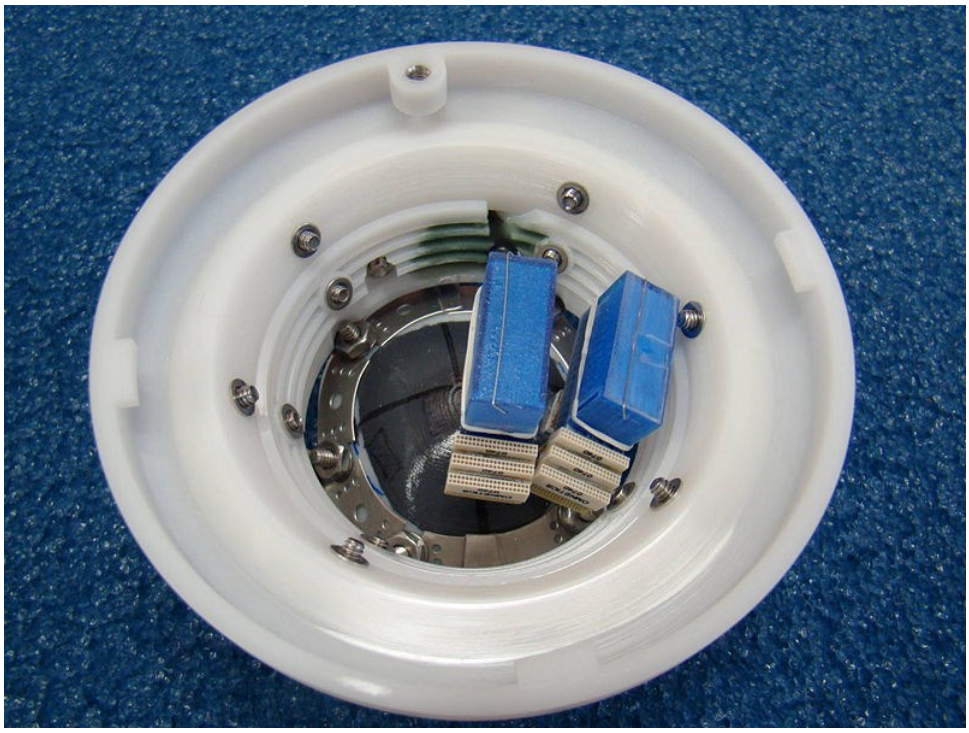

Figure 2.3. Top view of headcap assembly shown with cover plate removed and two electrodes installed onto a mock up skull. Blue plastic items cover the screws for moving electrodes.

Each bundle of triplets was separated by 1 mm. Each bundle contained three microwires of different lengths and diameters (Figure 2.4).

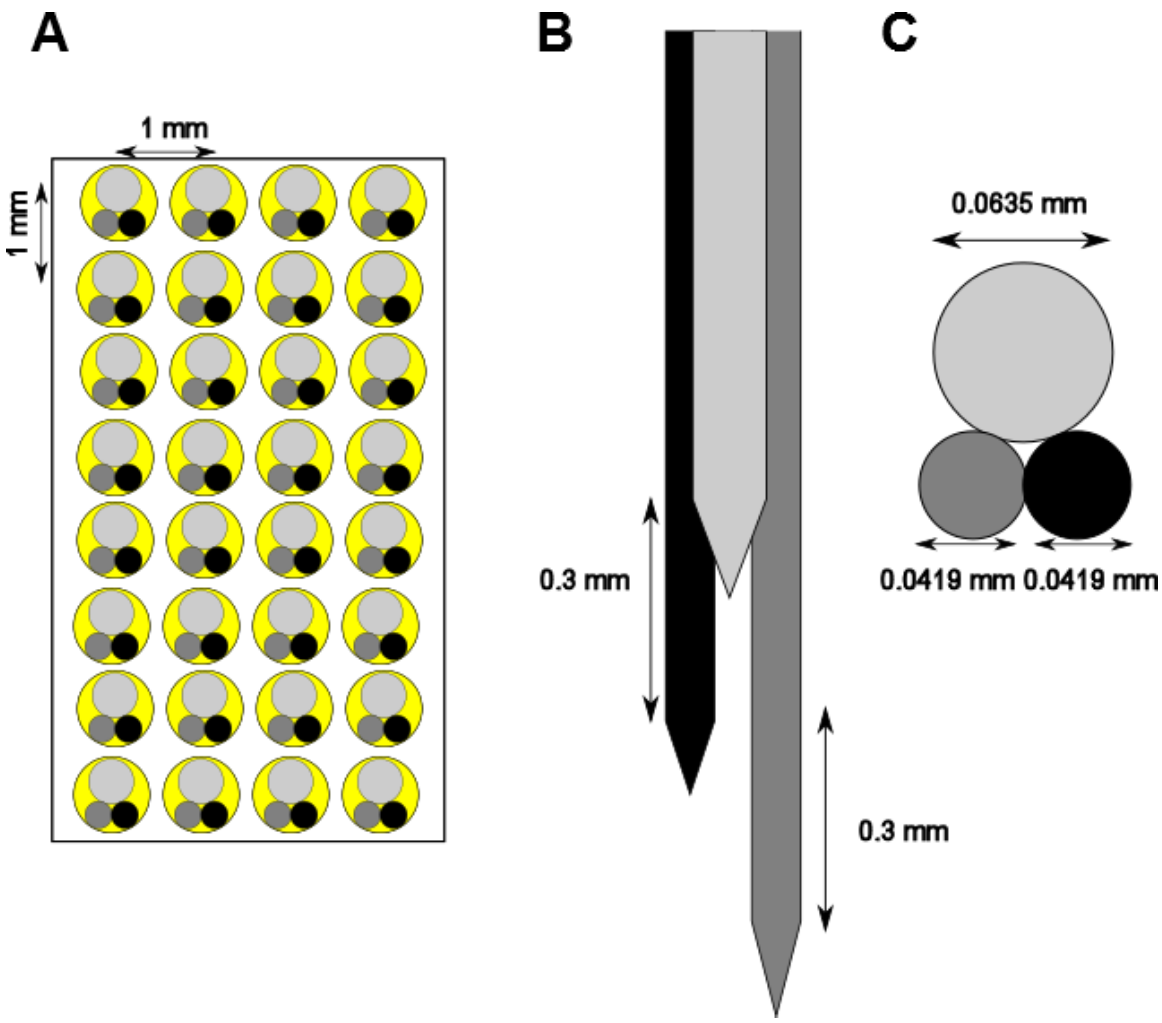

Figure 2.4. Electrode array design. A. Top view of one array of 96 microwires. B. Side view of a group of triplets of microwires. C. Top view of a group of triplets of microwires.

2.4. Microstimulation

ICMS was delivered using a multichannel stimulator designed and built in the Nicolelis laboratory (Hanson, Ómarsson et al. 2012). Both monkeys previously participated in a brain-machine-brain-interface (BMBI) task where they searched

through a set of visual targets, each associated with a pattern of ICMS applied to S1, and had to find a particular pattern (O'Doherty, Lebedev et al. 2011, Medina, Lebedev et al. 2012, O'Doherty, Lebedev et al. 2012). For this dissertation, the same implanted microelectrodes for ICMS delivery were used. In monkey M, ICMS was applied to the hand representation of S1 (Figure 2.1 A), whereas in monkey N, ICMS was applied to the leg representation of S1 (Figure 2.1 B). ICMS consisted of 100 Hz trains of symmetric, biphasic charge-balanced pulses delivered in bipolar form through two pairs of microwires. For both monkeys, positive and negative pulses of stimulation had amplitudes of 100 μA, pulse widths of 100 μs, and were separated by an interpulse delay of 25 μs.

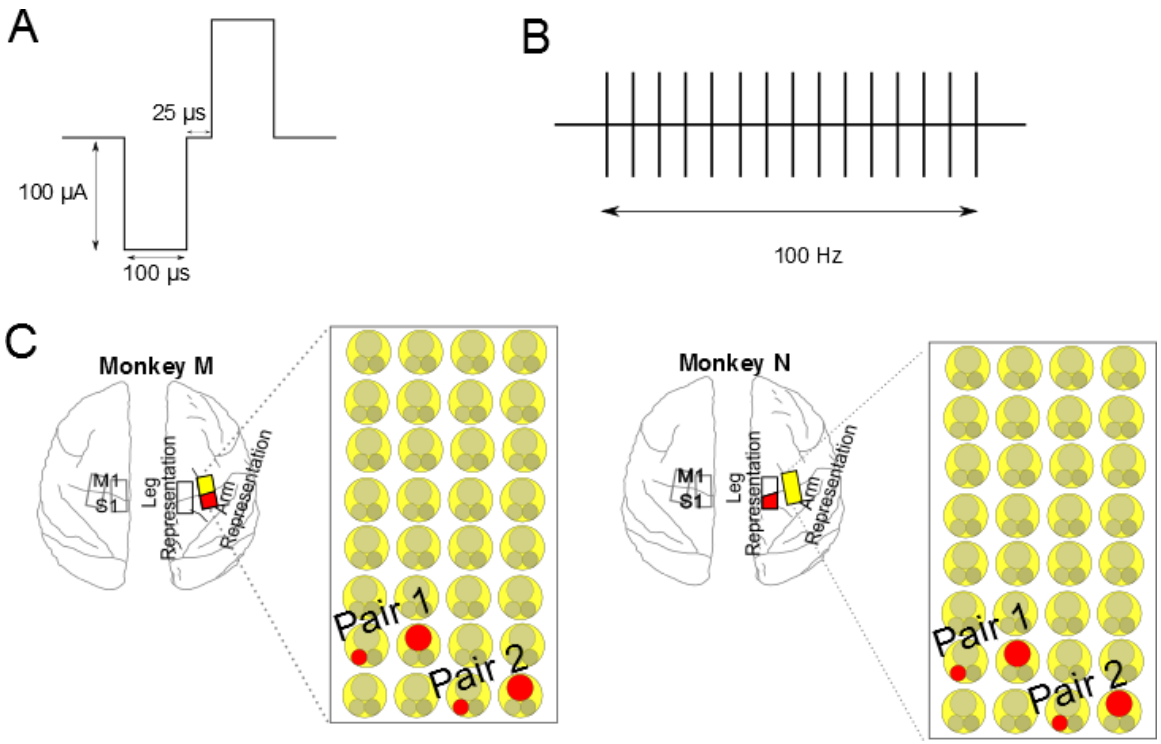

Figure 2.5. ICMS setup. A. Each pulse of microstimulation consisted of a cathodic-anodic pulse pair of 100 μA of amplitude, 100 μs duration and 25 μs interpulse delay. B. The primary frequency was 100 Hz. C. ICMS was delivered in two pairs of electrodes (red circles). Different electrodes were used for each monkey.

2.5. Additional Hardware

A Multichannel Acquisition Processor for 228 channel (Plexon Inc., Dallas TX. USA) was used for signal acquisition. This box was synchronized with the computer through a National Instruments digital acquisition (nidaq) card. Strobes were sent each time an event such as cursor movement occurred.

A 15 inch monitor was used to show the monkey the task display (cursor and target).

2.6. Behavioral setup

Both monkeys were proficient in joystick reaching tasks (Ifft, Lebedev et al. 2011, O'Doherty, Lebedev et al. 2011, Ifft, Lebedev et al. 2012, Medina, Lebedev et al. 2012, O'Doherty, Lebedev et al. 2012), which they had performed for more than four years. These previous tasks required reaching with a visible cursor towards visible targets. In the present study, the same monkeys were introduced to tasks in which they had to use ICMS feedback instead of relying on vision. For this purpose either the target or the cursor was made invisible.

Each monkey was seated in a Plexiglas primate chair, facing a 17-inch computer screen, which was placed 30-50 cm from the eyes from the monkey's eyes (Figure 2.6). A joystick was mounted at the monkey's waist level. The monkeys grasped the joystick with their left hands. The position of the joystick was mapped to the position of a screen

cursor (open circle, 0.5 cm in diameter; made invisible in some experiments). Rightward, leftward, forward and backward movements of the joystick were translated to rightward, leftward, upward and downward movements of the cursor, respectively.

A primate chair was customized to restrict monkeys' neck movements while allowing free arm movement so they could grab and move the joystick during experiments. A neckplate was used to prevent the monkeys from reaching their heads to remove the headstages and other wires used during experimental sessions.

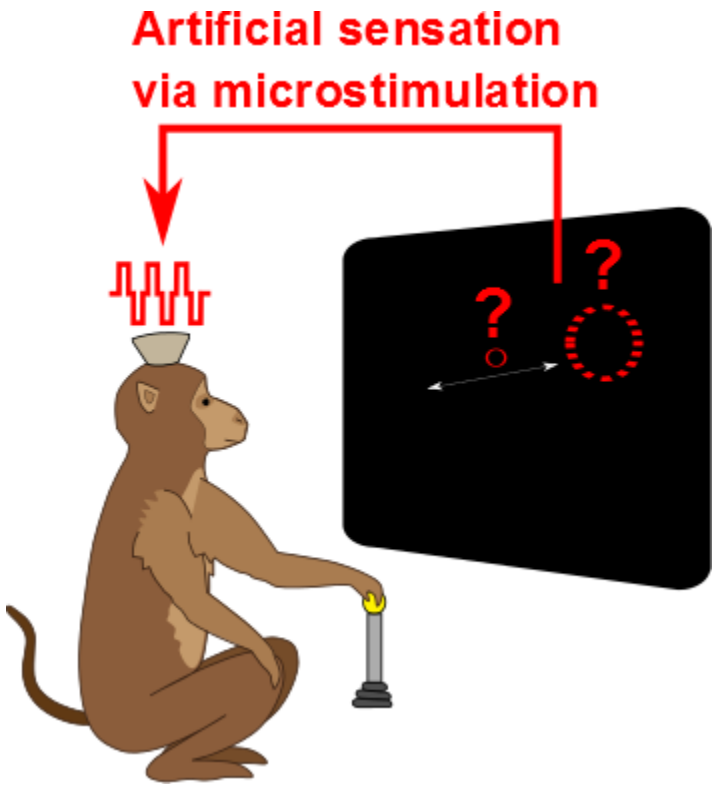

Figure 2.6. Behavioral setup. The monkey was placed on a chair that will allowed free movement of the arm so it could move the joystick. A computer screen was placed in

front of the monkey and it displayed the visible target or the visible cursor. Once the monkey placed the cursor in the target, ICMS was delivered.

All tasks required movements in only the horizontal dimension because targets were displayed at random locations along the horizontal axis.

In each trial, monkeys could place the cursor at any position and then move it to the target. There was no specific go-cue. Monkeys were rewarded with fruit juice for holding the cursor over the target for a randomly selected hold time (800-1200 ms) (Figure 2.7).

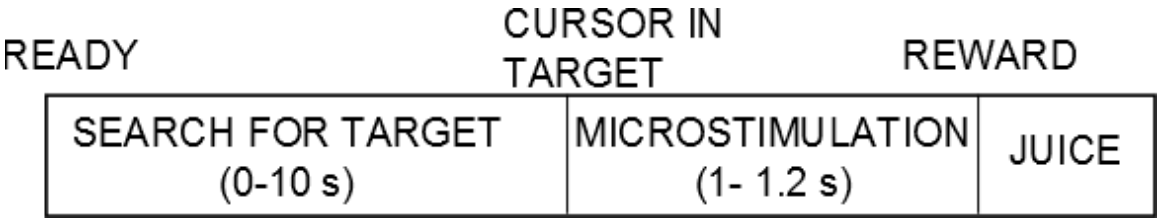

Figure 2.7. General trial setup.

If the monkey failed to reach the correct position of the target or did not hold enough time inside the target or exceeded a timeout interval of 10 s, no reward was given and a correction trial was issued with identical settings. The correction served to prevent the monkey from developing a strategy of always reaching in the same direction, with a 50% chance of getting a reward (Fitzsimmons, Drake et al. 2007, O'Doherty, Lebedev et al. 2009). These correction trials were not counted in calculating behavioral performance. Intertrial delay was 500 ms for all behavioral tasks. Each experimental session lasted from 40-120 minutes.

The visually guided task served as a baseline control. In that task, both the cursor and the target were visible throughout the trial (Figure 2.8). Each behavioral trial started with an appearance of a circular target (5 cm in diameter) 2.5-10 cm (drawn from a uniform distribution) to the left or to the right from screen center. Targets didn't appear at the resting position of the joystick which was the center of the screen (0 cm) because that position increased the probability of reward even if the monkey didn't move the joystick. Monkeys had to move the cursor over the target and hold it there for 800-1200 ms (randomly selected) to obtain a fruit juice reward. ICMS was never applied during this task.

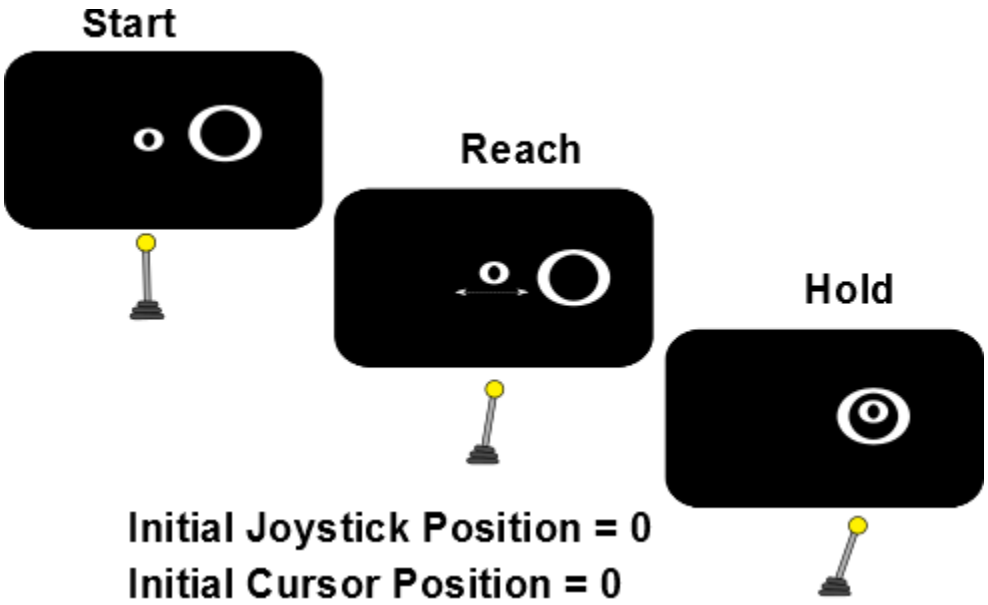

Figure 2.8. Visually guided task (control) setup.

In the invisible target task, the requirements were the same as in the visually guided task, but the target was invisible to the monkey and cursor contact with the target was signaled by ICMS instead of visual feedback (Figure 2.9). The transition to invisible target was the most difficult component of training for the monkeys. To ease this transition, two parameters were gradually adjusted: the brightness of the target and the duration of target visibility. During the training, the target initially was the same as in the visually guided task, and then its brightness was gradually decreased. Additionally the target initially remained on the screen for the entire duration of the trial, but gradually its duration was decreased to 0s, which was equivalent to making the target invisible. This training continued for several days (20 and 9 days for monkeys N and M, respectively), and then the monkeys performed the final task (10 and 8 sessions for monkeys N and M). In the final task, there was no other cue of the location of the target other than ICMS that was continuously applied when the cursor was placed inside the target. ICMS stopped immediately when the cursor moved outside of the target but it was delivered again if the cursor reentered the target. Multiple target entrances and exits were allowed, but a trial was rewarded only if the cursor was held inside the target for 0.8-1.2 s (randomly selected). Trials were unrewarded if the monkey failed to find and hold the target within 10s after the beginning of the trial. Catch trials

in which no ICMS was delivered were interweaved with regular trials (10% of total trials).

A modification of the invisible target task involved targets of variable size. The requirements remained the same, except that the target diameter varied from trial to trial from 2 to 5 cm.

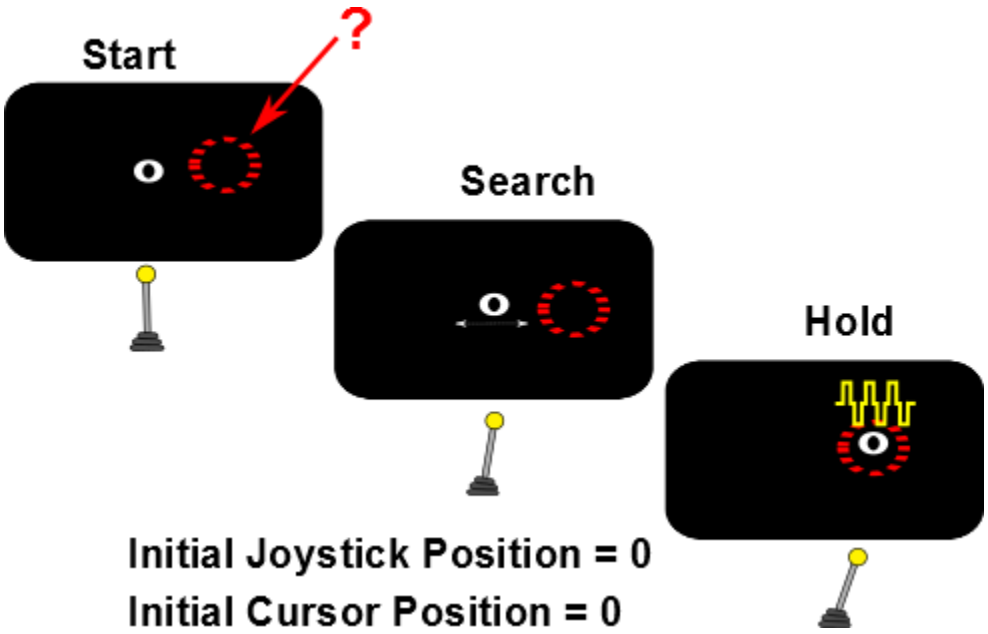

Figure 2.9. Invisible target task setup.

In the invisible cursor task, the requirements were the same as in the other tasks, but the cursor was invisible to the monkey (Figure 2.10). Cursor contact with the target was signaled to the monkey by ICMS, as in the invisible target task. For training purposes, the cursor was initially visible and then gradually decreased in opacity until it

became invisible while the target was visible throughout the trial. This initial training took 3 days in monkey N and 10 days in monkey M. Then, 5 and 6 sessions were recorded for monkeys N and M, respectively, with the invisible cursor. Catch trials in which no ICMS was delivered constituted 10% of total trials.

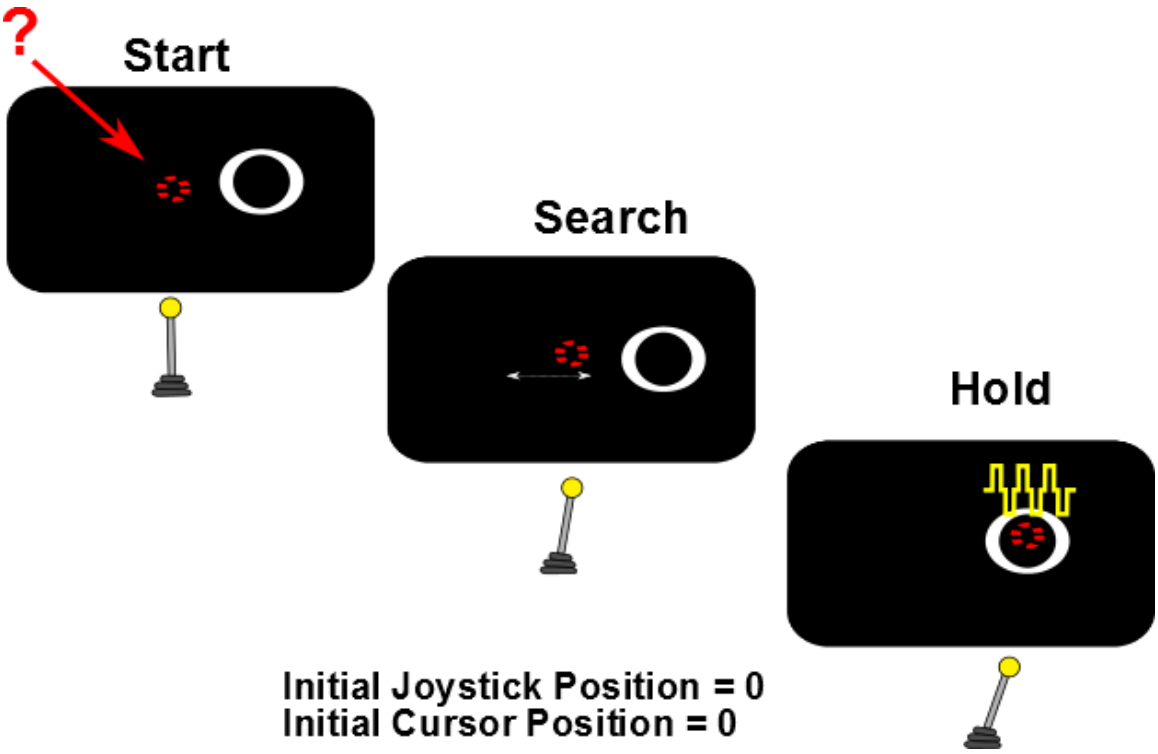

Figure 2.10. Invisible cursor task setup.

In the invisible cursor task with spatial bias (called Noisy Cursor Task for simplicity from now on) we introduced a random spatial bias to the position of the cursor. At the beginning of each trial, the position of the invisible cursor was shifted by a

constant horizontal offset randomly drawn from the range from -17 to 17 cm. The targets were visible (Figure 2.11). Catch trials in which no ICMS was delivered constituted 10% of total trials. We tested this paradigm after the subjects had learned the invisible cursor paradigm, so no initial training was needed with variable cursor visibility. 8 and9 sessions with this task were recorded in monkeys N and M, respectively.

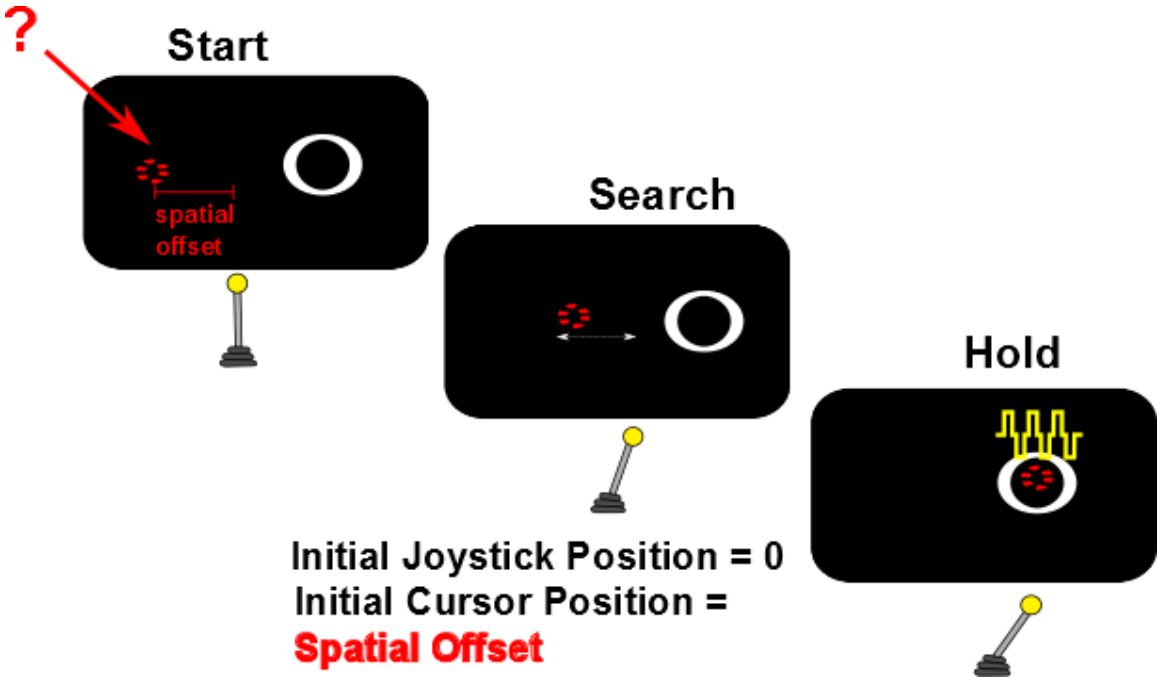

Figure 2.11. Invisible cursor with spatial offset task (noisy cursor) setup.

2.7 Software

A custom software suite called BMI3 built in the lab coded in C++ was used to control task parameters.

For the tasks, a state machine program was used so at any point the task was only in one state and a change of behavior would trigger change of state. The code was modified from existing tasks from the lab. There were seven states: Ready, Explore with Target, Explore without Target, In Target, Reward, Error Timeout Trial, and intertrial.

Ready: the start of the trial. It has the option to move to the next trial only if the monkey touches the joystick

Explore with Target: in this state the target can be made visible and a timer was added to transition to the state of Explore without Target. This state is most useful during training for a new task. No ICMS is delivered.

Explore without Target: the target is invisible, and if the cursor is placed inside the target then it moves to the In Target state. If the cursor doesn't move inside the target after a certain time then it is moved to the Error Canceled state. No ICMS is delivered.

In Target: if the cursor remains inside the target for a predetermined hold time, then the state changes to Reward. However if the cursor leaves the target area then it returns to Explore Without Target state. ICMS is delivered throughout this state.

Reward: juice is rewarded in this state and then is automatically transitioned into the Intertrial state. This is one of the two possible outcomes of the trial. No ICMS is delivered.

Error Timeout: the other possible outcome of the trial. A penalty time can be added here. It is automatically changed into Intertrial state after penalty time.

Intertrial: after a pause time between trials it is automatically changed into the Ready state.

3. Behavioral and neuronal responses under different visual feedback

3.1. Introduction

Ever since the pioneering studies of sensory and motor effects in response to electrical currents applied to nervous structures in animals (Fritsch and Hitzig 1870, Ferrier 1873, Ferrier 1875, Brown and Sherrington 1911) and humans (Ransom 1892, Penfield and Boldrey 1937, Penfield and Rasmussen 1950) electrical stimulation has evolved to become a widely used tool for exploration of the connectivity and function of the brain. Modern studies often employ injection of small electrical currents, termed intracortical microstimulation , to evoke local effects that mimic the function of the stimulated area (Tehovnik 1996, Cohen and Newsome 2004, DeAngelis and Newsome 2004, Tehovnik, Tolias et al. 2006). In particular, ICMS applied to different sensory areas in nonhuman primates has been shown to evoke sensations similar to vision (Bartlett, DeYoe et al. 2005), perception of visual motion (Salzman, Britten et al. 1990, Salzman, Murasugi et al. 1992, Britten and van Wezel 1998) and the somatosensory sensation of flutter (Romo, Hernández et al. 1998, Romo, Hernández et al. 2000, de Lafuente and Romo 2005). In humans, ICMS of the visual cortex has been shown to evoke sensations of light (Bak, Girvin et al. 1990, Schmidt, Bak et al. 1996).

With the emergence of multielectrode implants (Nicolelis, Dimitrov et al. 2003) and rapid development of brain–machine interfaces (BMIs) (Chapin, Moxon et al. 1999,

Wessberg, Stambaugh et al. 2000, Taylor, Tillery et al. 2002, Carmena, Lebedev et al. 2003, Lebedev, Carmena et al. 2005, Lebedev and Nicolelis 2006), there have been an increased interest in ICMS as the method of delivering artificial sensory inputs to the brain (Fitzsimmons, Drake et al. 2007, O'Doherty, Lebedev et al. 2009, O'Doherty, Lebedev et al. 2011, O'Doherty, Lebedev et al. 2012, Johnson, Wander et al. 2013). Such artificial sensations could act as communication channels (Fitzsimmons, Drake et al. 2007, Weber, Friesen et al. 2012, Johnson, Wander et al. 2013) or could provide sensory feedback from prosthetic limbs (Berger, Ahuja et al. 2005, Middlebrooks, Bierer et al. 2005, Lebedev and Nicolelis 2006, Wickelgren 2006). Recent studies support that ICMS of S1 can be a solution to providing sensory feedback for BMI devices. It has been demonstrated that monkeys can gradually learn to discriminate temporal and spatio-temporal ICMS patterns delivered to S1 through chronically implanted microelectrode arrays (Fitzsimmons, Drake et al. 2007). Moreover, we have developed a brain-machine-brain interface (BMBI), where motor signals are extracted from an M1 implant go control avatar search, and an S1 implant is used to deliver an ICMS feedback that mimics active touch (O'Doherty, Lebedev et al. 2011, O'Doherty, Lebedev et al. 2012).

Notwithstanding these demonstrations, it is still not well understood to what extent ICMS could be useful in clinical neuroprosthetic devices to substitute normal somatic sensations. In particular, it is unknown if ICMS-based feedback could be used

alone, without a need for visual feedback, to subserve exploratory tasks, such as locating (Murthy and Fetz 1992) and apprehending objects through touch (Klatzky, Lederman et al. 1985). The ability to use the limb and receive sensations from it without having it in sight is one of the primary needs of the users of prosthetic limbs (Atkins, Heard et al. 1996). To explore ICMS as the means to provide this ability, we chronically implanted two rhesus monkeys with cortical multielectrode arrays and introduced them to behavioral tasks that required relying on ICMS of S1 instead of vision as the sensory feedback that guided arm reaching.

3.2. Methods

3.2.1. Analysis of behavioral performance

The performance was evaluated as 1) the percentage of correct random trials and 2) the number of rewarded trials per minute (Fig. 3.1). Correction trials were excluded from both analyses, and catch trials were analyzed separately.

The monkeys' behavior was compared to chance performance, which was evaluated using two approaches. In the first approach, we applied a shuffle test to recorded behavioral data. Target locations were randomly reassigned for each trial. We then tested if the cursor trajectory could satisfy the successful performance requirements for those random target locations. In the second approach, we analyzed behavioral

performance in catch trials in which monkeys did not receive ICMS feedback. Chance performance was estimated using two approaches (figure 3.1).

For the task with variable target size we analyzed the time to target acquisition (Fig. 3.2). This metric was defined as the time from the start of the trial to the final entrance of the cursor into the target (i.e., the entrance followed by holding the target for the required duration).

The time to target acquisition was defined as the time from the start of the trial to the onset of the cursor position that was within the target for the established hold time and immediately before juice reward.

The length of cursor trajectory was calculated as the sum of cursor position difference until the onset of the successful target hold time.

3.2.2. Analysis of neuronal responses

Peri-event time histograms (PETHs) were used to analyze neuronal modulations for different neurons, target locations and tasks. PETHs were visualized for the entire neuronal population using color plots in which horizontal rows represented neurons, position in the row represented time, and firing rate was color coded (Figures 3.8 and 3.9). PETHs were aligned to peak velocity <10 cm/s. A maximum peak detection analysis was used to detect the start of the highest normalized firing rate of each neuron. Only neurons that had a maximum peak >1.2 were used. For monkey M a window of -1 to 0 s

from the peak of velocity was used while for monkey N a window of -0.5 to 0 s was used.

Neuronal tuning to position and velocity was analyzed using color diagrams, where the x-axis represented position and the y-axis represented velocity, and color represented average firing rate (Figures 3.11 and 3.12). In these diagrams, position and velocity were binned into 2 cm and 2 cm/s bins, respectively, and it was required that each square bin represented average data for at least 4 data points. If the number of data points was insufficient, the bin was left blank.

The tuning to position and velocity was also quantified using a multiple linear regression:

$$y = b_1 pos_x + b_2 vel_x + b_3 {pos_x}^2 + b_4 {vel_x}^2 + b_5 \quad (3.1)$$

where f is firing rate of a neuron, pos_x is x coordinate, vel_x is the x component of velocity, b_1 and b_2 are coefficient for linear terms, and b_3 and $b_4$are coefficients for quadratic terms.

To estimate stability of neuronal recordings across different sessions, we plotted probability density of the interspike interval each neuron of one session and compared it to the interspike interval of the same neuron and other neurons recorded in the same channel in a different session. Neurons were considered stable if the p value of the

Kolmogorov–Smirnov test for binned probability distribution of interspike intervals (ISI) during reward times was more than 0.05 (Ganguly and Carmena 2009).

3.3. Results

3.3.1. Behavioral results in the absence of visual feedback

3.3.1.1. Visually Guided paradigm

Because of previous overtraining, both monkeys achieved better than 90% correct performance from the very first session of the visually guided task. Their performance remained at this high level for the rest of the visually guided sessions.

3.3.1.2. Invisible Target paradigm

In the invisible target task, following preliminary training with barely visible and short-duration targets (9 and 20 days for monkeys M and N, respectively), both monkeys reached 90 % correct performance on the very first day of the final task (Fig. 3.3). Their performance remained at this high level during the next recording sessions. This level of performance was highly statistically different ($P<0.05$; t-test) from the performance on catch trials and baseline level (Fig. 3.3).

The pattern of movements was different in the invisible target task compared to the visually guided task. Both the velocity and the position traces become less stereotypical and there were more variability in the before and after the peak velocity

(Figure 3.8 and 3.9 B,C,E,F). Both monkeys increased the number of cursor direction changes, the number of crossing the target, but not holding, and the length of cursor trajectory (Table 1).

For monkey M, under this paradigm, the time to movement initiation was much less than in the visually guided case (Table 1) and as the monkey was overtrained the time to movement initiation decreased (0.29 $\pm$ 0.21 s in session 1 to 0.16 $\pm$ 0.11 s in session 8). There was no clear cue to trial start as the target was always invisible and the cursor was always visible.

For monkey N, the time to movement initiation was not different than in the visually guided paradigm (Table 1) as there was no significant difference among sessions.

The time to reward was longer as the size of the target became smaller (figure 3.1). This was expected as the size of the target increased the probability of the monkeys finding an area where ICMS was delivered increased.

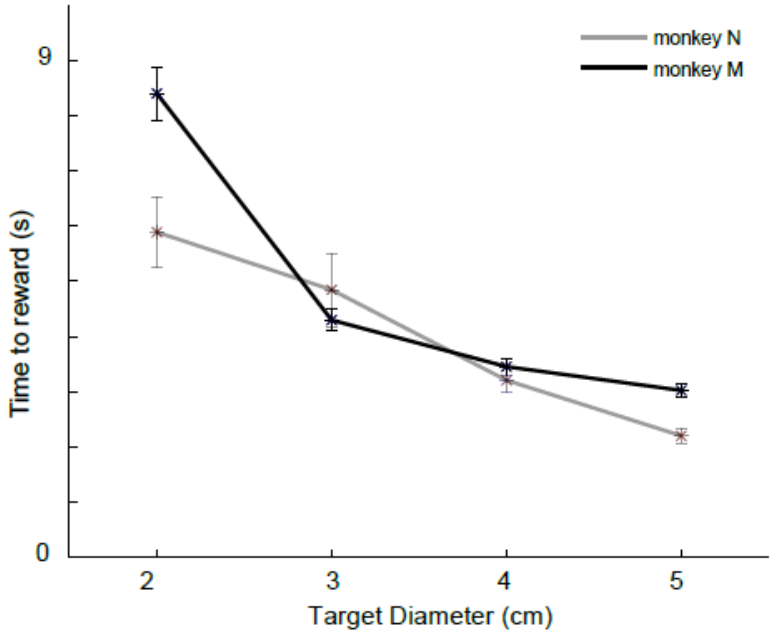

Figure 3.1. The effect of target size on the time from the start of the trial until reward under the invisible target paradigm for both monkeys.

3.3.1.3. Invisible Cursor paradigm

Once the invisible target task was learned, the next question was whether monkeys could perform without visual feedback of the end-effector, the cursor. Both monkeys were able to learn the task (9 sessions for monkey M and 3 sessions in monkey N). Monkey M's performance of catch trials was higher than monkey N's suggesting that they developed different strategies to perform in the task (Fig. 3.3). Monkey M probably relied on its sense of joystick position's correspondence to the cursor position and ICMS while monkey N relied mainly on ICMS only to identify whether the cursor

was placed on the target. For the invisible cursor task, similarly to the invisible target task, training was needed for the monkeys to perform this task. During the initial training sessions, monkeys couldn't perform trials in which the cursor was completely invisible thus the dimness of the cursor was gradually decreased. Monkeys M started to perform the invisible cursor task after 9 days of training, and monkey N after 3 days and their performance improved to more than 90% and remained at >90% for the rest of the sessions. Monkey M's performance of catch trials (56 $\pm$ 9%) was higher than monkey N's performance (31 $\pm$ 5 %) and higher than the baseline level (18%), which possibly indicated that monkey M was able to derive the cursor position from the position of the joystick position, which it felt through the arm proprioception. The task was then modified to make this behavioral strategy impractical.

3.3.1.4. Invisible Cursor with bias (noisy cursor) paradigm

To effectively uncouple the very well trained sense of joystick position and cursor position, a random spatial bias was added to each trial. This spatial bias consisted of shifting the start position of the invisible cursor in each trial. The spatial bias did not decrease the performance of regular trials but it did affect the performance of catch trials (Fig. 3.3). The monkeys were able to perform without any additional learning (they achieved >90% performance from session 1 indicating that they were mostly paying attention to the ICMS rather than its own joystick position sense.

The cursor bias did not affect the time that the monkeys needed to reach the reward further suggesting that monkeys were guided by the ICMS rather than the joystick sense (figure 3.2).

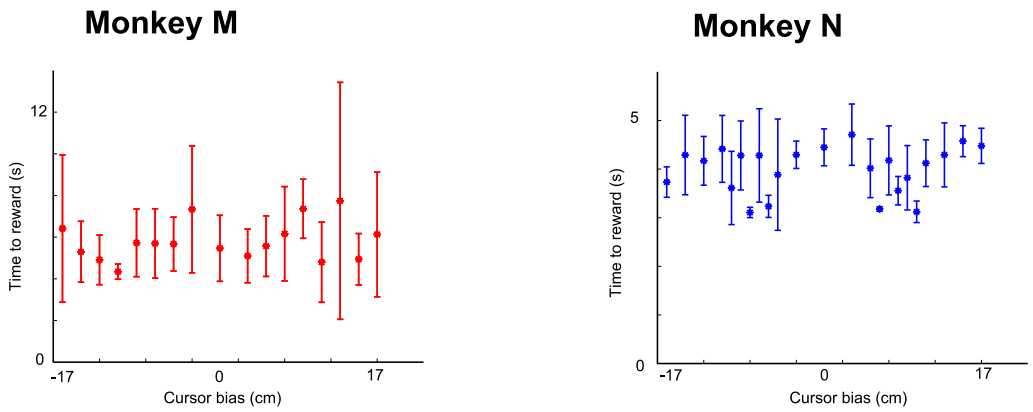

Figure 3.2. The effect of cursor bias on time from the start of the time trial until reward for both monkeys.

However this task proved to be the most difficult task that required most exploratory movement for both monkeys given the greatest number of cursor direction change and cursor trajectory length (table 1).

For monkey M, under this paradigm this premovement phase (period in which the movement is planned) was much longer than in control paradigm. The movement was exploratory with many more target touches, cursor direction changes, and trajectory length compared to Visually Guided paradigm. But as the monkey learned the paradigm better, the time to movement initiation period was reduced (reaction time of session 1 for noisy cursor was 0.456 $\pm$ 0.14 s but the reaction time of session 6 was 0.315 $\pm$

0.21 s). For monkey N, the time to movement initiation in this task is comparable to the visually guided.

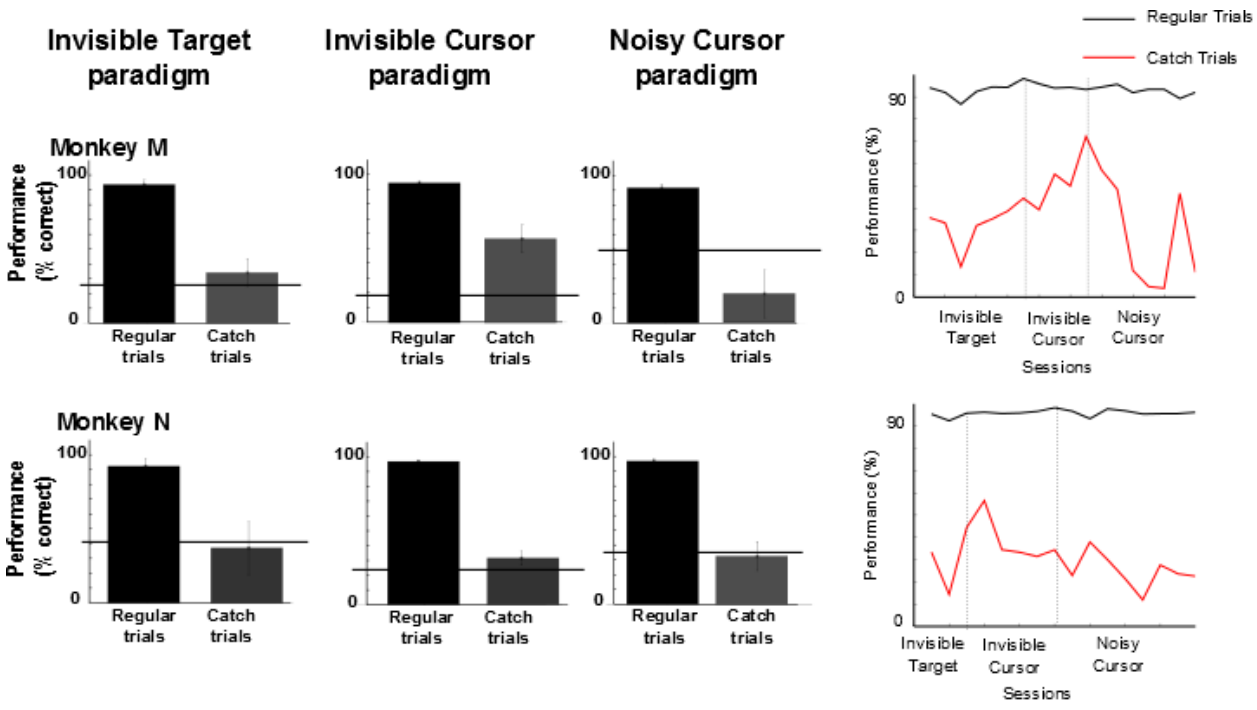

Figure 3.3. Behavioral results under different paradigms for both monkeys. Top row contains data for monkey M and the bottom row contains data for monkey N. The performance of regular trials for each paradigm was significantly higher than the performance of the catch trials (t-test, $p<0.05$) and higher than the baseline level indicated by a horizontal bar. The data from each session is plotted on the right column.

3.3.1.5. Comparison of all paradigms

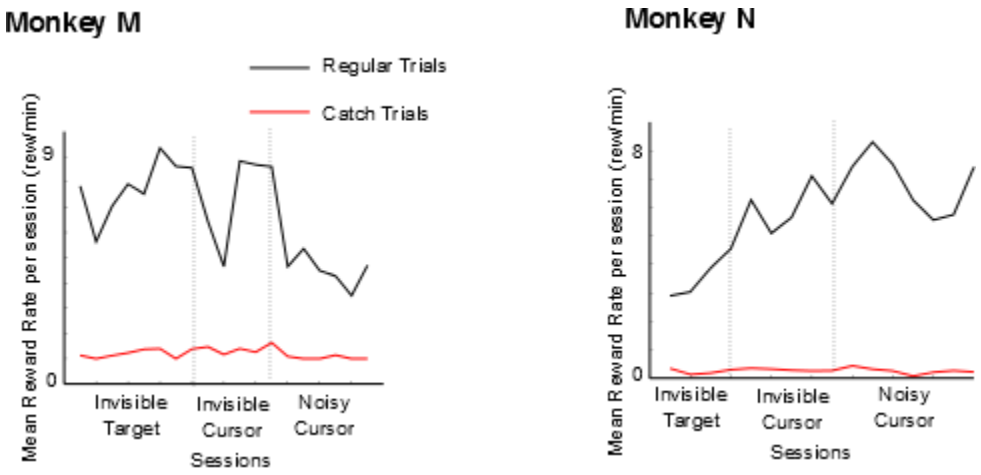

Figure 3.4. Mean reward rate per session per monkey.

The mean reward rate was always higher for regular trials than catch trials for both monkeys under all conditions (the Visually Guided paradigm did not have catch trials thus their data are not depicted in this figure).

No significant differences of time from the start of trial to reward were found based the starting point of the trial within a paradigm for neither monkeys (figure 3.6).

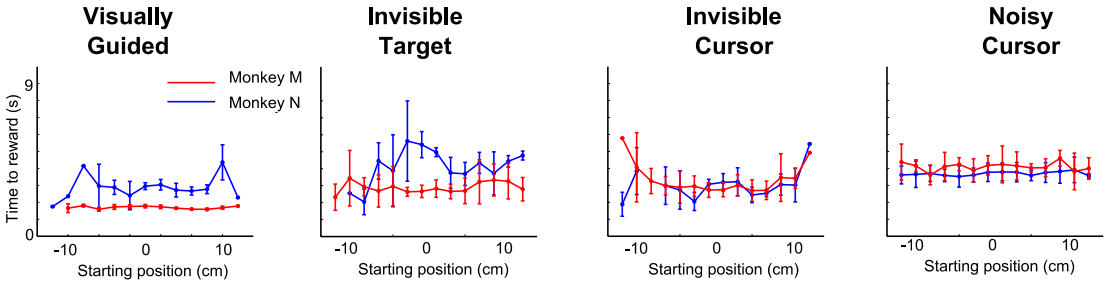

Figure 3.5. The effect of starting cursor position under different paradigms for both monkeys (errorbars represent s.t.d).

There was a significant difference of time to reach the target and hold the position for monkey M under different paradigms. The time was much longer under the Noisy Cursor paradigm (Figure 3.6). This was due to the exploratory behavior of the movement indicated by the increased number of target touches, cursor trajectory length, and movement direction changes. For monkey N, there was no significant difference of time to reach the target and hold the position under different paradigms but the data was more variable (Figure 3.6).

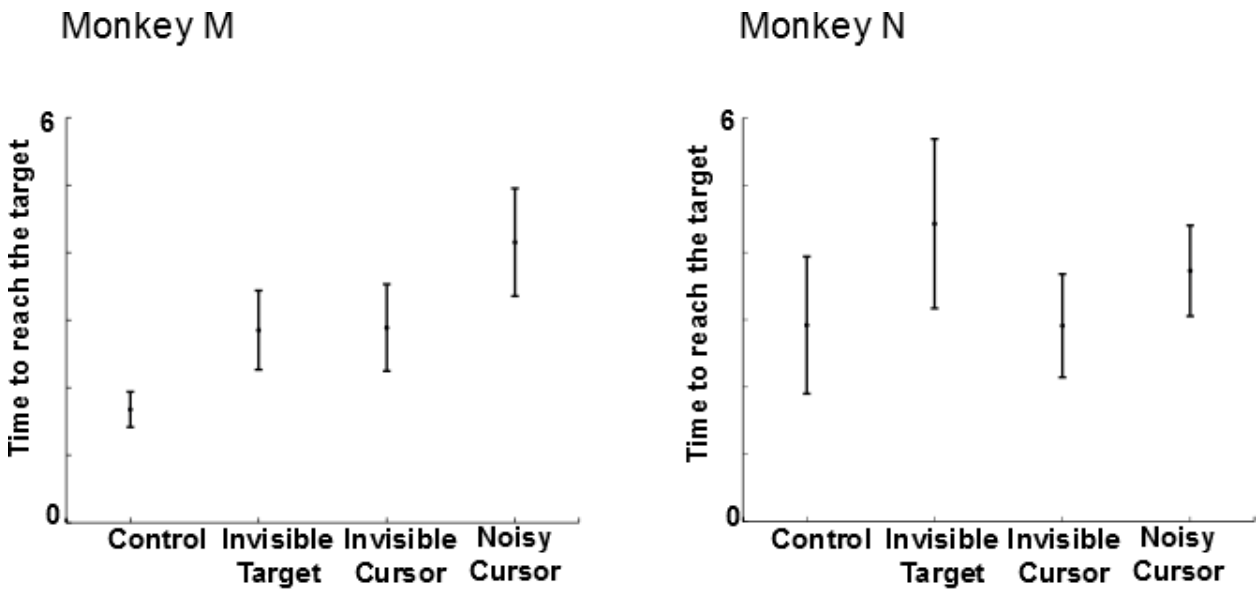

Figure 3.6. Average time to reach the target from the start of the trial under different paradigms for both monkeys.

Table 3.1 Behavioral parameters of both subjects under different experimental paradigms.

		Visually Guided	Invisible Target	Invisible Cursor	Noisy Cursor
Number of Target touch ± s.t.d.	Monkey M	1.06 ± 0.27	2.32 ± 1.71	2.04 ± 1.30	4.15 ± 4.40
	Monkey N	1.50 ± 0.88	1.72 ± 1.21	2.40 ± 2.29	2.55 ± 2.22

Number of Cursor direction change ± s.t.d.	Monkey M Monkey N	1.05 ± 0.62 1.98 ± 1.34	2.79 ± 2.35 3.09 ± 2.26	2.06 ± 1.76 2.91 ± 2.91	6.08 ± 5.4 4.20 ± 3.03
Cursor trajectory length (cm) ± s.t.d.	Monkey M Monkey N	9.67 ± 2.09 18.12 ± 9.96	54.19 ± 12.60 39.22 ± 2.55	31.99 ± 8.08 33.14 ± 1.58	147.00 ± 41.98 85.06 ± 3.96
Average initial velocity peak (cm/s) ± s.t.d.	Monkey M Monkey N	1.97 ± 0.12 2.58 ± 0.18	4.15 ± 0.40 2.05 ± 0.14	3.39 ± 0.27 2.20 ± 0.13	4.71 ± 0.23 3.44 ± 0.73
Time to movement initiation (s)	Monkey M Monkey N	0.28 ± 0.01 0.49 ± 0.01	0.19 ± 0.04 0.43 ± 0.06	0.26 ± 0.05 0.27 ± 0.04	0.34 ± 0.11 0.41 ± 0.03

3.3.2. Neuronal ensemble responses in absence of visual feedback

3.3.2.1. Visually Guided paradigm

PETHs aligned on peak velocity revealed clear modulation patterns in cortical neurons during the visually guided task for both monkey M (figure 3.7) and monkey N (figure 3.8). In monkey M, M1 and S1 neurons had similar modulation patterns, but M1

modulations led those in S1 for both leftward and rightward directions of movements (Table 3.2) as was evident from the analysis of the difference of maximum firing time. In monkey N, M1 and S1 had different firing patterns. While the majority of M1 neurons modulated, S1 neurons didn't modulate significantly and those S1 neurons that did modulate were asynchronous with each other. Thus the difference between M1 and S1 maximum peak time was not significant for movements to both leftward and rightward directions of movements.

3.3.2.2. Invisible Target paradigm

PETHs constructed for the invisible target task and aligned on peak were clearly different from similar PETHs for the visually guided task (Figures 3.7 and 3.8). For monkey M, both M1 and S1 neurons modulated simultaneously as there was no significant difference in their maximum peak firing time for both leftward and rightward directions of movements (Table 3.2). The overall peak of velocity was higher than in the Visually Guided sessions (Table 3.1.) and the activity before and after the velocity peak was variable. For monkey N, there was more dispersion in timing of their peak firing rate (more in the leftward movement) and there was no significant difference between M1 and S1 maximum firing peak timing. There was an overall decrease of peak velocity compared to the Visually Guided sessions (Table 3.1).

3.3.2.3. Invisible Cursor paradigm

PETHs constructed for the Invisible Cursor task and aligned on peak were different from the Invisible Target paradigm but comparable to the Visually Guided paradigm except that there was a slight increase activity of S1 before reaching their peak firing rate. For monkey M, modulations of M1 and S1 cells were synchronous thus no significant difference in maximum firing peak timing (table 3.2.) for both leftward and rightward movements. The activity after the velocity peak was much less variable than the Invisible Target sessions as was the variability of position traces. The velocity peak was comparable to the Invisible Target sessions (Table 3.2). For monkey N, there was a significant difference of maximum firing peak timing for M1 and S1 (Table 3.2), S1 maximum peak activity preceded M1 activity. The peak of velocity was comparable to the Invisible Target sessions (Table 3.1)

3.3.2.4. Invisible Cursor with bias (Noisy Cursor) paradigm

PETHs constructed for the Noisy Cursor task and aligned on peak were different from the other paradigms. For both monkeys M1 cells modulated synchronously. For monkey M, S1 cells modulated synchronously while for monkey N S1 cells had more dispersion in timing of their peak firing rate. The criteria used for only analyzing velocity peaks <10 cm/s resulted in selection of <20% of total number of regular trials per session. For both monkeys, the maximum firing peak activity of S1 preceded M1 in a

statistically significant manner for both leftward and rightward movements. For both monkeys, there was an increase of velocity peak (Table 3.1) and an increased activity post velocity peak (Figure 3.8).

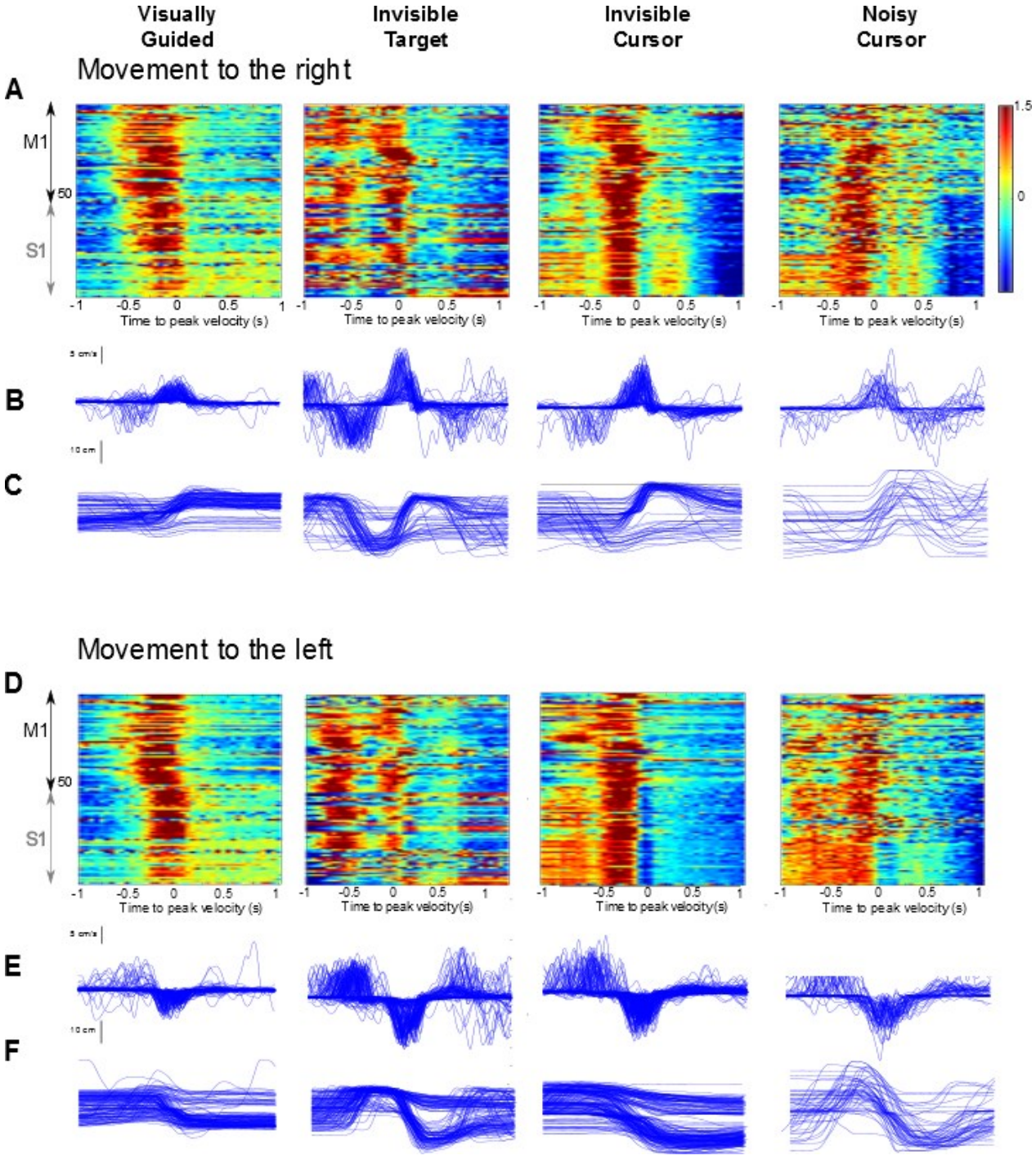
Visually Guided
Invisible Target
Invisible Cursor
Noisy Cursor
Movement to the right
A
M1
50
S1
1.5
0
-1 -0.5 0 0.5 1
Time to peak velocity (s)
B
5 cm/s
10 cm
C
Movement to the left
D
M1
50
S1
Time to peak velocity(s)
E
F

Figure 3.7. Population response of monkey M under different experimental paradigms. A. Averaged PETHs for M1 and S1 neurons aligned to the peak of velocity for each trial when the joystick movement was to the right. B. Overlayed velocity traces of each trial when the joystick movement was to the right. C. Overlayed joystick position traces of each trial when the joystick movement was to the right. D. Averaged PETHs for M1 and S1 neurons aligned to the peak of velocity for each trial when the joystick movement was to the left. E. Overlayed velocity traces of each trial when the joystick movement was to the left. F. Overlayed joystick position traces of each trial when the joystick movement was to the left.

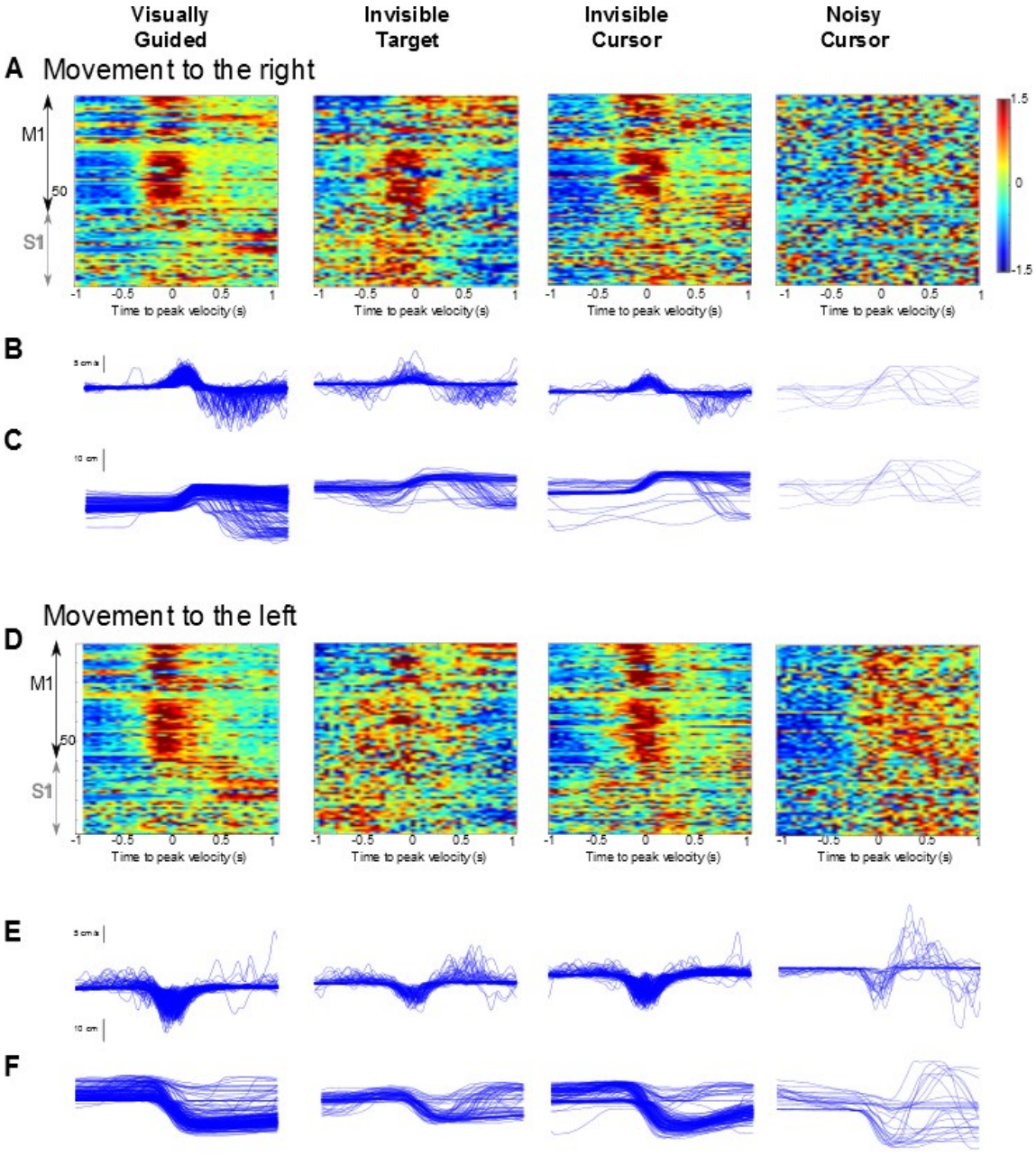
Visually Guided
Invisible Target
Invisible Cursor
Noisy Cursor
A Movement to the right
M1
50
S1
Time to peak velocity (s)
1.5
0
-1.5
B
C
Movement to the left
D
E
F

Figure 3.8. Population response of monkey N under different experimental paradigms. A. Averaged PETHs for M1 and S1 neurons aligned to the peak of velocity for each trial when the joystick movement was to the right. B. Overlayed velocity traces of each trial when the joystick movement was to the right. C. Overlayed joystick position traces of each trial when the joystick movement was to the right. D. Averaged PETHs for M1 and S1 neurons aligned to the peak of velocity for each trial when the joystick movement was to the left. E. Overlayed velocity traces of each trial when the joystick movement was to the left. F. Overlayed joystick position traces of each trial when the joystick movement was to the left.

The effect of ICMS on the normalized firing rate of the neuronal ensemble was analyzed (figure 3.9). During regular trials where ICMS was applied during the hold time (0.8-1.2 s), the normalized firing rate of the cells appear to be inhibitory by decreasing the firing rate compared to the rate during the reward period (figure 3.9A). However in a minority of cells, the effect seems excitatory. It is not clear the effect of ICMS on the cells during ICMS thus there was no analysis performed on data contained during ICMS.

As expected, during catch trials when ICMS was not applied, there was no significant difference during the hold period and the reward period (figure 3.9B).

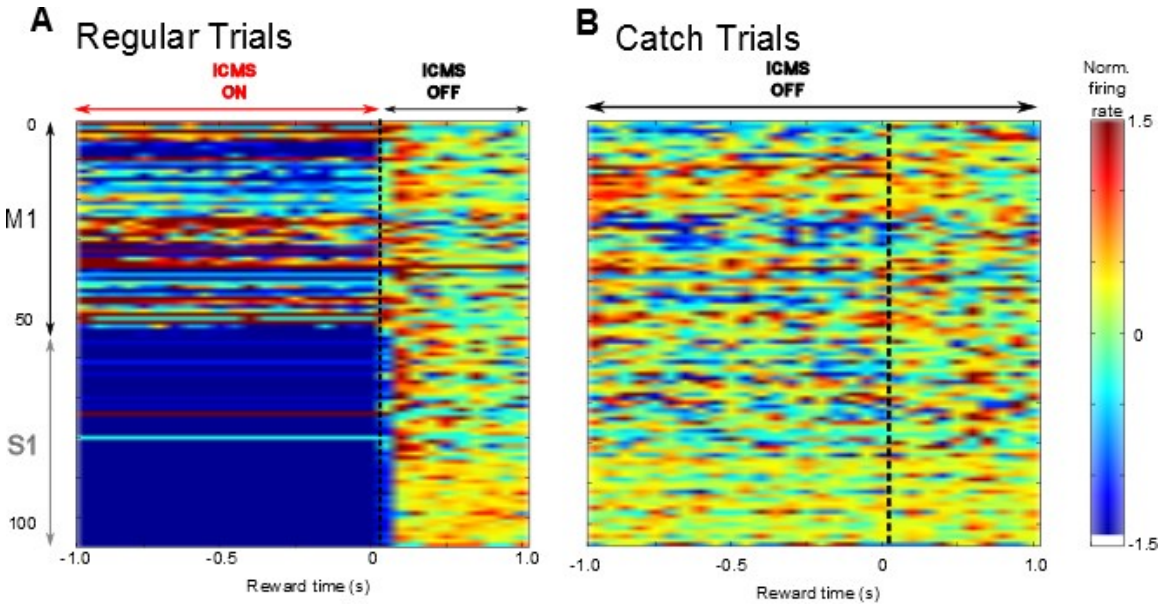

Figure 3.9. Population response to regular trials and catch trials. A. Averaged PETHs for M1 and S1 neurons aligned to the reward time for regular trials within a session. B. Averaged PETHs for M1 and S1 neurons aligned to the reward time for each catch trials within a session.

Additional PETH analysis was performed. The normalization of firing rate was performed by subtracting the average binned firing rate of each cell from the start of the trial to the peak velocity (1s) to each bin and then dividing by the standard deviation of the same period from the start of the trial to the peak velocity. This analysis revealed no significant difference (figure 3.10) between using the period of 1s before and 1s after peak velocity as the average and standard deviation of normalization as performed for figures 3.7 and 3.8.

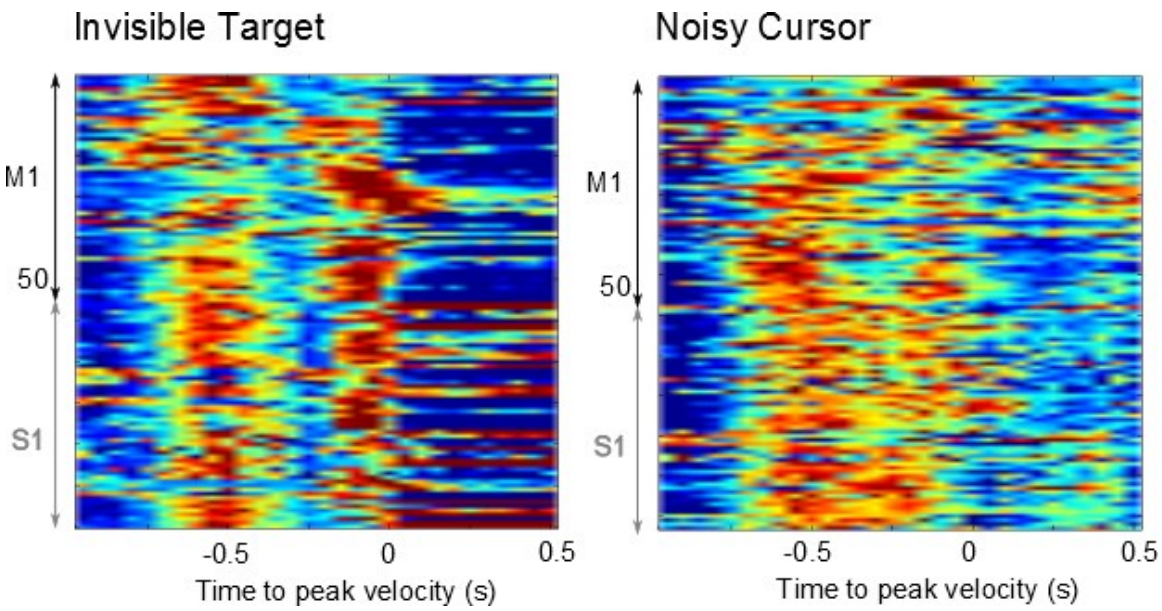

Figure 3.10. Averaged PETHs for M1 and S1 neurons aligned to the peak of velocity for each trial when the joystick movement was to the right with different normalization procedure for monkey M under two different paradigms. Same color scale as figures 3.7-3.9.

Table 3.2. Maximum peak detection for M1 and S1 cells (mean ± s.t.d. in ms). The time was centered at the peak of velocity as in figures 3.8 and 3.9.

	Monkey M		Monkey N	
	M1	S1	M1	S1
Visually Guided (R)	-468 ± 32 *	-364 ± 54	-192 ± 29	-219 ± 45
Visually Guided (L)	-441 ± 38 *	-299 ± 39	-190 ± 16	-218 ± 57
Invisible Target (R)	-526 ± 74	-547 ± 177	-234 ± 16	-230 ± 18
Invisible Target (L)	-509 ±113	-537 ± 64	-253 ± 74	265 ± 54
Invisible Cursor (R)	-461 ± 78	-429 ± 50	-190 ± 24 *	-220 ± 21
Invisible Cursor (L)	-510 ± 89	-670 ± 173	-180 ± 5 *	-281 ± 26
Noisy Cursor (R)	-386 ± 120 *	-449 ± 140	-168 ± 70 *	-248 ± 33
Noisy Cursor (L)	-461 ± 93 *	-499 ± 104	-197 ± 63 *	-253 ± 74

3.3.3. Individual neuronal responses in the absence of visual feedback

To compare the pattern of individual neurons across different sessions and experimental paradigms, stable neurons were analyzed. Stable neurons were determined as neurons that did not have significantly different intertrial spike interval (ISI) during the reward period from session to session (figure 3.9).

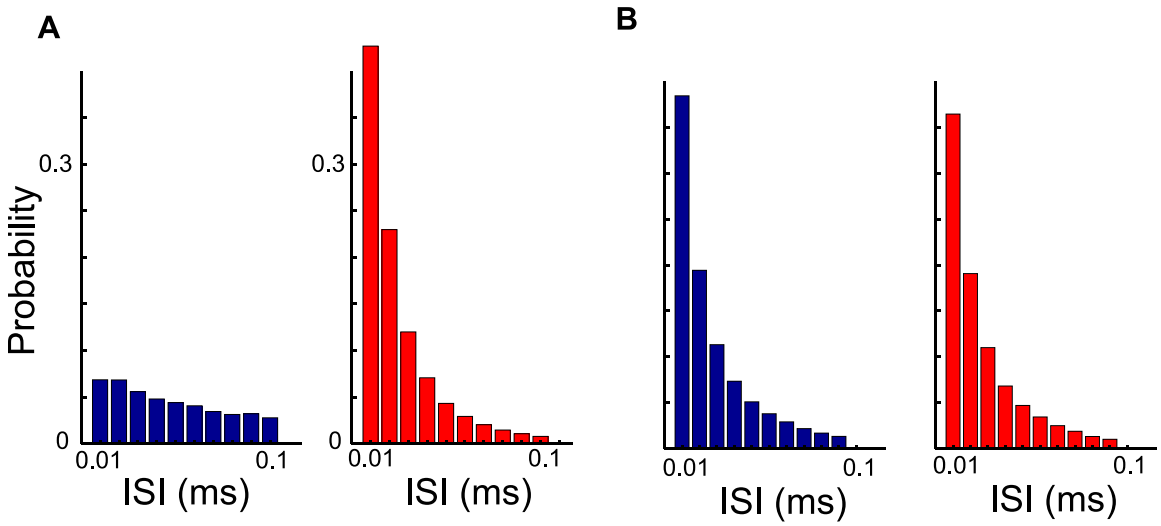

Figure 3.11. Example of probability distribution of ISI in neurons. A. Example of a neuron considered unstable (p<0.05 Kolmogorov-Smirnov test). B. A. Example of a neuron considered stable (p>0.05 Kolmogorov-Smirnov test).

Decreased visual feedback of target and cursor affected the neuronal firing (Figures 3.10-3.12). The firing rate of cells modulated to different ranges of position and velocity under different paradigms. To illustrate this result, represented cells (two from monkey M, figure 3.10 and two from monkey N, figure 3.11) are presented.

Under the Visually Guided paradigm where both the target and the cursor were visible, Cell 1 (figure 3.10 A) was strongly tuned to velocity of both directions. Under Invisible Target paradigm, strong velocity tuning still remained but the range of velocity for which the cell modulated its firing rate increased. Under the Invisible Cursor paradigm, the cell also had strong tuning to velocity but the range of both position and velocity were not significantly different from the Visually Guided paradigm.

The most dramatic change of tuning occurred under the Noisy Cursor paradigm. Tuning to velocity was strong and the range of velocity and position to which the cell modulated was much wider compared to the other paradigms. This trend can observed in the 3D tuning model (Figure 3.10 B) as the model curvature to velocity significantly decreased from the Visually Guided paradigm to Noisy Cursor paradigm. Tuning to position did not change significantly despite the increased range of cell modulation to position.

Cell 2 of Figure 3.10 also had a significant change of tuning to both velocity and position. Under the Visually Guided paradigm the cell was tuned to both directions of velocity and positions. Under the Invisible Target paradigm, the cell was mostly tuned to the positive direction of velocity. In addition the range of velocity for which the cell modulated its firing rate also increased. Under Invisible Cursor paradigm the strong tuning to the positive direction of velocity remained while the range of velocity for which the cell modulated its firing rate was more comparable to the Visually Guided tuning. As in Cell 1, under the Noisy Cursor paradigm, the range of velocity and position for which the cell modulated its firing rate increased significantly compared to other paradigms. The cell was strongly tuned to velocity in the positive direction only.

Cells of monkey N also had change of tuning under different experimental conditions. Cell 1 of figure 3.11 was tuned to both directions of velocity under the

Visually Guided paradigm. Under the Invisible Target paradigm there was no clear tuning to either position but there was a slight tuning to velocity. In addition, the range of position to which the cell modulated its firing rate was decreased. Under the Invisible Cursor there was clear tuning to velocity. Under the Noisy Cursor paradigm, as the cells of figure 3.11, the range of velocity and position for which the cell modulated its firing rate increased significantly. Tuning to velocity also remained strong.

Cell 2 of figure 3.11 showed a strong tuning to velocity and position under the Visually Guided paradigm. Under the Invisible Target paradigm the cell was slightly tuned to velocity while the range of position for which the cell modulated its firing rate. Under the Invisible Cursor paradigm, the cell also had a slight tuning to velocity while the range of position and velocity for which the cell fired remained comparable to the Invisible Target paradigm. Under the Noisy Cursor paradigm, as in previous cells, the range of velocity and position for which the cell modulated its firing rate increased. Tuning to velocity became strong to both directions of velocity but not for position.

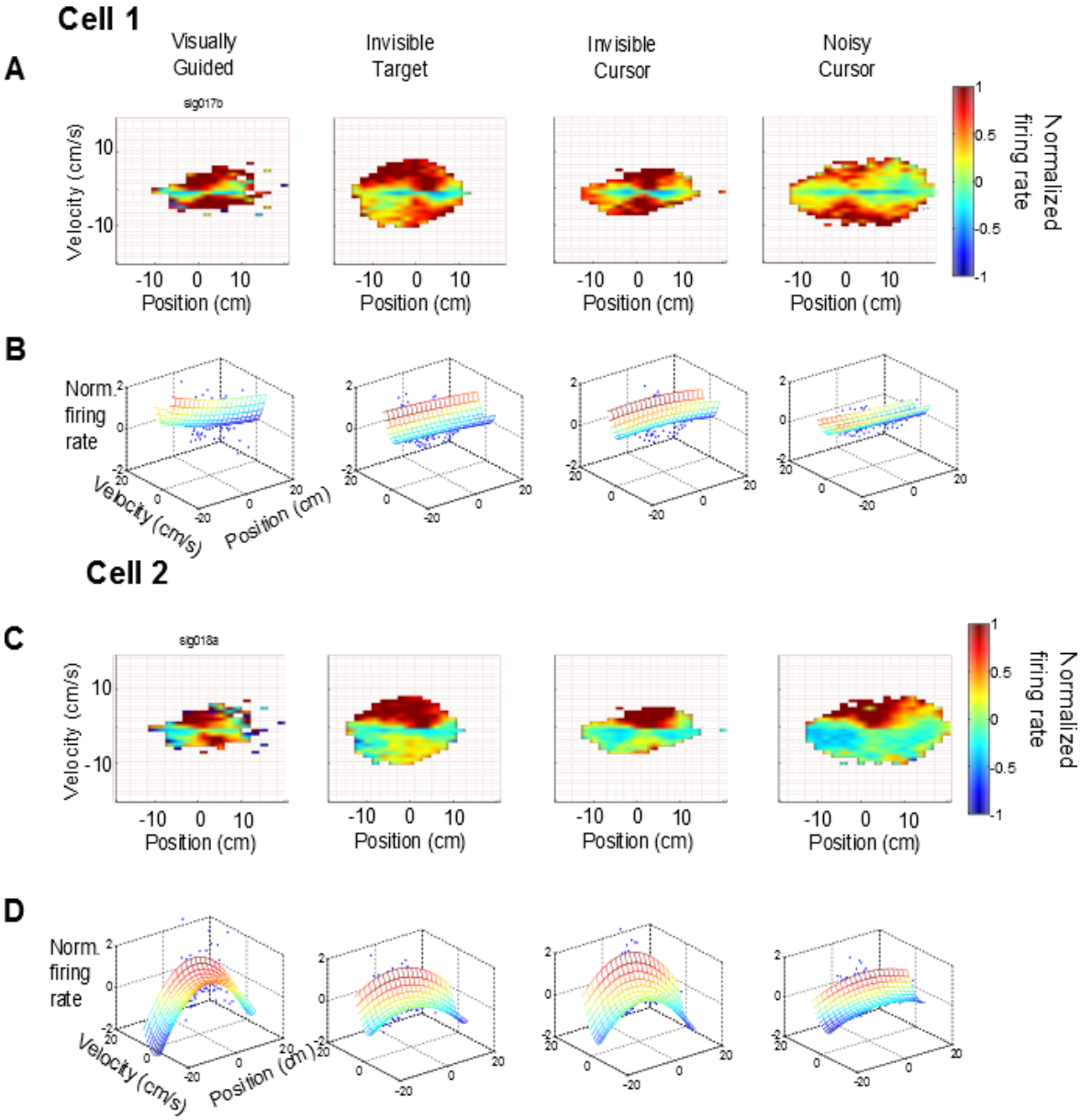

Figure 3.12. Individual cell tuning to velocity and position in monkey M. A. This cell exhibits different tuning width and intensity to both directions of velocity under different experimental paradigms. B. A regression 3D model fitted to match the data from A. C. This cell exhibits different tuning width and intensity to positive velocity under different experimental paradigms. D. A regression 3D model fitted to match the data from C.

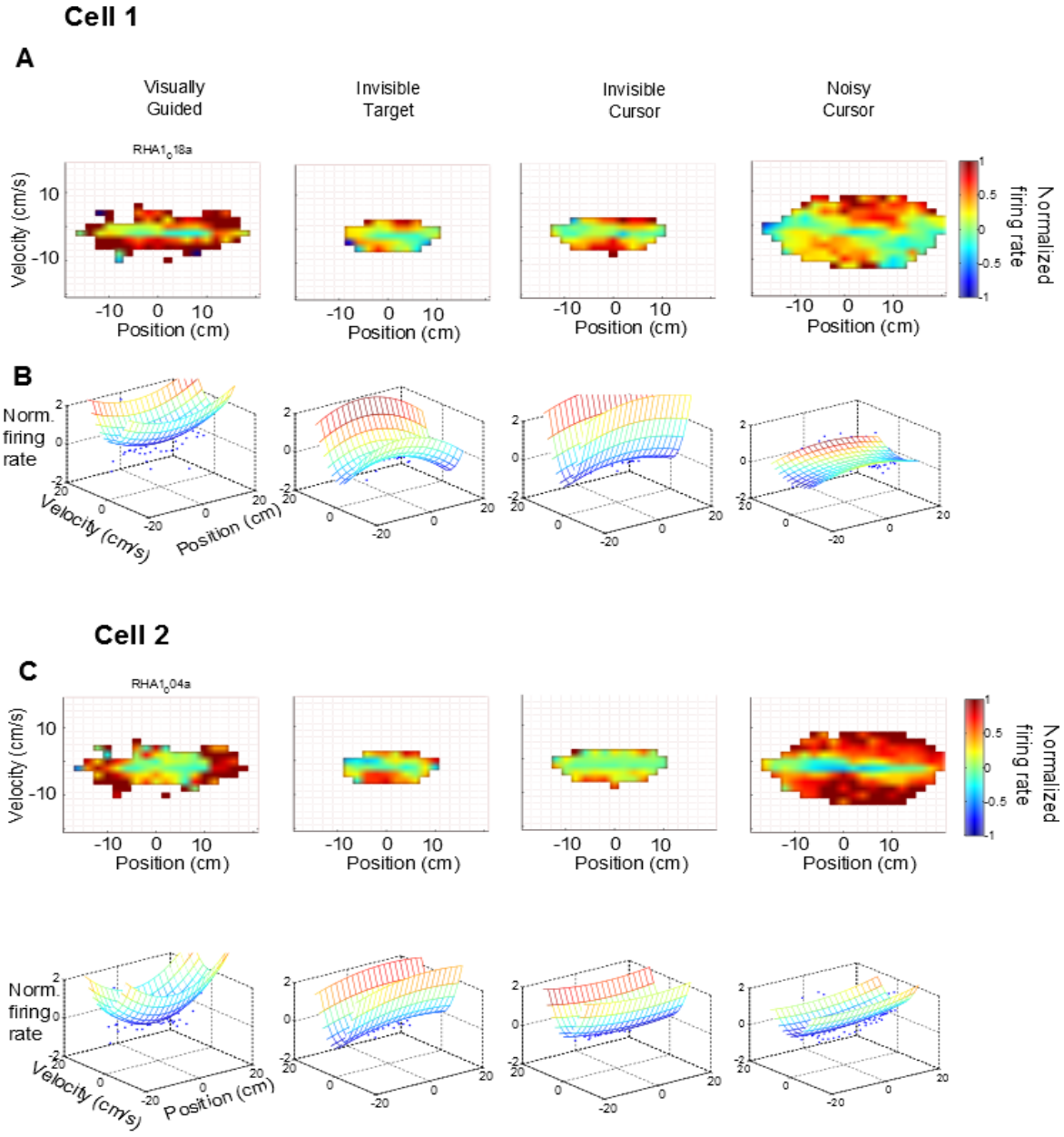

Figure 3.13. Individual cell tuning to velocity and position in monkey N. A. This cell exhibits different tuning width and intensity to velocity under different experimental paradigms. B. A regression 3D model fitted to match the data from A. C. This cell exhibits different tuning width and intensity to positive velocity under different experimental paradigms. D. A regression 3D model fitted to match the data from C.

The change of tuning for velocity and position was further examined by aligning the normalized firing rate of each neuron to velocity and position for both monkeys (figure 3.12). There was a clear increase in the range of velocity for which cells modulated their firing rates from Visually Guided paradigm to Noisy Cursor paradigm while the normalized firing rates remain comparable for both monkeys. The ranges of velocity under Visually Guided paradigm were -4 to 8 cm/s for monkey M and -6 to 6 cm/s for monkey M. The ranges under Noisy Cursor were -12 to 16 cm/s for both monkeys. When the normalized firing rate was aligned with position, the range for which the cells modulated their firing rates remained stable but the maximum and minimum velocities under Visually Guided, Invisible Target, and Invisible Cursor greatly decreased under Noisy Cursor paradigm for both monkeys.

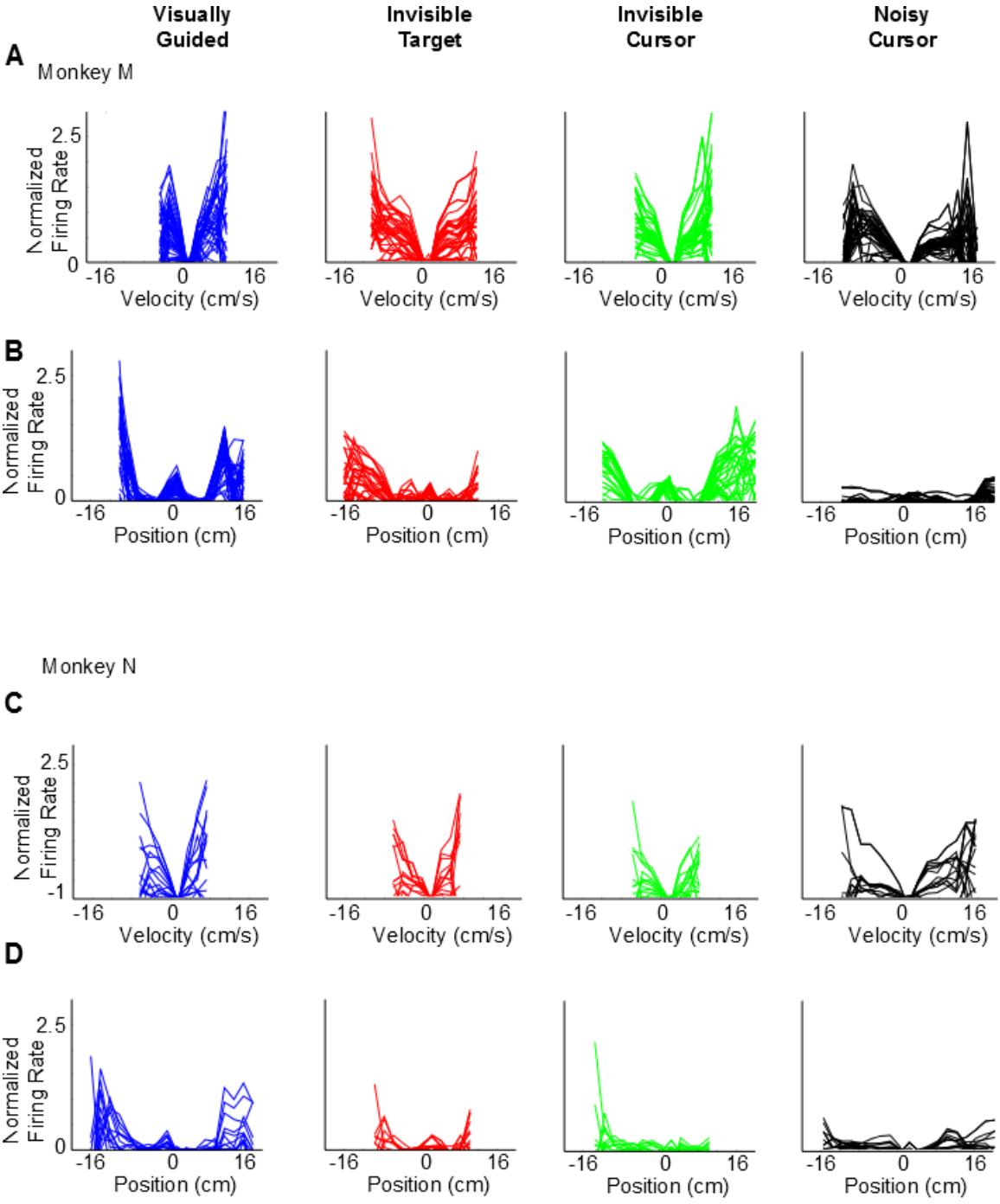
Visually Guided
Invisible Target
Invisible Cursor
Noisy Cursor
A
Monkey M
Normalized Firing Rate
2.5
0
-16
0
16
Velocity (cm/s)
B
Position (cm)
Monkey N
C
-1
D

Figure 3.15. Cell tuning to velocity and position under different experimental paradigms. A. Overlayed cell tuning to velocity in monkey M. Each trace represents one cell. The tuning width widens significantly in noisy cursor paradigm compared to visually guided. B. Overlayed cell tuning to position in monkey M. C. Overlayed cell tuning to velocity in monkey N. Each trace represents one cell. The tuning width widens significantly in noisy cursor paradigm compared to visually guided. D. Overlayed cell tuning to position in monkey N.

3.4. Discussion

Here we show for the first time that ICMS can be used to detect a target. These results compliment previous results of using ICMS to provide sensorized neuroprosthetics (London, Jordan et al. 2008, O'Doherty, Lebedev et al. 2011, Venkatraman and Carmena 2011, Weber, London et al. 2011, O'Doherty, Lebedev et al. 2012). This is a step closer to providing sensory feedback that can aid reaching movements for those suffering of diminished or lack of somatosensory feedback and alleviate phantom limb pain caused by somatosensory cortical reorganization as described in chapter 1.

3.4.1. ICMS as artificial texture

Active sensing has been a recent area of interest in the BMI field. Recent studies showed that active tactile exploration of virtual objects was possible in monkeys using ICMS of different frequencies to code for different identical-looking virtual objects and the monkeys are able to discriminate the correct virtual "texture" (O'Doherty, Lebedev et al. 2011, O'Doherty, Lebedev et al. 2012). Venkatraman and Carmena (Venkatraman and Carmena 2011) also showed that rats could use their whiskers to detect a software-defined target indicated by ICMS although not necessarily by active searching but by high frequency of whisker movement.

3.4.2. Reaching for an invisible target

The Invisible Target paradigm forces the monkeys perform an exploratory movement rather than a goal-directed movement since the end-point is not visible. If the target location is provided via visual feedback, then the information is first processed in the retina and there is a visuomotor transformation and the target is described in a retinotopic coordinates, while when the location of the target is provided purely by somatosensory feedback then the position of the target might be trunk-referenced (Neggers and Bekkering 1999). The view of planning for movement based on the visual feedback of the target does not apply here but it is possible that the monkeys had a plan on how to perform an exploratory movement.

These ideas explain the different behavior under this paradigm compared to the Visually Guided paradigm when visual feedback of the target and cursor were provided. This task proved more difficult than the Visually Guided given the increased number of target touches, direction changes, and cursor trajectory length (Table 3.1). The increase of these variables were consistent with other tactile exploration strategy without visual feedback in which human subjects performed several back and forth right-left sweeping movements (Smith, Gosselin et al. 2002). However the time to movement initiation is less than in the Visually Guided paradigm possibly correlated to less planning of movement given the lack of visual feedback of the target. It is

conceivable that monkey M interpreted the appearance of the target as the go-signal in the Visually Guided task but in this paradigm the target was always invisible thus there was no particular cue to when to start the trial which led to the exploration behavior of starting the movement at the beginning of the trial.

The size of the target has an impact on the trial duration again in accordance to human active tactile exploration task in which the time to find small target was significantly greater (Smith, Gosselin et al. 2002). In human experiments, higher force and slower speed are used when searching for smaller targets (Fitts 1954, Ifft, Lebedev et al. 2011) although this relationship was observed only in experiments with visual targets.

3.4.3. Reaching with an invisible cursor and invisible cursor with bias

During a reaching movement, subjects make a plan according to the location of the desired end point, e.g. a target, and the initial position of the arm by integrating visual and proprioceptive feedback from the body (Sober and Sabes 2003).

A study has suggested that cursor feedback is more important than the target location to the visual representations within M1 especially when constant feedback is required for movement (Eisenberg, Shmuelof et al. 2011). They reasoned that in their reaching task in which human subjects were required to perform a center-out task with and without a 45 degree rotation of the cursor while the activity of M1 was monitored

through fMRI M1 activity had a visual component that was not present in other studies which contained a visual target. The results of that study agrees with the results from the Noisy Cursor task in which more target touches, cursor direction changes and cursor trajectory length (Table 3.1) were needed to complete the Noisy Cursor paradigm compared to the Invisible Target paradigm.

The high percentage of correct catch trials under the Invisible Cursor paradigm by monkey M could be due the strategy of relying on its well learned sense of joystick movement and cursor position which enabled it to estimate the approximate position of the invisible cursor. This strategy did not work under the Noisy Cursor task in which the mapping of joystick position to cursor position was altered at every single trial. Trained monkeys that received surgical deafferentiation of the limb can still perform the trained task of reaching to a target with just the visual feedback of target position even without visual feedback of the position of their arm but when their posture was changed by moving the shoulder and elbow, the deafferented monkeys could not perform the task (Polit and Bizzi 1979). Deafferented monkeys also took longer time to reach the target (Taub, Goldberg et al. 1975). The results from the deafferented monkeys support our results of monkeys able to perform simple invisible end-effector tasks (Invisible Cursor) but when the task is slightly changed (Noisy Cursor) they have difficulty performing unless guided by an additional feedback such as ICMS.

3.4.4. Neuronal: ensemble

Given that the motor cortex changes behavior when visual information is modified (Eisenberg, Shmuelof et al. 2011) coupled with movement and it shows no response when the feedback is visual only it can be expected that when visual feedback of the target or the cursor disappear the pattern of neurons firing could be affected.

When the target or the cursor becomes invisible, the cell changes its strategy and maybe optimize whether change in velocity or position is more important.

It can hypothesized that the increased activity before movement onset in control of the neuronal ensemble is because when the target or the cursor are visible, the brain forms a plan to reach but when the target and the cursor are invisible the brain has to explore and search for the target, thus no clear initial plan of movement is formed.

The timing of maximum peak of firing rate of S1 occurs before the timing of maximum peak of firing rate of M1 under the Noisy Cursor paradigm (Table 3.2) could be that during exploratory movement, movement planning is first dependent on sensory feedback. This is a different type of movement from visually cued experiments in which M1 neurons increase activity 60-80 ms before S1 neurons activity (Evarts 1972).

3.4.5. Neuronal: single neuron

M1 cells represent multiple parameters such as muscles and movements (Kakei, Hoffman et al. 1999) and usually they represent the most relevant parameter during a particular task. Furthermore, M1 controls the muscle, direction of movement in space, and the direction of movement at the joints (Kakei, Hoffman et al. 1999) and are tuned to hand position, speed, direction of motion, and force (Paninski, Fellows et al. 2004) and individual cortical neurons can encode more than one of these parameters (Ashe and Georgopoulos 1994, Sergio and Kalaska 1998, Carmena, Lebedev et al. 2003). Another subset is known to have limb-dependent preparatory activity by increasing activity before a flexion or extension regardless of the direction of the target (Alexander and Crutcher 1990, Shen and Alexander 1997) and complex neurons that respond to both. Tuning properties of neurons in M1 can change when perturbations are applied during reaching movements (Gandolfo, Li et al. 2000) or learning new visually guided movements (Paz, Boraud et al. 2003). The plasticity and tuning of cells have shown to change during BMI learning and control (Carmena, Lebedev et al. 2003, Lebedev, Carmena et al. 2005, Jarosiewicz, Chase et al. 2008, Koralek, Jin et al. 2012).

In this chapter it is shown for the first time that M1 and S1 cells can also modulate the range of velocity for which they modulate their firing rate (Figure 3.12). This result suggests that the brain controls neuronal modulation. Each neuron has a

fixed firing modulation range and this range is modified to represent an important parameter, in this case, velocity, and the cell optimizes the firing modulation range to match the task. Other studies have shown that M1 neurons can be tuned to velocity and position or either and that velocity tuning can be temporary during pursuit task (Paninski, Fellows et al. 2004) and that M1 cells can be tuning to position only, velocity only, to both position and velocity, as well as to neither (Wang, Chan et al. 2007)showing the adaptability of M1 neurons.

Moran and Schwartz (Moran and Schwartz 1999) reported that both speed and movement are continuously changing during reaching in a center-out task. Speed profiles for movements to the different targets were similar across targets although there was some variety within profiles reaching the same targets. Furthermore they found that the firing rate of the neurons increase with increase of speed to any direction but the amount of change is dependent of direction. Our result is due to the exploratory movement of our tasks thus even at different velocities the firing rate of the cells remain comparable.

The results shown in this chapter demonstrate once again that cortical cells in particular M1 cells are very plastic to different parameters and provide evidence for optimal feedback control theory which describes the motor system as a stochastic

feedback controller that optimizes only those motor parameters that are necessary to achieve task goals (Lebedev, Carmena et al. 2005).

4. Decoding of movement parameters under different visual feedback conditions

4.1. Introduction

It has been more than ten years since the first BMI paper was published (Chapin, Moxon et al. 1999). Since then there has been many seminal BMI studies and there has been an interest in characterizing the neuronal behavior during BMI experiments. Most experiments report results from one experimental paradigm such as center out tasks or pursuit tasks. However as technical advances in the field are achieved as well as for clinical purposes it is necessary to learn how the neural ensemble behaves under several different conditions. The purpose of this chapter was to investigate the behavior of the neuronal ensemble and single neurons under four different experimental paradigms.

BMI implant and recording techniques have improved dramatically by increasing the number of neurons to be recorded and by maintaining signal stability for longer periods, hopefully lasting a life-time. As the recording techniques and electrode designs have improved, so have the life of implants since one group has reported recording for seven years (Krüger, Caruana et al. 2010) and our lab has shown that signal quality in owl monkeys can easily remain stable for over five years (Fitzsimmons 2009) and the subjects used for this dissertation have been implanted since 2009 and even currently they possess stable and reliable quality of cell recording. Given the longevity of implants in animal experimental subjects it is not unexpected for these

subjects to perform different kinds of experiments thus decreasing the number of animals needed to perform experimental tasks. Candidates for BMI implants will use variety of movements related to everyday life not just restricted currently found in BMI experiments. Thus as BMI research is advanced, more complex movement pattern and operations as well as the neuronal changes related to these paradigms should be studied.

4.2. Methods

4.2.1. Wiener Filter

To characterize the relationship between firing of individual neurons and their populations with movements, we used a linear decoding algorithm Wiener Filter; (Haykin 2005). The decoding for an individual neuron was represented by the equation:

$$X(t) = b + \sum_{i=1}^{N} w_i n\,[t - (i-1)\tau] + \epsilon(t) \quad (4.1)$$

where *X(t)* is the value of the decoded parameter (e.g., joystick position) at time *t*, *n* is the firing rate of the neuron, N is the number of taps, $(i-1)\tau$ is the time delay for tap *i*, w_i is the weight at time tap *i*, *b* is the y-intercept, and $\epsilon(t)$ is the residual error. The model weights were calculated first by converting equation 4.1 into

$$\mathbf{X} = \mathbf{NW} + \varepsilon \text{ (3)} \quad (4.2)$$

Where **X** is the matrix of kinematics (position), **N** is the matrix of binned firing rate with taps, and ε was the residual error. Then **W** can be solved using ridge regression

$$\mathbf{W} = \left(\mathbf{N}^{\mathrm{T}}\mathbf{N} + \lambda_W \mathbf{I}\right)^{-1}\mathbf{N}^{\mathrm{T}}\mathbf{X} \tag{4.3}$$

where λ_W is the ridge regression parameter and **I** is the identity matrix (Haykin 2005).

The decoding for neuronal populations was represented by the equation:

$$X(t) = b + \sum_{i=1}^{N}\sum_{j=1}^{M} w_{ij} n_i \left[t - (j-1)\tau\right] + \epsilon(t) \tag{4.4}$$

where *X(t)* is the value of the decoded parameter (e.g., joystick position) at time *t*, *n* is the firing rate of the neuron, N is the number of taps, $(i-1)\tau$ is the time delay for tap *i*, w_i is the weight at time tap *i*, *b* is the y-intercept, and $\epsilon(t)$ is the residual error. The model weights were calculated using equations 4.2 and 4.3 (Haykin 2005).

The Wiener filter was trained using 80% of the session data to get the weights for the model and then the remaining 20% was used for analyze our prediction accuracy with five taps and a bin size of 100 ms.

4.2.2. Signal-to-Noise Ratio and Correlation Coefficient

Decoding accuracy was evaluated using two metrics. The signal to noise ratio (SNR) was calculated as:

$$SNR(X, \hat{X}) = 10 \text{ x } log_{10}\frac{var\,(X)}{mse(\hat{X})} \tag{4.5}$$

where X is the actual parameter and $\hat{X}$ is the predicted value of that parameter. *Var* is the variance and *mse* is the mean squared error, that is mean squared difference between the actual and predicted parameter.

The decoding accuracy was also quantified as Pearson's correlation coefficient (CC):

$$\mathrm{CC}\left(\mathrm{X},\widehat{\mathrm{X}}\right) = \frac{\mathrm{cov}\,(\mathrm{X},\widehat{\mathrm{X}})}{\sigma_X \sigma_{\widehat{\mathrm{X}}}} \tag{4.6}$$

where X is the actual data and $\widehat{\mathrm{X}}$ is the predicted data, cov is the covariance, and σ_X is the standard deviation of X and $\sigma_{\widehat{\mathrm{X}}}$ is the standard deviation of $\widehat{\mathrm{X}}$.

4.2.3. Linear Discriminant Analysis

To predict whether a trial was an attention trial or a non-attention trial, linear discriminant analysis (LDA (Fisher 1936) was performed per session. An attention trial was considered as a trial in which the monkey tried to reach the target by moving the joystick and non-attention trial was considered as a trial a monkey was not paying attention to the task and didn't even touch the joystick.

The firing rate of each neuron for 1.5s from the start of the trial was binned in 100 ms bin per trial. Each trial was grouped into attention or non-attention trial. A multivariate normal density was fit for each group so the mean, the variance and the covariance were estimated. Then likelihood ratios using the training data are used to create boundary linear equation

$$k + \overrightarrow{x} * \vec{L} \tag{4.7}$$

where k represents a constant term, $\vec{x}$ represents the observation set and $\vec{L}$ is the weights assigned to each observation.

If equation 4.7 was larger than zero then that observation set was determined to be an attention trial and if equation 4.7 was less than zero then that observation set was determined to be a non-attention trial (figure 4.1). Then the outcome of the classifier was compared to the actual outcome during experiments and their ratio was computed in percentage values. 80% of each type of trials was used for training sets and the reminder was used to verify the accuracy of the classifier.

For single neuron LDA, the training and the sample sets contained only the firing rates of that particular neuron while for ensemble LDA, the training and the sample sets contained the firing rates of all the neurons.

The accuracy of the classifier was cross-validated using the real group of the sample set.

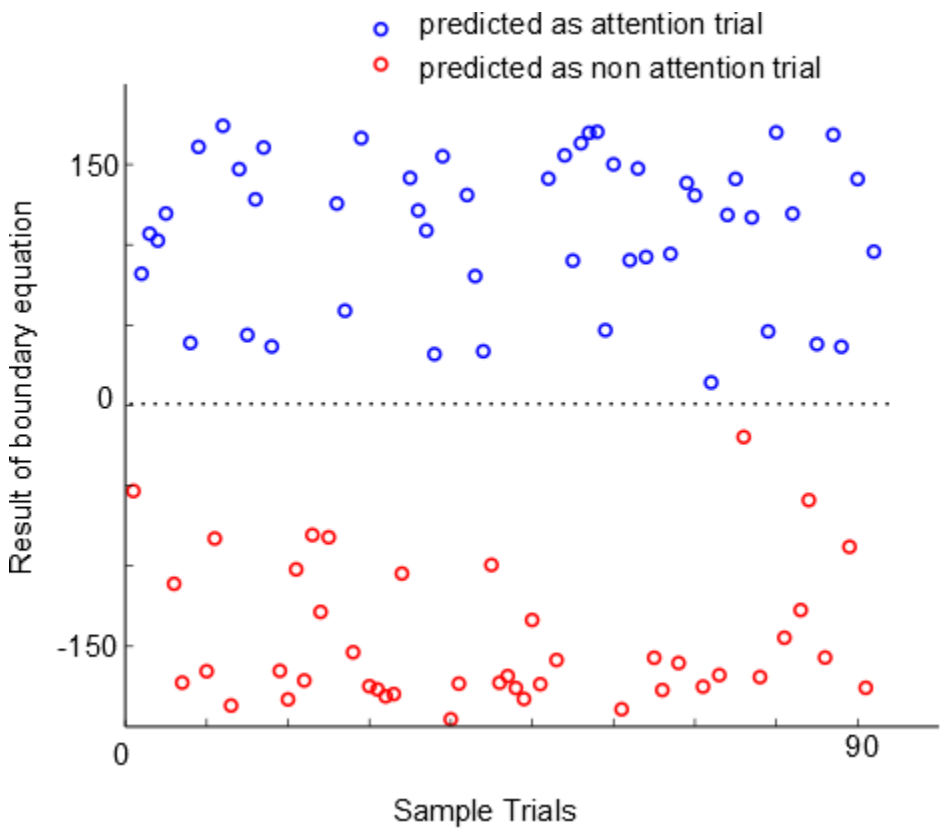

Figure 4.1. Graphical example of trial type decoding using LDA.

4.2.4. Neuron dropping analysis

Based on previous studies (Wessberg, Stambaugh et al. 2000, Carmena, Lebedev et al. 2003), the data from the entire ensemble was used to predict the joystick position. One neuron was randomly removed from the ensemble, then a new prediction was generated. This process was repeated 100 times.

4.3. Results

4.3.1. Correlation of single neuron decoding

We investigated the decoding power of the neuronal ensemble and individual neurons under different conditions. We found that under the same experimental condition, the decoding correlation of each neuron of one session is strongly correlated to the decoding correlation of other sessions (Figures 4.1 and 4.2 top row). However under different experimental conditions, there is almost no correlation (Figures 4.1 and 4.2 row row).

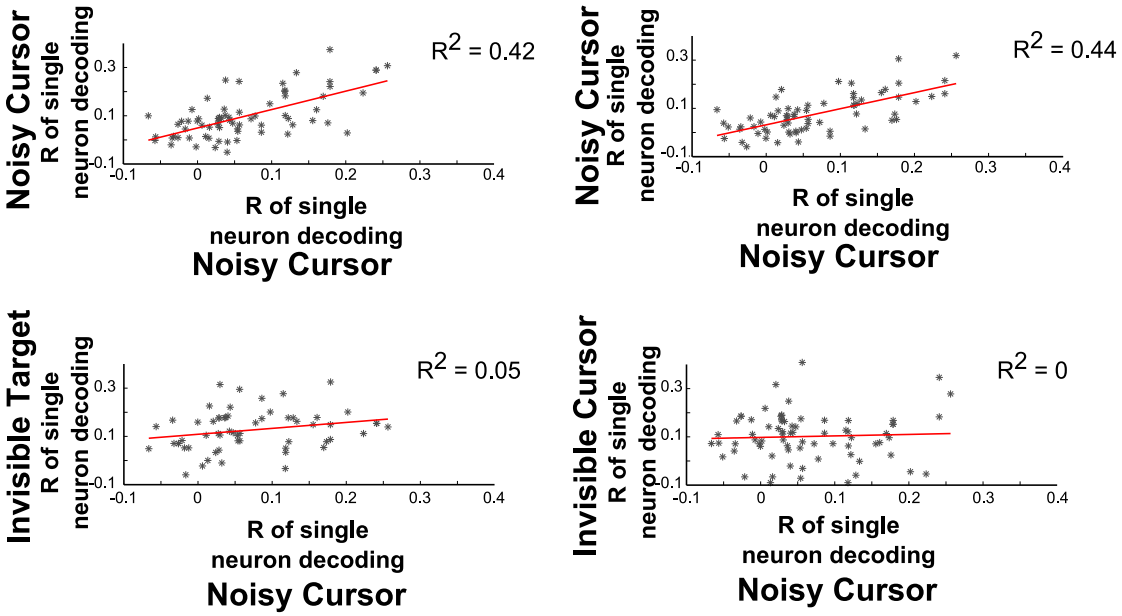

Figure 4.2. Correlation of decoding SNR for joystick position of single neuron under different task conditions.

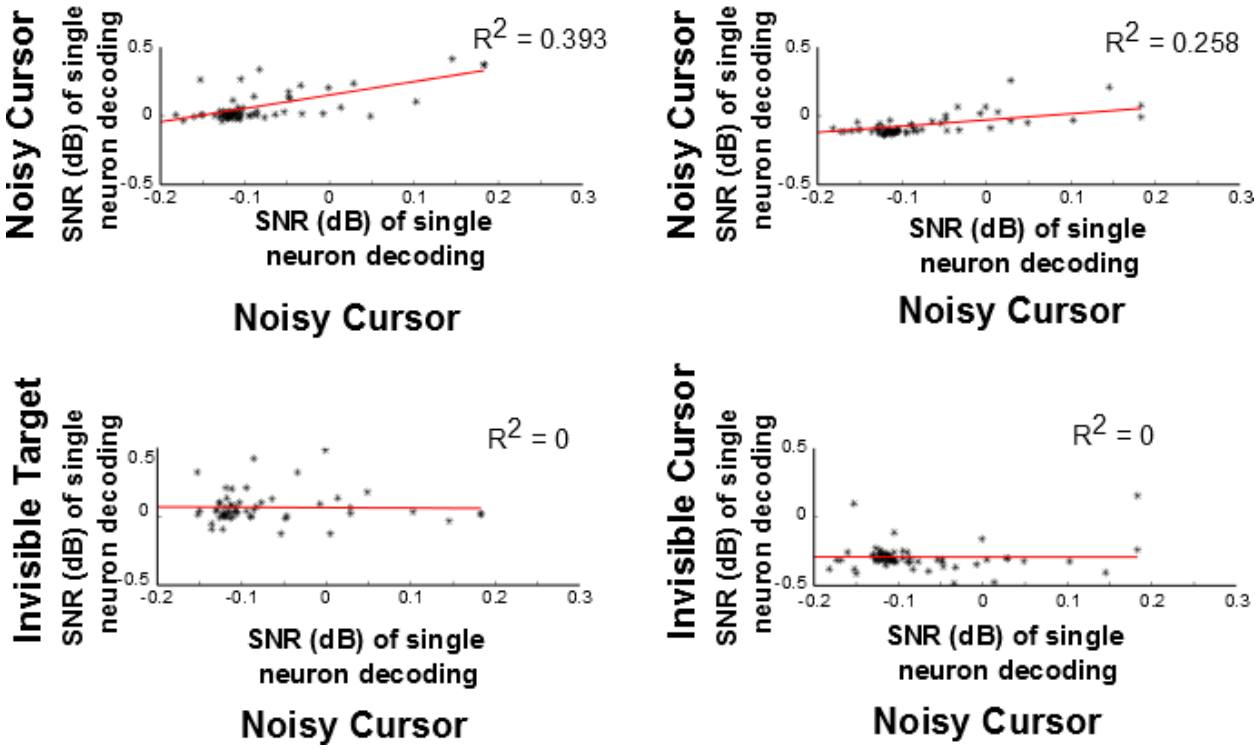

Figure 4.3. Correlation of decoding correlation coefficient (R) for joystick position of single neuron under different task conditions.

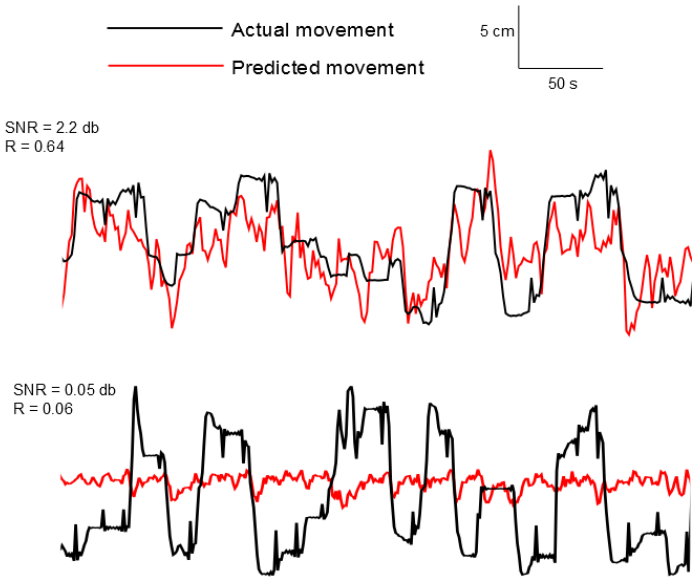

Figure 4.4. Example of decoding performance. The top row is a total ensemble of 81 neurons decoding of position. The bottom row is decoding of position by one neuron.

The decoding capability was much higher for the data for the entire ensemble was used (top row) versus the decoding of one single neuron (bottom row).

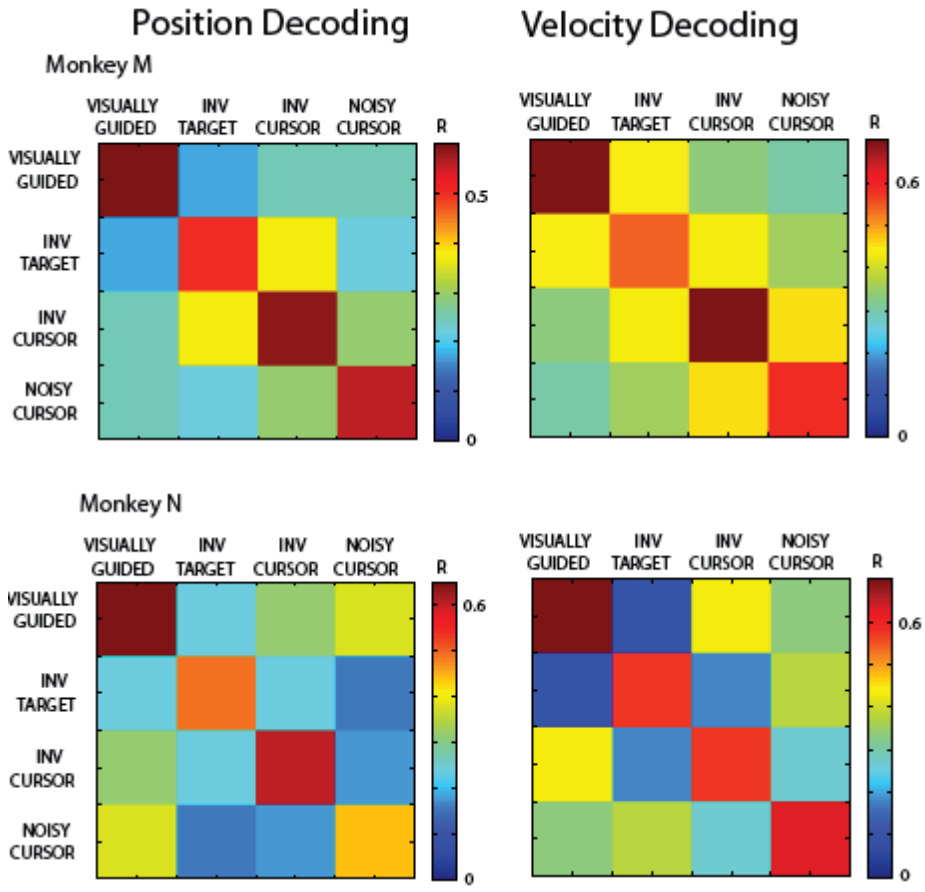

Figure 4.5. Average correlation of the decoding SNRs of single neurons of one session to the decoding SNRs of single neurons of another session.

The correlation of the decoding SNRs of single neurons was the strongest when the sessions of the same paradigm were compared for both monkeys (Figure 4.4). This strong correlation among sessions for decoding was for joystick position and joystick velocity. There is a slight correlation between Invisible Target and Invisible Cursor. This

might be due to the fact that the Invisible Cursor sessions were recorded immediately after the Invisible Target sessions.

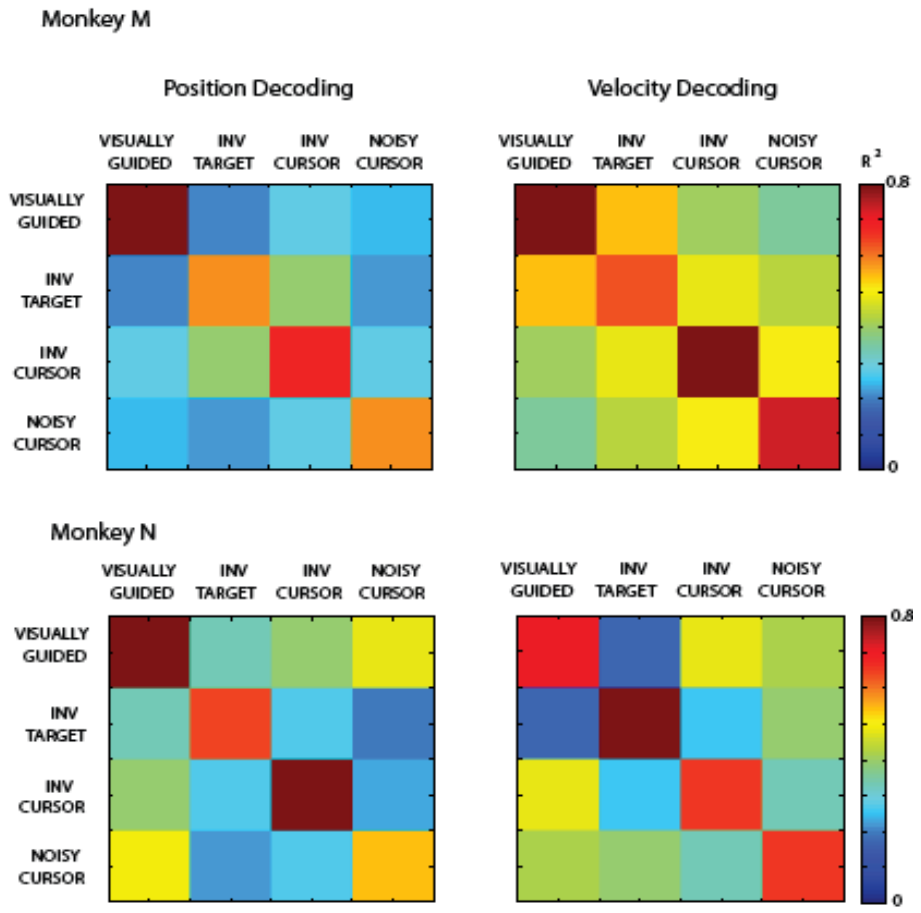

Figure 4.6. Average correlation of the decoding correlation coefficients of single neurons of one session to the decoding correlation coefficients of single neurons of another session.

Similarly, the correlation of the decoding correlation coefficients of single neurons was the strongest when the sessions of the same paradigm were compared for

both monkeys (Figure 4.5). This strong correlation among sessions was for decoding for joystick position and joystick velocity.

The correlation of decoding SNR's during learning sessions was much lower. The correlation of single neuron decoding SNR during training for the Invisible Target was 0.22 dB for monkey M and monkey N. The correlation for neuron decoding SNR during learning the Invisible Cursor task was 11 % for monkey M.

4.3.2. Single neuron and ensemble decoding for position

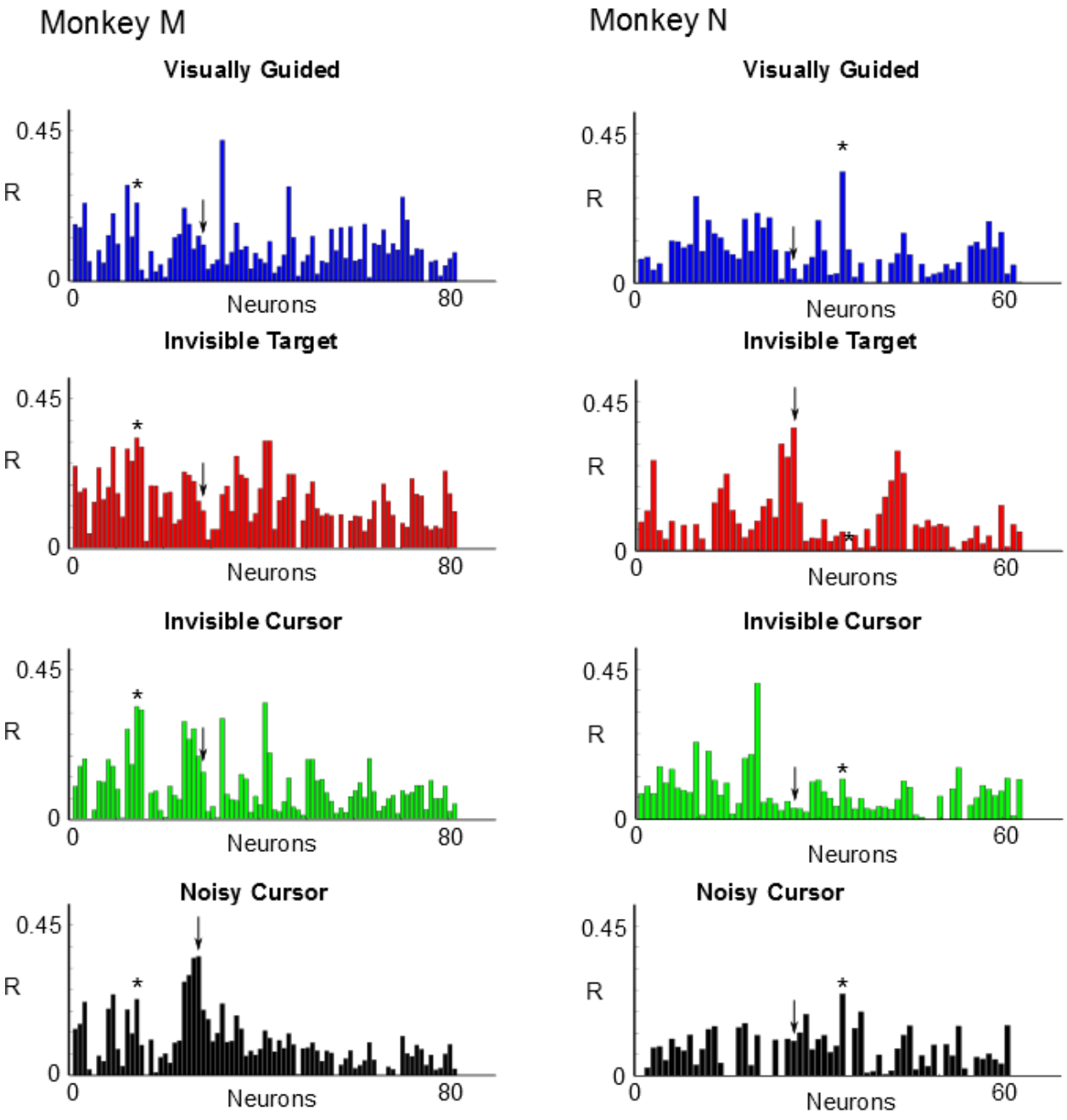

Figure 4.7. Single neuron decoding correlation under different experimental paradigms for both monkeys.

Some individual neurons contributed strongly to decoding only under certain paradigms, while some others have a strong decoding power under all conditions. In monkey M, an example of a neuron whose decoding correlation coefficient is task-dependent is marked with an arrow in Figure 4.6. This neuron's strongest decoding correlation coefficient is under the Noisy Cursor paradigm at 0.35, while under other conditions is 0.14, 0.14, and 0.18 for Visually Guided, Invisible Target, and Invisible Cursor respectively. An example of a neuron that has a stronger decoding correlation coefficient under all conditions is marked with an asterisk in Figure 4.6. In Monkey M, that neuron's decoding correlation coefficient was 0.24, 0.33, 0.33, and 0.23 for Visually Guided, Invisible Target, Invisible Cursor, and Noisy Cursor respectively. In monkey N, an example of a neuron whose decoding correlation coefficient is task-dependent had the strongest value under the Invisible Target paradigm of 0.36 while under other conditions had a value of 0.04, 0.03, 0.10, under Visually Guided, Invisible Cursor, and Noisy Cursor respectively. An example of non-tasks dependent neuron is marked with a asterisk and had the decoding correlation coefficient of 0.32, 0.06, 0.12, and 0.24 under Visually Guided, Invisible Target, Invisible Cursor, and Noisy Cursor respectively.

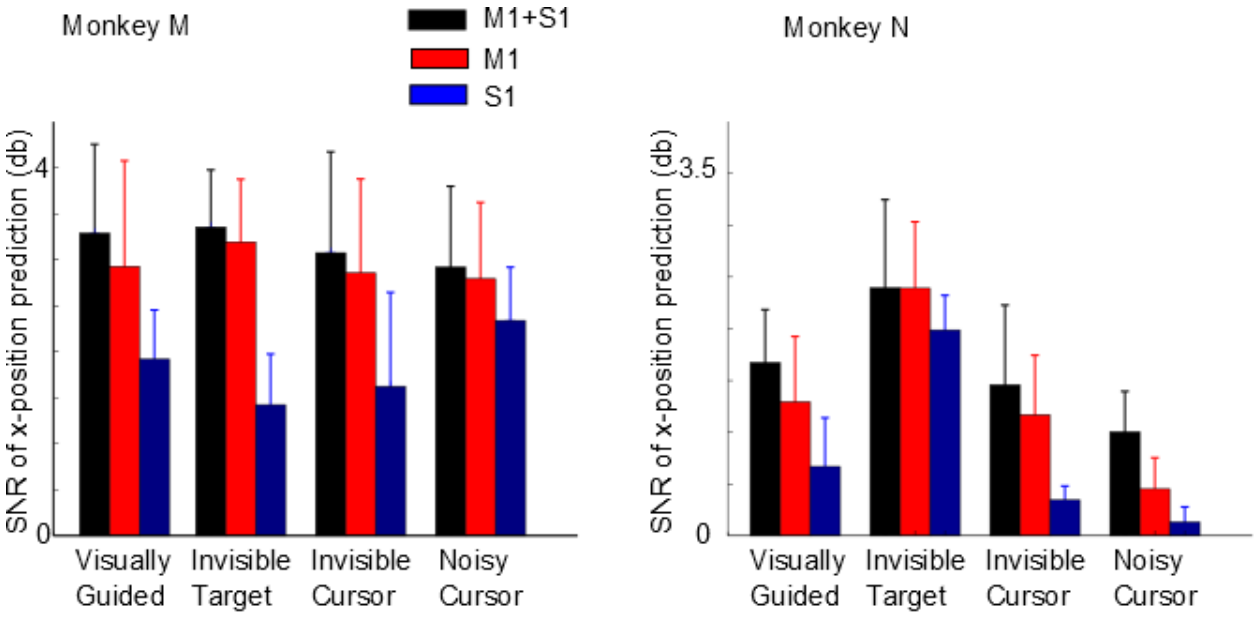

Figure 4.8. Decoding of position by the total neuronal ensemble, by M1 neurons only, and by S1 neurons only under different experimental paradigms for both monkeys.

Predictive power of position was always greater when more of the entire neuronal ensemble was used to train the decoding filter. Decoding using just M1 neurons yielded comparable decoding power but it was less than the decoding of using the entire ensemble. Predictive power using just S1 neurons resulted in the least decoding power under all paradigms and for both monkeys.

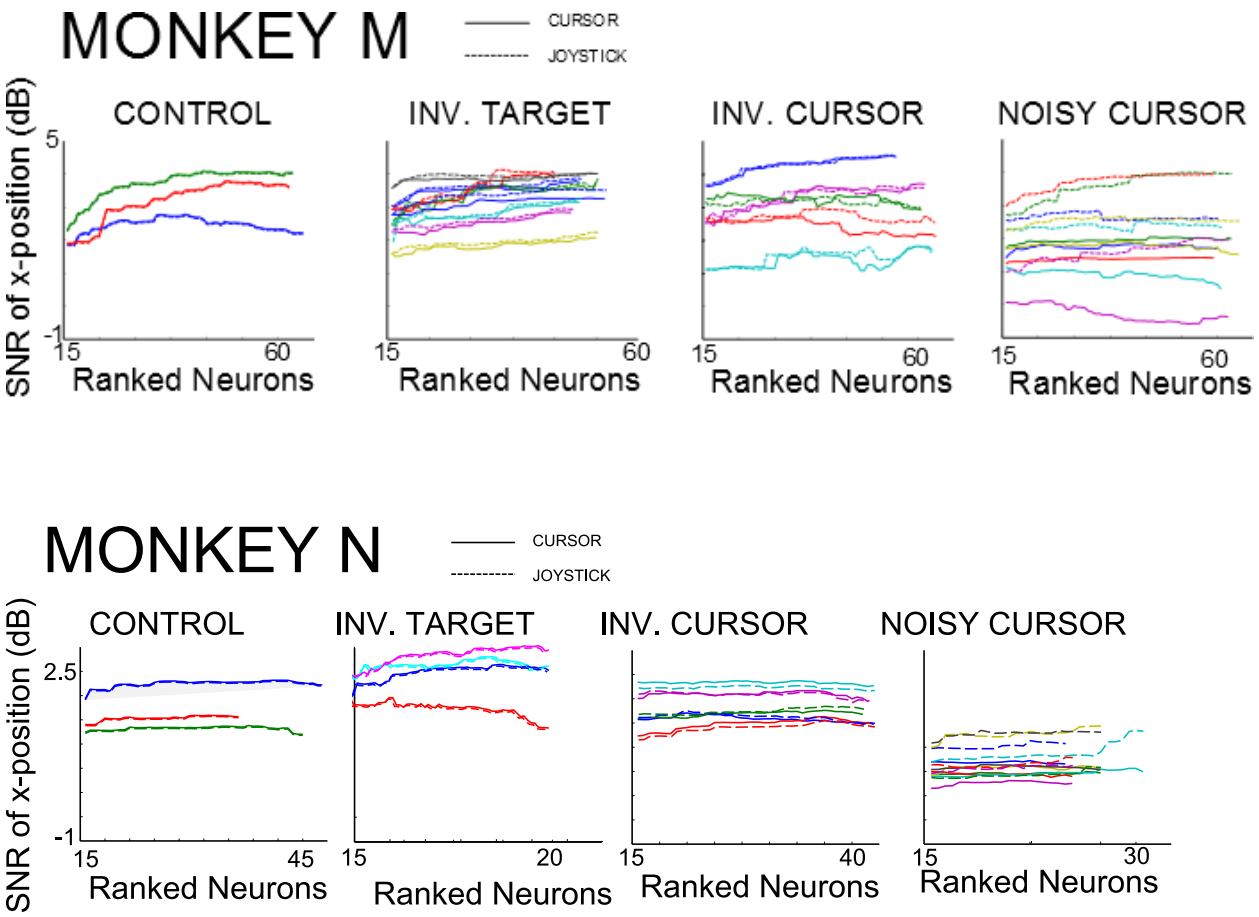

Figure 4.9. Decoding performance of cursor position vs. joystick position for all sessions under different experimental paradigm for both monkeys. Each trace represents one session.

Due to the large ensembles, similar decoding was achieved for different paradigms (Figure 4.8). However under the Noisy Cursor paradigm, decoding for joystick position resulted in higher decoding SNR than decoding for cursor position.

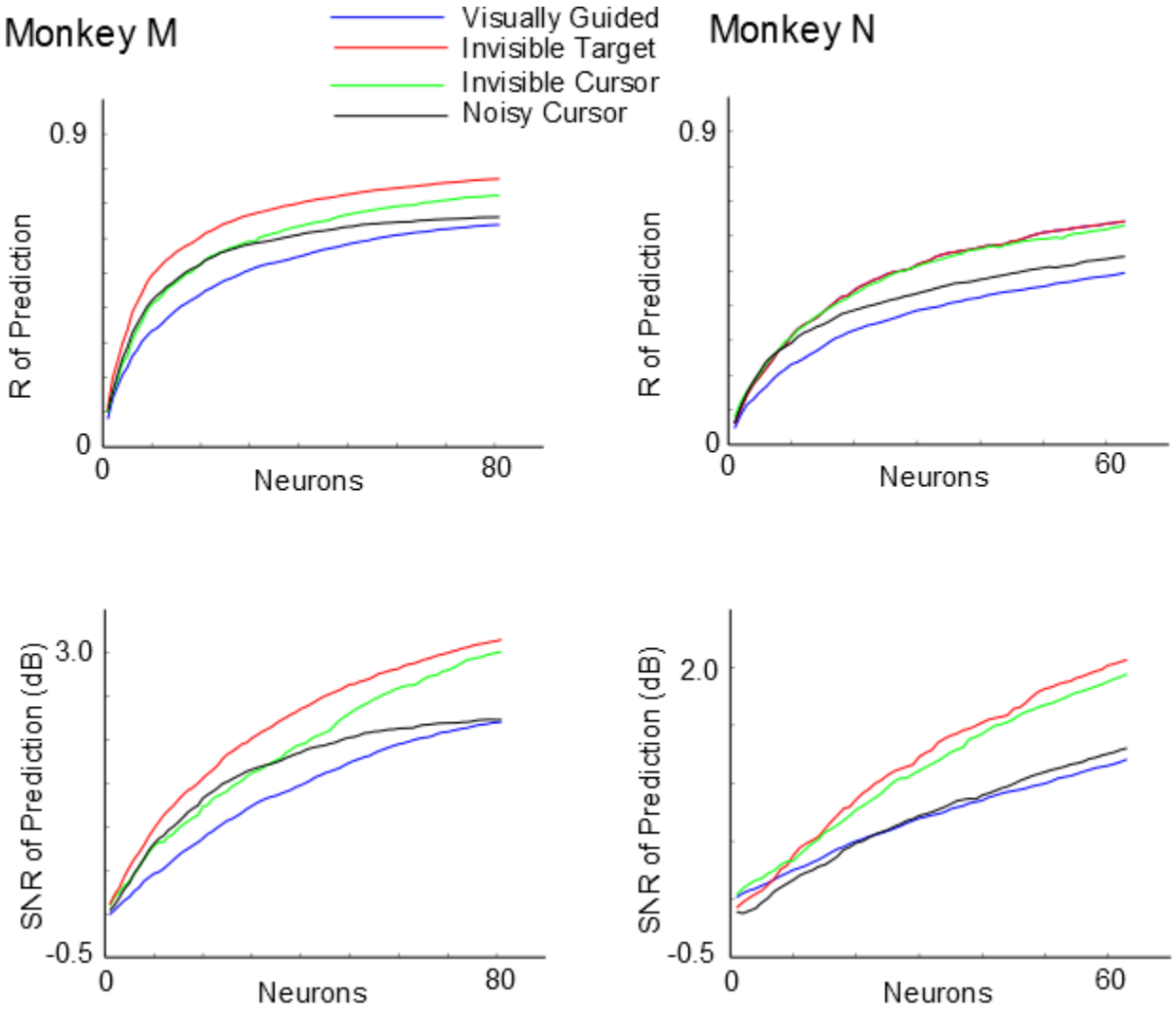

Figure 4.10. Neuron-dropping curves of monkeys M and N under different paradigms for both monkeys. Top row shows R of prediction and bottom row shows SNR of prediction.

As the number of contributing neurons increased, whether it had a very low single contribution, as an ensemble the prediction of position improved. This increasing trend is consistent with both R and SNR metrics.

4.3.3. Single neuron decoding and population decoding for trial type

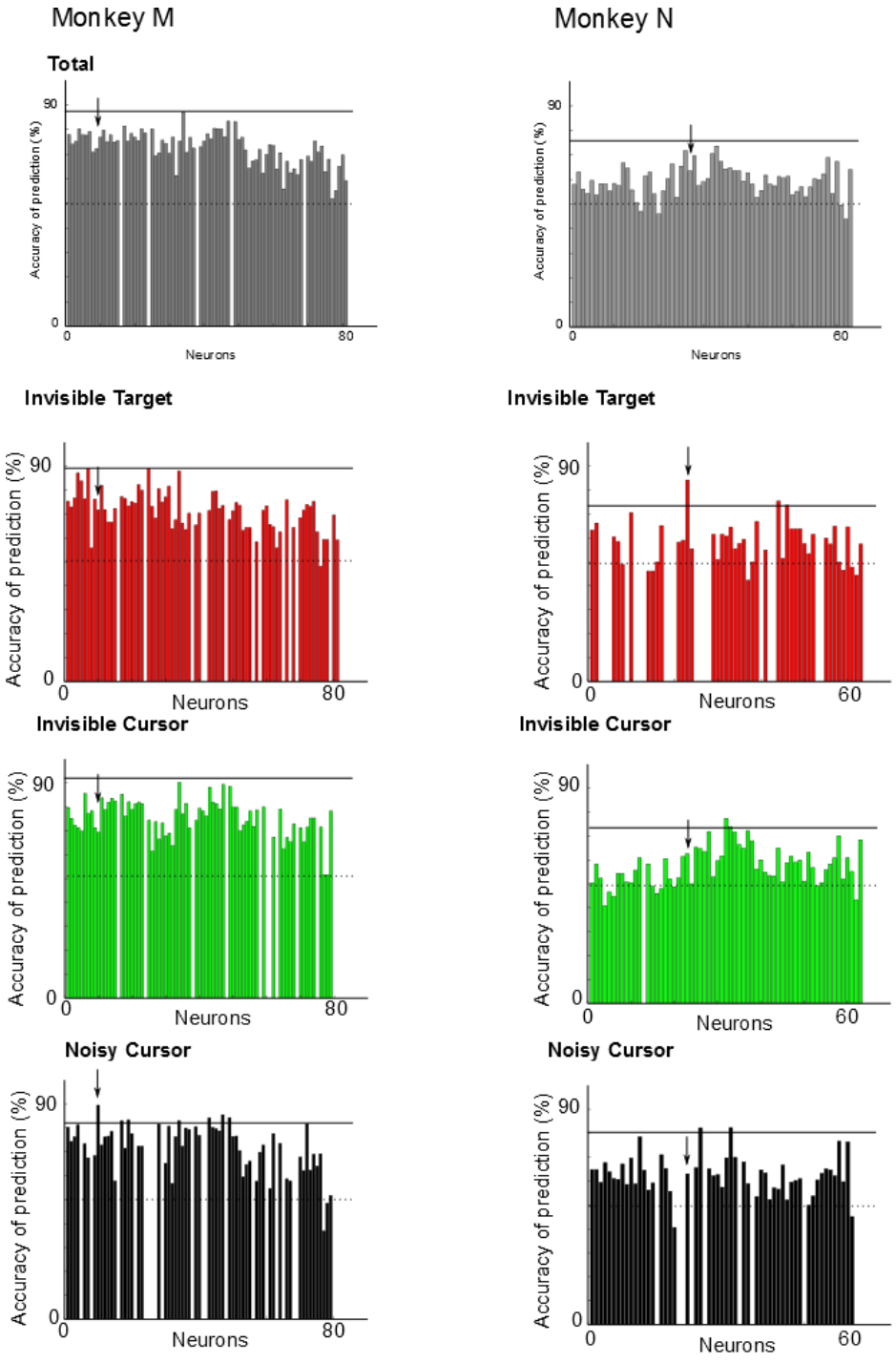

Figure 4.11. Prediction of attention trials vs. non-attention trials under an average of all conditions and under Invisible Target, Invisible Cursor, and Noisy Cursor paradigms for both monkeys. The solid horizontal bar represents accuracy of prediction using the neuronal ensemble. The dashed horizontal bar represents the baseline probability of accuracy of prediction.

Using LDA, non-attention trials in which the monkey didn't move the joystick and did not participate in the task and attention trials in which the monkey performed the trial were predicted. Most single neurons' decoding are above chance and several perform the decoding to the level of the neuronal ensemble accuracy. However, similar to the decoding for positive case, the neurons that have the highest decoding power vary from condition to condition.

At first it may appear that some single neurons have better predictive power than the ensemble. However these neurons have strong predictive power only under specific conditions. For example, in monkey M, the neuron indicated by an arrow in Figure 4.10 has a decoding accuracy of 89% under the Noisy Cursor condition greater than the accuracy of prediction by the ensemble of 83 $\pm$ 1 %. However this neuron gives a lower accuracy than the neuronal ensemble in all other conditions (77%, 72%, 69% in overall average, Invisible Target, and Invisible Cursor respectively). Similarly, in monkey N, the neuron indicated by an arrow in Figure 4.10 has a decoding accuracy of 84 % under the Invisible Target paradigm which is higher than the one given by the ensemble (73 $\pm$ 10%). However the same neuron underperforms the neuronal ensemble under all other paradigms (66 %, 63%, and 63% in overall average, Invisible Cursor, and Noisy Cursor respectively). These results suggest that the predictive power of an entire

neuronal ensemble is more reliable than the prediction of one single neuron under general conditions.

4.4. Discussion

The results from this chapter show for the first time how decoding of movement of single neurons and population of neurons can vary under different visual feedback and ICMS paradigms because neurons contribute differently to decoding depending on the feedback condition and the variable that it decodes. They also show that some single neuron decoding might appear to be as powerful as the decoding given by an ensemble of multiple neurons, but the ensemble's performance is superior overall.

4.4.1. Decoding under different paradigms

The possibility that the decoding differences in single neurons and ensemble observed in my results was due to the inherent variability of neurons was considered but discarded. Although some variability of neurons is expected (Carmena, Lebedev et al. 2003, Carmena, Lebedev et al. 2005, Suner, Fellows et al. 2005, Chestek, Batista et al. 2007, Chestek, Gilja et al. 2011) and change of preferred direction (PD) is also expected (Carmena, Lebedev et al. 2003, Carmena, Lebedev et al. 2005, Chestek, Batista et al. 2007) overall neurons have been shown to maintain good quality and high SNR during recording sessions spanning 61-210 days (Suner, Fellows et al. 2005). Chestek found

that the change in firing rate, PD change, and contribution of single neurons to kinematic decoding remain very stable over time and even in a long experimental session lasting over 6 hours (Chestek, Batista et al. 2007). Furthermore the contribution of a single neuron decoding stays very stable over time as measured by the correlation coefficient between the predicted and the actually kinematic parameter of the actual data.

Given that neurons of monkey in M1 change tuning properties during learning to reach in different environments and maintain that change after learning (Gandolfo, Li et al. 2000, Zach, Inbar et al. 2008) the results of my experiments are likely due to adjusting to a new experimental condition when the visual feedback was modified and ICMS was added.

It has also been shown that an ensemble of motor cortex neurons for prosthetic control can remain stable across time once it has been formed and consolidated through overtraining (Suner, Fellows et al. 2005, Ganguly and Carmena 2009). A neuronal unit is considered stable if its firing properties does not significantly change from day to day (Ganguly and Carmena 2009). Waveform shapes have been shown to vary between days suggesting different neuronal population recorded (Suner, Fellows et al. 2005) although a stable population tends to maintain a similar waveform shapes (Ganguly and Carmena 2009) and if the probability distribution of the interspike interval (ISI)

throughout sessions (Dickey, Suminski et al. 2009, Ganguly and Carmena 2009). Once the ensemble is stable, it would be expected that the tuning properties of the units and its contribution to the decoder to remain stable. Ganguly and Carmena found that the tuning properties of the units remain stable in an ensemble of 15 units and that the ensemble achieved high performance with a fixed decoder after several sessions (Ganguly and Carmena 2009).

My subjects were implanted over four years ago thus any variability associated with initial implant surgery issues such as edema and necrosis (Polikov, Tresco et al. 2005) can be discarded. Intra-day signal instabilities which affect decoding performance (Perge, Homer et al. 2013) have been reported. However, their observed instability might be due to the data being from early post-implantation in which the acute and initial chronic response to the presence of electrodes is still expected (Polikov, Tresco et al. 2005) although it isn't specified whether the data collected was from early days. It could also be that during a "learning" period of cursor control there might not be stability and the neuronal population ensemble has not consolidated. Their findings are useful nonetheless since they point out that the change of waveform shape might make a particular unit not cross the firing threshold thus affecting the performance of the decoder, which is dependent on the number of units and the firing rate of those units, although there was a study suggesting that spiking sort does not improve decoder

performance (Fraser, Chase et al. 2009). Also firing rate of a neuron might be dependent on the attention that the subject is paying to the task as the state of attention or inattention indicated by moving the joystick (Figure 4.13) can be reliably predicted. My data does not suggest intra-day instability and only neurons that have been shown to be stable were analyzed.

M1 has better predictive power than S1. That is not surprising given that the activity of S1 was very variable (chapter 3). However the combination of both neuronal ensembles gives a superior decoding performance than each ensemble alone suggesting that both ensembles carry movement-related information content (Figure 4.7).

The performance of the decoder can be affected by the parameter being decoded as suggested by the significant difference between cursor position decoding and joystick position decoding under the Noisy Cursor paradigm (Figure 4.8). This difference might be especially significant under this paradigm because the sense of cursor position was uncoupled from the joystick position due to the invisible initial cursor bias and that the monkeys were more certain of the joystick position that the cursor.

4.4.2. Single neuron vs. population decoding

This finding is in accordance with other studies which also show that the decoding power of single neurons is very weak compared to the decoding power of an entire ensemble (Wessberg, Stambaugh et al. 2000, Carmena, Lebedev et al. 2003,

Carmena, Lebedev et al. 2005) and that contribution of single neuron to position, velocity and gripping force are different (Carmena, Lebedev et al. 2003). However it hasn't been studied whether the same neurons contribute equally to decoding of parameters that are useful during BMI control such as position.

However, studying single neuron decoding can yield an important insight if the goal of the study is to examine a specific cell type under different conditions.

5. Discussion

5.1. ICMS

This dissertation presents ICMS as a possible solution to delivering somatosensation that can act alone without the need of other sensory modalities. However there remain many issues that need to be solved before ICMS can be clinically relevant such as the use of ICMS for continuous feedback.

I tried delivering spatial sense to monkeys by using different ICMS frequencies (figure 5.1) but failed. Although several experiments have shown that rat, monkeys, and humans can discriminate ICMS frequencies (Romo, Hernández et al. 1998, Fitzsimmons, Drake et al. 2007, O'Doherty, Lebedev et al. 2011), my experiments using four different frequencies to signal their position failed because either of the two monkeys, who learned the experiments from the previous chapter, never became proficient in this task.

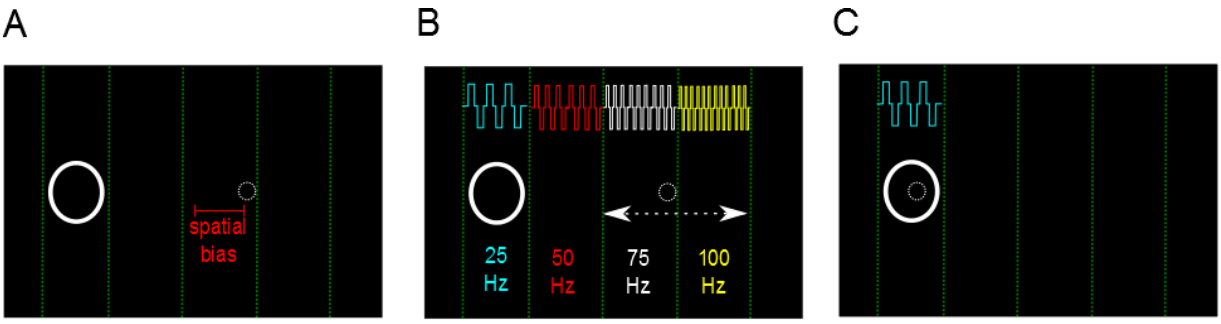

Figure 5.1. Schematic of invisible cursor with continuous ICMS task. A. When the trial starts the target was visible and the cursor was invisible. Initial cursor position changed in every trial with a spatial bias. B. ICMS was delivered throughout the entire trial depending on the position of the cursor. If the cursor was in the first area, an ICMS of 25 Hz was delivered. C. Once the cursor was in the target, the ICMS

corresponding to the area was delivered. If the cursor remained in the target for a pre-determined time (0.8-1.4 s) then reward in form of juice was delivered.

Different parameters of ICMS and experimental parameters were changed to train the subjects to learn the task. I used different frequency parameters (25, 50, 75, 100 Hz) as well as 10, 20, 40, 80, Hz. Four different pairs of stimulating electrodes with different RF areas were also used. I also added visual feedback (bars and color and intensity) per different stimulation frequency area. The target duration and target size were increased. But even after 6 months of training neither monkeys had learned the task.

There are several possibilities of why this experiment did not work. 1) The monkeys were overtrained to only detect the onset of detect and they were not accustomed to continuous ICMS. 2) The transition from one frequency to the next was too fast. 3) ICMS should be delivered to areas with very different RF and even different parts of the body such as from hand, forearm, and shoulder 4) More complex patterns of ICMS frequency that increases gradually to one direction but decreases to another could be used. Overall, my negative results suggest that more complex sensory feedback might need more complex ICMS patterns.

Another important yet unsolved issue in the field of ICMS research is the "sensation" that the subjects feel when ICMS is applied initially and in a chronic matter.

It is impossible to know what the monkeys felt but what is clear is that ICMS produces a sensation whether artificial or natural and that they can use this sensation as a source of information to detect that the cursor is inside the target without any additional information.

For the tasks in this dissertation, the arm representation area of S1 was used for ICMS application in monkey M and the leg representation of area S1 was used for monkey N. These locations were chosen based on the area in each monkey that presented the strongest receptive fields. There was no significant difference in ICMS efficacy in terms of sessions that each monkey required for learning the tasks and the ICMS parameters (amplitude, frequency and duration). This is possibly due to the fact that the sensation given by ICMS was strong enough to be detectable during the task once they were accustomed.

ICMS produces artifacts during recording (Heffer and Fallon 2008). Thus for the data shown in this dissertation data from periods that contain ICMS application was not analyzed. However, despite the artifacts created by ICMS, ICMS is very useful as monkeys in this dissertation learned the tasks and it is still a viable option for sensory BMIs because it has been shown that blacking of neuronal data of up to 10 ms after stimulation that contain potential artifact has no significant difference on position decoding accuracy (O'Doherty, Lebedev et al. 2012)

5.2. BMI recording

In the future more neurons from different cortical and deeper structures of the primate brain should be recorded. The Nicolelis lab reported recordings from 1874 neurons from S1 and M1 of monkeys in 2013. The motor and the sensory systems involve many different structures of the brain and I predict that simultaneous recording of neurons from all different areas will provide better decoding of movement parameters and will also serve as a valuable tool to study the motor and the sensory system.

5.3. BMI for humans

For patients with severe SCI, locked-in syndrome, and patients without any residual limb control or complete sensory denervation, invasive BMIs could be an only solution. Furthermore invasive BMIs utilize the brain directly to extract and to implant information which leads to the possibility of a seamless integration in the future. Peripheral prosthetics have the advantage of being less invasive but they will always have the disadvantage of interfering with the current use of a particular limb. For example, providing vibration as sensation of movement of a prosthetic arm to the elbow will always interface with the natural sensory sensation of the elbow.

However, for invasive BMIs to be as common as pacemakers, first of all the long term effects of BMI arrays should be examined. The longest recording that has been

reported was seven years (Krüger, Caruana et al. 2010) however in a human an implant should guarantee a lifetime efficiency especially since implants in the brain pose great risks when they are attempted to be removed. Maybe to alleviate the acute and chronic effects of the implants mentioned in Chapter 2 neurotrophic factors used in some implants (Kennedy and Bakay 1998) could be considered.

Another important issue that needs to be solved is that the BMI system should be small, wireless, and power-efficient so it could ideally fit under the patient's scalp. Exposed headcaps can be susceptible to infections and greater risk of being broken.

I believe if these issues are solved BMIs could become as common of DBS systems and pacemakers. In the future, somatosensory feedback will be as essential as the haptic feedback provided in smartphones nowadays. The patient will be able to voluntarily switch the feedback on and off or set it on an "automatic" mode such the somatosensory feedback is provided when the light conditions prevents visual feedback or a fine motor control is needed.

Bibliography

Afraz, S.-R., R. Kiani and H. Esteky (2006). "Microstimulation of inferotemporal cortex influences face categorization." Nature **442**(7103): 692-695.

Alexander, G. and M. Crutcher (1990). "Neural representations of the target (goal) of visually guided arm movements in three motor areas of the monkey." Journal of neurophysiology **64**(1): 164-178.

Alles, D. S. (1970). "Information Transmission by Phantom Sensations." Man-Machine Systems, IEEE Transactions on **11**(1): 85-91.

Ashe, J. and A. Georgopoulos (1994). "Movement parameters and neural activity in motor cortex and area 5." Cerebral Cortex.

Atkins, D. J., D. C. Y. Heard and W. H. Donovan (1996). "Epidemiologic Overview of Individuals with Upper-Limb Loss and Their Reported Research Priorities." JPO: Journal of Prosthetics and Orthotics **8**(1): 2-11.

Bak, M., J. Girvin, F. Hambrecht, C. Kufta, G. Loeb and E. Schmidt (1990). "Visual sensations produced by intracortical microstimulation of the human occipital cortex." Medical & biological engineering & computing **28**(3): 257-259.

Bartlett, J., E. DeYoe, R. Doty, B. Lee, J. Lewine, N. Negrão and W. Overman (2005). "Psychophysics of electrical stimulation of striate cortex in macaques." Journal of neurophysiology **94**(5): 3430-3442.

Batista, A. P., C. A. Buneo, L. H. Snyder and R. A. Andersen (1999). "Reach Plans in Eye-Centered Coordinates." Science **285**(5425): 257-260.

Berger, T., A. Ahuja, S. Courellis, S. Deadwyler, G. Erinjippurath, G. Gerhardt, G. Gholmieh, J. Granacki, R. Hampson, M. Hsaio, J. LaCoss, V. Marmarelis, P. Nasiatka, V. Srinivasan, D. Song, A. Tanguay and J. Wills (2005). "Restoring lost cognitive function." IEEE engineering in medicine and biology magazine : the quarterly magazine of the Engineering in Medicine & Biology Society **24**(5): 30-44.

Blank, A., A. M. Okamura and K. J. Kuchenbecker (2008). "Identifying the role of proprioception in upper-limb prosthesis control: Studies on targeted motion." ACM Trans. Appl. Percept. **7**(3): 1-23.

Brindley, G. S. and W. S. Lewin (1968). "The sensations produced by electrical stimulation of the visual cortex." The Journal of Physiology **196**(2): 479-493.

Britten, K. and R. van Wezel (1998). "Electrical microstimulation of cortical area MST biases heading perception in monkeys." Nature neuroscience **1**(1): 59-63.

Brown, T. and C. Sherrington (1911). "Observations on the localisation in the motor cortex of the baboon ("Papio anubis")." The Journal of physiology **43**(2): 209-218.

Carmena, J., M. Lebedev, R. Crist, J. O'Doherty, D. Santucci, D. Dimitrov, P. Patil, C. Henriquez and M. Nicolelis (2003). "Learning to control a brain-machine interface for reaching and grasping by primates." PLoS biology **1**(2).

Carmena, J., M. Lebedev, C. Henriquez and M. Nicolelis (2005). "Stable ensemble performance with single-neuron variability during reaching movements in primates." The Journal of neuroscience **25**(46): 10712-10716
.
Carrozza, M. C., F. Vecchi, F. Sebastiani, G. Cappiello, S. Roccella, M. Zecca, R. Lazzarini and P. Dario (2003). Experimental analysis of an innovative prosthetic hand with proprioceptive sensors. Robotics and Automation, 2003. Proceedings. ICRA '03. IEEE International Conference on. **2:** 2230-2235 vol.2232

Chapin, J., K. Moxon, R. Markowitz and M. Nicolelis (1999). "Real-time control of a robot arm using simultaneously recorded neurons in the motor cortex." Nature neuroscience **2**(7): 664-670.

Chestek, C., A. Batista, G. Santhanam, B. Yu, A. Afshar, J. Cunningham, V. Gilja, S. Ryu, M. Churchland and K. Shenoy (2007). "Single-neuron stability during repeated reaching in macaque premotor cortex." The Journal of neuroscience **27**(40): 10742-10750.

Chestek, C., V. Gilja, P. Nuyujukian, J. Foster, J. Fan, M. Kaufman, M. Churchland, Z. Rivera-Alvidrez, J. Cunningham, S. Ryu and K. Shenoy (2011). "Long-term stability of neural prosthetic control signals from silicon cortical arrays in rhesus macaque motor cortex." Journal of neural engineering **8**(4): 45005.

Cohen, M. and W. Newsome (2004). "What electrical microstimulation has revealed about the neural basis of cognition." Current opinion in neurobiology **14**(2): 169-177.
de Lafuente, V. and R. Romo (2005). "Neuronal correlates of subjective sensory experience." Nature neuroscience **8**(12): 1698-1703.

DeAngelis, G. and W. Newsome (2004). "Perceptual "read-out" of conjoined direction and disparity maps in extrastriate area MT." PLoS biology **2**(3).

Dickey, A., A. Suminski, Y. Amit and N. Hatsopoulos (2009). "Single-unit stability using chronically implanted multielectrode arrays." Journal of neurophysiology **102**(2): 1331-1339.

Dobelle, W. and M. Mladejovsky (1974). "Phosphenes produced by electrical stimulation of human occipital cortex, and their application to the development of a prosthesis for the blind." The Journal of physiology.

Dobelle, W. H., M. G. Mladejovsky, J. R. Evans, T. S. Roberts and J. P. Girvin (1976). "/`Braille/' reading by a blind volunteer by visual cortex stimulation." Nature **259**(5539): 111-112.

Doty, R., L. Rutledge and R. Larsen (1956). "Conditioned reflexes established to electrical stimulation of cat cerebral cortex." Journal of neurophysiology.

Eisenberg, M., L. Shmuelof, E. Vaadia and E. Zohary (2011). "The representation of visual and motor aspects of reaching movements in the human motor cortex." The Journal of neuroscience **31**(34): 12377-12384.

Ethier, C., E. Oby, M. Bauman and L. Miller (2012). "Restoration of grasp following paralysis through brain-controlled stimulation of muscles." Nature **485**(7398): 368-371.

Evarts, E. (1972). "Contrasts between activity of precentral and postcentral neurons of cerebral cortex during movement in the monkey." Brain research **40**(1): 25-31.

Ferrier, D. (1873). "Experimental Researches in Cerebral Physiology and Pathology." BMJ **1**.

Ferrier, D. (1875). "The Croonian Lecture: Experiments on the Brain of Monkeys (Second Series)." Philosophical Transactions of the Royal Society of London **165**.

Fetz, E. (1969). "Operant conditioning of cortical unit activity." Science **163**(3870): 955-958.

Fisher, R. A. (1936). "The use of multiple measurements in taxonomic problems." Annals of eugenics **7**(2): 179-188.

Fitts, P. (1954). "The information capacity of the human motor system in controlling the amplitude of movement." Journal of experimental psychology **47**(6): 381-391.

Fitzsimmons, N. (2009). "A study of extracting information from neuronal ensemble activity and sending information to the brain using microstimulation in two experimental models: bipedal locomotion in rhesus macaques and instructed reaching movements in owl monkeys." PhD thesis Duke University.

Fitzsimmons, N., W. Drake, T. Hanson, M. Lebedev and M. Nicolelis (2007). "Primate reaching cued by multichannel spatiotemporal cortical microstimulation." The Journal of neuroscience :**27**(21): 5593-5602.

Flor, H., T. Elbert, W. Mühlnickel, C. Pantev, C. Wienbruch and E. Taub (1998). "Cortical reorganization and phantom phenomena in congenital and traumatic upper-extremity amputees." Experimental brain research **119**(2): 205-212.

Fraser, G., S. Chase, A. Whitford and A. Schwartz (2009). "Control of a brain–computer interface without spike sorting." Journal of Neural Engineering **6**(5): 055004.

Fritsch, G. and E. Hitzig (1870). "Ueber die elektrische Erregbarkeit des Grosshirns."

Gallace, A. and C. Spence (2008). "The cognitive and neural correlates of "tactile consciousness": A multisensory perspective." Consciousness and Cognition **17**(1): 370-407

Gandolfo, F., C. Li, B. Benda, C. Schioppa and E. Bizzi (2000). "Cortical correlates of learning in monkeys adapting to a new dynamical environment." Proceedings of the National Academy of Sciences of the United States of America **97**(5): 2259-2263.

Ganguly, K. and J. Carmena (2009). "Emergence of a stable cortical map for neuroprosthetic control." PLoS biology **7**(7).

Georgopoulos, A., A. Schwartz and R. Kettner (1986). "Neuronal population coding of movement direction." Science **233**(4771): 1416-1419.

Ghez, C., J. Gordon and M. Ghilardi (1995). "Impairments of reaching movements in patients without proprioception. II. Effects of visual information on accuracy." Journal of neurophysiology **73**(1): 361-372.

Graziano, M., C. Taylor and T. Moore (2002). "Complex movements evoked by microstimulation of precentral cortex." Neuron **34**(5): 841-851.

Grill, W., S. Norman and R. Bellamkonda (2009). "Implanted neural interfaces: biochallenges and engineered solutions." Annual review of biomedical engineering **11**: 1-24.

Hanson, T., B. Ómarsson, J. O'Doherty, I. Peikon, M. Lebedev and M. Nicolelis (2012). "High-side digitally current controlled biphasic bipolar microstimulator." IEEE transactions on neural systems and rehabilitation engineering : a publication of the IEEE Engineering in Medicine and Biology Society **20**(3): 331-340.

Haykin, S. S. (2005). Adaptive Filter Theory, 4/e, Pearson Education India.

Heffer, L. F. and J. B. Fallon (2008). "A novel stimulus artifact removal technique for high-rate electrical stimulation." Journal of Neuroscience Methods **170**(2): 277-284.

Heming, E. A., R. Choo, J. N. Davies and Z. H. T. Kiss (2011). "Designing a Thalamic Somatosensory Neural Prosthesis: Consistency and Persistence of Percepts Evoked by Electrical Stimulation." Neural Systems and Rehabilitation Engineering, IEEE Transactions on **19**(5): 477-482.

Hochberg, L. R., D. Bacher, B. Jarosiewicz, N. Y. Masse, J. D. Simeral, J. Vogel, S. Haddadin, J. Liu, S. S. Cash, P. van der Smagt and J. P. Donoghue (2012). "Reach and grasp by people with tetraplegia using a neurally controlled robotic arm." Nature **485**(7398): 372-375.

Hochberg, L. R., M. D. Serruya, G. M. Friehs, J. A. Mukand, M. Saleh, A. H. Caplan, A. Branner, D. Chen, R. D. Penn and J. P. Donoghue (2006). "Neuronal ensemble control of prosthetic devices by a human with tetraplegia." Nature **442**(7099): 164-171.

Humphrey, D., E. Schmidt and W. Thompson (1970). "Predicting measures of motor performance from multiple cortical spike trains." Science **170**(3959): 758-762.

Ifft, P., M. Lebedev and M. Nicolelis (2011). "Cortical correlates of fitts' law." Frontiers in integrative neuroscience **5**: 85.

Ifft, P., M. Lebedev and M. Nicolelis (2012). "Reprogramming movements: extraction of motor intentions from cortical ensemble activity when movement goals change." Frontiers in neuroengineering **5**: 16.

Jarosiewicz, B., S. Chase, G. Fraser, M. Velliste, R. Kass and A. Schwartz (2008). "Functional network reorganization during learning in a brain-computer interface paradigm." Proceedings of the National Academy of Sciences of the United States of America **105**(49): 19486-19491.

Johnson, L., J. Wander, D. Sarma, D. Su, E. Fetz and J. Ojemann (2013). "Direct electrical stimulation of the somatosensory cortex in humans using electrocorticography electrodes: a qualitative and quantitative report." Journal of neural engineering **10**(3): 36021.

Kakei, S., D. Hoffman and P. Strick (1999). "Muscle and movement representations in the primary motor cortex." Science **285**(5436): 2136-2139.

Kennedy, P. and R. Bakay (1998). "Restoration of neural output from a paralyzed patient by a direct brain connection." Neuroreport **9**(8): 1707-1711.

Klatzky, R., S. Lederman and V. Metzger (1985). "Identifying objects by touch: an "expert system"." Perception & psychophysics **37**(4): 299-302.

Koralek, A., X. Jin, J. Long, R. Costa and J. Carmena (2012). "Corticostriatal plasticity is necessary for learning intentional neuroprosthetic skills." Nature **483**(7389): 331-335.

Krüger, J., F. Caruana, R. Volta and G. Rizzolatti (2010). "Seven years of recording from monkey cortex with a chronically implanted multiple microelectrode." Frontiers in neuroengineering **3**: 6.

Kuiken, T. A., G. A. Dumanian, R. D. Lipschutz, L. A. Miller and K. A. Stubblefield (2004). "The use of targeted muscle reinnervation for improved myoelectric prosthesis control in a bilateral shoulder disarticulation amputee." Prosthet Orthot Int **28**(3): 245-253

Kuiken, T. A., P. D. Marasco, B. A. Lock, R. N. Harden and J. P. A. Dewald (2007). "Redirection of cutaneous sensation from the hand to the chest skin of human amputees with targeted reinnervation." Proceedings of the National Academy of Sciences **104**(50): 20061 -20066

Lebedev, M., J. Carmena, J. O'Doherty, M. Zacksenhouse, C. Henriquez, J. Principe and M. Nicolelis (2005). "Cortical ensemble adaptation to represent velocity of an artificial actuator controlled by a brain-machine interface." The Journal of neuroscience **25**(19): 4681-4693.

Lebedev, M. and M. Nicolelis (2006). "Brain-machine interfaces: past, present and future." Trends in neurosciences **29**(9): 536-546.

Lebedev, M., A. Tate, T. Hanson, Z. Li, J. O'Doherty, J. Winans, P. Ifft, K. Zhuang, N. Fitzsimmons, D. Schwarz, A. Fuller, J. An and M. Nicolelis (2011). "Future developments in brain-machine interface research." Clinics (São Paulo, Brazil) **66 Suppl 1**: 25-32.

Leuthardt, E. C., G. Schalk, J. R. Wolpaw, J. G. Ojemann and D. W. Moran (2004). "A brain–computer interface using electrocorticographic signals in humans." Journal of neural engineering **1**(2): 63.

London, B., L. Jordan, C. Jackson and L. Miller (2008). "Electrical stimulation of the proprioceptive cortex (area 3a) used to instruct a behaving monkey." IEEE transactions on neural systems and rehabilitation engineering : a publication of the IEEE Engineering in Medicine and Biology Society **16**(1): 32-36.

Mann, R. W. and S. D. Reimers (1970). "Kinesthetic Sensing for the EMG Controlled "Boston Arm"." Man-Machine Systems, IEEE Transactions on **11**(1): 110-115.

Marzullo, T. C., M. J. Lehmkuhle, G. J. Gage and D. R. Kipke (2010). "Development of Closed-Loop Neural Interface Technology in a Rat Model: Combining Motor Cortex Operant Conditioning With Visual Cortex Microstimulation." Neural Systems and Rehabilitation Engineering, IEEE Transactions on **18**(2): 117-126.

McDonald, J. and C. Sadowsky (2002). "Spinal-cord injury." Lancet **359**(9304): 417-425.
Medina, L., M. Lebedev, J. O'Doherty and M. Nicolelis (2012). "Stochastic facilitation of artificial tactile sensation in primates." The Journal of neuroscience **32**(41): 14271-14275.

Micera, S., X. Navarro, J. Carpaneto, L. Citi, O. Tonet, P. M. Rossini, M. C. Carrozza, K. P. Hoffmann, M. Vivo, K. Yoshida and P. Dario (2008). "On the Use of Longitudinal Intrafascicular Peripheral Interfaces for the Control of Cybernetic Hand Prostheses in Amputees." Neural Systems and Rehabilitation Engineering, IEEE Transactions on **16**(5): 453-472.

Middlebrooks, J., J. Bierer and R. Snyder (2005). "Cochlear implants: the view from the brain." Current opinion in neurobiology **15**(4): 488-493.

Moran, D. and A. Schwartz (1999). "Motor cortical representation of speed and direction during reaching." Journal of Neurophysiology.

Moritz, C. T., S. I. Perlmutter and E. E. Fetz (2008). "Direct control of paralysed muscles by cortical neurons." Nature **456**(7222): 639-642.

Murphey, D. K. and J. H. R. Maunsell (2007). "Behavioral Detection of Electrical Microstimulation in Different Cortical Visual Areas." Current Biology **17**(10): 862-867.

Murthy, V. and E. Fetz (1992). "Coherent 25- to 35-Hz oscillations in the sensorimotor cortex of awake behaving monkeys." Proceedings of the National Academy of Sciences of the United States of America **89**(12): 5670-5674.

Musallam, S., B. Corneil, B. Greger, H. Scherberger and R. Andersen (2004). "Cognitive control signals for neural prosthetics." Science **305**(5681): 258-262.

Neggers, S. and H. Bekkering (1999). "Integration of visual and somatosensory target information in goal-directed eye and arm movements." Experimental brain research. Experimentelle Hirnforschung. Expérimentation cérébrale **125**(1): 97-107.

Nicolelis, M., L. Baccala, R. Lin and J. Chapin (1995). "Sensorimotor encoding by synchronous neural ensemble activity at multiple levels of the somatosensory system." Science **268**.

Nicolelis, M., D. Dimitrov, J. Carmena, R. Crist, G. Lehew, J. Kralik and S. Wise (2003). "Chronic, multisite, multielectrode recordings in macaque monkeys." Proceedings of the National Academy of Sciences of the United States of America **100**(19): 11041-11046.

Nicolelis, M. A. (2007). Methods for neural ensemble recordings, CRC press.

Nohama, P., A. V. Lopes and A. Cliquet (1995). "Electrotactile Stimulator for Artificial Proprioception." Artificial Organs **19**(3): 225-230

O'Doherty, J., M. Lebedev, T. Hanson, N. Fitzsimmons and M. Nicolelis (2009). "A brain-machine interface instructed by direct intracortical microstimulation." Frontiers in integrative neuroscience **3**: 20.

O'Doherty, J., M. Lebedev, P. Ifft, K. Zhuang, S. Shokur, H. Bleuler and M. Nicolelis (2011). "Active tactile exploration using a brain-machine-brain interface." Nature **479**(7372): 228-231.

O'Doherty, J., M. Lebedev, Z. Li and M. Nicolelis (2012). "Virtual active touch using randomly patterned intracortical microstimulation." IEEE transactions on neural systems and rehabilitation engineering : a publication of the IEEE Engineering in Medicine and Biology Society **20**(1): 85-93.

O'Doherty, J. E., M. A. Lebedev, T. L. Hanson, N. A. Fitzsimmons and M. A. L. Nicolelis (2009). "A Brain-Machine Interface Instructed by Direct Intracortical Microstimulation." Frontiers in integrative neuroscience **3**: 1-10.

Otto, K. J., P. J. Rousche and D. R. Kipke (2005). "Microstimulation in auditory cortex provides a substrate for detailed behaviors." Hearing Research **210**(1–2): 112-117.

Pais-Vieira, M., M. Lebedev, C. Kunicki, J. Wang and M. Nicolelis (2013). "A brain-to-brain interface for real-time sharing of sensorimotor information." Scientific reports **3**: 1319.

Paninski, L., M. Fellows, N. Hatsopoulos and J. Donoghue (2004). "Spatiotemporal tuning of motor cortical neurons for hand position and velocity." Journal of neurophysiology **91**(1): 515-532.

Paz, R., T. Boraud, C. Natan, H. Bergman and E. Vaadia (2003). "Preparatory activity in motor cortex reflects learning of local visuomotor skills." Nature neuroscience **6**(8): 882-890.

Penfield, W. and E. Boldrey (1937). " Somatic motor and sensory representation in the cerebral cortex of man as studied by electrical stimulation." Brain **60**(4): 389-443.

Penfield, W. and P. Perot (1963). "The brain's record of auditory and visual experience." Brain **86**(4): 595-696.

Penfield, W. and T. Rasmussen (1950). "The cerebral cortex of man; a clinical study of localization of function."

Perge, J., M. Homer, W. Malik, S. Cash, E. Eskandar, G. Friehs, J. Donoghue and L. Hochberg (2013). "Intra-day signal instabilities affect decoding performance in an intracortical neural interface system." Journal of neural engineering **10**(3): 36004.

Polikov, V., P. Tresco and W. Reichert (2005). "Response of brain tissue to chronically implanted neural electrodes." Journal of neuroscience methods **148**(1): 1-18.

Polit, A. and E. Bizzi (1979). "Characteristics of motor programs underlying arm movements in monkeys." Journal of neurophysiology **42**(1 Pt 1): 183-194.

Ransom, W. B. (1892). "A case illustrating kinaesthesis." Brain **15**(3-4): 437-442.

Rincon-Gonzalez, L., J. P. Warren, D. M. Meller and S. Helms Tillery (2011). "Haptic Interaction of Touch and Proprioception: Implications for Neuroprosthetics." Neural Systems and Rehabilitation Engineering, IEEE Transactions on **19**(5): 490-500.

Romo, R., A. Hernández, A. Zainos, C. Brody and L. Lemus (2000). "Sensing without touching: psychophysical performance based on cortical microstimulation." Neuron **26**(1): 273-278.

Romo, R., A. Hernandez, A. Zainos and E. Salinas (1998). "Somatosensory discrimination based on cortical microstimulation." Nature **392**(6674): 387-390.

Salzman, C., K. Britten and W. Newsome (1990). "Cortical microstimulation influences perceptual judgements of motion direction." Nature **346**(6280): 174-177.

Salzman, C., C. Murasugi, K. Britten and W. Newsome (1992). "Microstimulation in visual area MT: effects on direction discrimination performance." The Journal of neuroscience : the official journal of the Society for Neuroscience **12**(6): 2331-2355.

Salzman, C. D., K. H. Britten and W. T. Newsome (1990). "Cortical microstimulation influences perceptual judgements of motion direction." Nature **346**(6280): 174-177.

Schmidt, E. (1980). "Single neuron recording from motor cortex as a possible source of signals for control of external devices." Annals of biomedical engineering **8**(4-6): 339-349.

Schmidt, E., M. Bak, F. Hambrecht, C. Kufta, D. O'Rourke and P. Vallabhanath (1996). "Feasibility of a visual prosthesis for the blind based on intracortical microstimulation of the visual cortex." Brain : a journal of neurology **119 (Pt 2)**: 507-522.

Sergio, L. and J. Kalaska (1998). "Changes in the temporal pattern of primary motor cortex activity in a directional isometric force versus limb movement task." Journal of neurophysiology **80**(3): 1577-1583.

Shen, L. and G. Alexander (1997). "Neural correlates of a spatial sensory-to-motor transformation in primary motor cortex." Journal of neurophysiology **77**(3): 1171-1194.

Smith, A., G. Gosselin and B. Houde (2002). "Deployment of fingertip forces in tactile exploration." Experimental brain research. Experimentelle Hirnforschung. Expérimentation cérébrale **147**(2): 209-218.

Sober, S. and P. Sabes (2003). "Multisensory integration during motor planning." The Journal of neuroscience **23**(18): 6982-6992.

Sober, S. J. and P. N. Sabes (2005). "Flexible strategies for sensory integration during motor planning." Nat Neurosci **8**(4): 490-497.

Suminski, A. J., D. C. Tkach, A. H. Fagg and N. G. Hatsopoulos (2010). "Incorporating feedback from multiple sensory modalities enhances brain-machine interface control." The Journal of neuroscience **30**(50): 16777-16787.

Suner, S., M. Fellows, C. Vargas-Irwin, G. Nakata and J. Donoghue (2005). "Reliability of signals from a chronically implanted, silicon-based electrode array in non-human primate primary motor cortex." IEEE transactions on neural systems and rehabilitation engineering : a publication of the IEEE Engineering in Medicine and Biology Society **13**(4): 524-541.

Talwar, S., S. Xu, E. Hawley, S. Weiss, K. Moxon and J. Chapin (2002). "Rat navigation guided by remote control." Nature **417**(6884): 37-38.

Taub, E., I. Goldberg and P. Taub (1975). "Deafferentation in monkeys: pointing at a target without visual feedback." Experimental neurology **46**(1): 178-186.

Taylor, D., S. Tillery and A. Schwartz (2002). "Direct cortical control of 3D neuroprosthetic devices." Science **296**(5574): 1829-1832.

Tehovnik, E. (1996). "Electrical stimulation of neural tissue to evoke behavioral responses." Journal of neuroscience methods **65**(1): 1-17.

Tehovnik, E., A. Tolias, F. Sultan, W. Slocum and N. Logothetis (2006). "Direct and indirect activation of cortical neurons by electrical microstimulation." Journal of neurophysiology **96**(2): 512-521.

Thomson, E., R. Carra and M. Nicolelis (2013). "Perceiving invisible light through a somatosensory cortical prosthesis." Nature communications **4**: 1482.

Velliste, M., S. Perel, M. C. Spalding, A. S. Whitford and A. B. Schwartz (2008). "Cortical control of a prosthetic arm for self-feeding." Nature **453**(7198): 1098-1101.

Venkatraman, S. and J. Carmena (2011). "Active sensing of target location encoded by cortical microstimulation." IEEE transactions on neural systems and rehabilitation engineering : a publication of the IEEE Engineering in Medicine and Biology Society **19**(3): 317-324.

Wang, W., S. Chan, D. Heldman and D. Moran (2007). "Motor cortical representation of position and velocity during reaching." Journal of neurophysiology **97**(6): 4258-4270.

Weber, D., R. Friesen and L. Miller (2012). "Interfacing the somatosensory system to restore touch and proprioception: essential considerations." Journal of motor behavior **44**(6): 403-418.

Weber, D., B. London, J. Hokanson, C. Ayers, R. Gaunt, R. Torres, B. Zaaimi and L. Miller (2011). "Limb-state information encoded by peripheral and central somatosensory neurons: implications for an afferent interface." IEEE transactions on neural systems and rehabilitation engineering : a publication of the IEEE Engineering in Medicine and Biology Society **19**(5): 501-513.

Wessberg, J., C. Stambaugh, J. Kralik, P. Beck, M. Laubach, J. Chapin, J. Kim, S. Biggs, M. Srinivasan and M. Nicolelis (2000). "Real-time prediction of hand trajectory by ensembles of cortical neurons in primates." Nature **408**(6810): 361-365.

Wickelgren, I. (2006). "Biomedical engineering. A vision for the blind." Science **312**(5777): 1124-1126.

Wilson, B. S. and M. F. Dorman (2008). "Cochlear implants: A remarkable past and a brilliant future." Hearing Research **242**(1–2): 3-21.

Zach, N., D. Inbar, Y. Grinvald, H. Bergman and E. Vaadia (2008). "Emergence of novel representations in primary motor cortex and premotor neurons during associative learning." The Journal of neuroscience **28**(38): 9545-9556.

Zainos, A., H. Merchant, A. Hernández, E. Salinas and R. Romo (1997). "Role of primary somatic sensory cortex in the categorization of tactile stimuli: effects of lesions." Experimental Brain Research **115**(2): 357-360.

Ziegler-Graham, K., E. MacKenzie, P. Ephraim, T. Travison and R. Brookmeyer (2008). "Estimating the prevalence of limb loss in the United States: 2005 to 2050." Archives of physical medicine and rehabilitation **89**(3): 422-429.

Biography

Je Hi An was born in Seoul, South Korea on October 15, 1984. She lived in Buenos Aires, Argentina from 1993 to 2002.

She attended the Macaulay Honors College at The City College of New York where she graduated with Bachelors in Engineering *magna cum laude*. During her undergraduate years, she worked in Prof. Marom Bikson's laboratory where she published *Effects of glucose and glutamine concentration in the formulation of the artificial cerebrospinal fluid (ACSF)* and co-authored *Spike timing amplifies the effect of electric fields on neurons: implications for endogenous field effects.*

In the summer of 2007 she interned in the laboratory of Prof. Eric Perrault where she co-authored *The differential role of motor cortex in stretch reflex modulation induced by changes in environmental mechanics and verbal instruction*.

She was recipient of the NSF Graduate Fellowship in 2009. She was also a BOOST coach from 2012-2013.